ALFRED-WEGENER-INSTITUT
HELMHOLTZ-ZENTRUM FÜR POLAR- UND MEERESFORSCHUNG

744
2020

Berichte
zur Polar- und Meeresforschung

Reports on Polar and Marine Research

The Expedition AF122/1 Setting up the MOSAiC Distributed Network in October 2019 with Research Vessel AKADEMIK FEDOROV

Edited by

Thomas Krumpen and Vladimir Sokolov

with contributions of the participants

HELMHOLTZ

Die Berichte zur Polar- und Meeresforschung werden vom Alfred-Wegener-Institut, Helmholtz-Zentrum für Polar- und Meeresforschung (AWI) in Bremerhaven, Deutschland, in Fortsetzung der vormaligen Berichte zur Polarforschung herausgegeben. Sie erscheinen in unregelmäßiger Abfolge.

Die Berichte zur Polar- und Meeresforschung enthalten Darstellungen und Ergebnisse der vom AWI selbst oder mit seiner Unterstützung durchgeführten Forschungsarbeiten in den Polargebieten und in den Meeren.

Die Publikationen umfassen Expeditionsberichte der vom AWI betriebenen Schiffe, Flugzeuge und Stationen, Forschungsergebnisse (inkl. Dissertationen) des Instituts und des Archivs für deutsche Polarforschung, sowie Abstracts und Proceedings von nationalen und internationalen Tagungen und Workshops des AWI.

Die Beiträge geben nicht notwendigerweise die Auffassung des AWI wider.

Herausgeber
Dr. Horst Bornemann

Redaktionelle Bearbeitung und Layout
Birgit Reimann

Alfred-Wegener-Institut
Helmholtz-Zentrum für Polar- und Meeresforschung
Am Handelshafen 12
27570 Bremerhaven
Germany

www.awi.de
www.awi.de/reports

Der Erstautor bzw. herausgebende Autor eines Bandes der Berichte zur Polar- und Meeresforschung versichert, dass er über alle Rechte am Werk verfügt und überträgt sämtliche Rechte auch im Namen seiner Koautoren an das AWI. Ein einfaches Nutzungsrecht verbleibt, wenn nicht anders angegeben, beim Autor (bei den Autoren). Das AWI beansprucht die Publikation der eingereichten Manuskripte über sein Repositorium ePIC (electronic Publication Information Center, s. Innenseite am Rückdeckel) mit optionalem print-on-demand.

The Reports on Polar and Marine Research are issued by the Alfred Wegener Institute, Helmholtz Centre for Polar and Marine Research (AWI) in Bremerhaven, Germany, succeeding the former Reports on Polar Research. They are published at irregular intervals.

The Reports on Polar and Marine Research contain presentations and results of research activities in polar regions and in the seas either carried out by the AWI or with its support.

Publications comprise expedition reports of the ships, aircrafts, and stations operated by the AWI, research results (incl. dissertations) of the Institute and the Archiv für deutsche Polarforschung, as well as abstracts and proceedings of national and international conferences and workshops of the AWI.

The papers contained in the Reports do not necessarily reflect the opinion of the AWI.

Editor
Dr. Horst Bornemann

Editorial editing and layout
Birgit Reimann

Alfred-Wegener-Institut
Helmholtz-Zentrum für Polar- und Meeresforschung
Am Handelshafen 12
27570 Bremerhaven
Germany

www.awi.de
www.awi.de/en/reports

The first or editing author of an issue of Reports on Polar and Marine Research ensures that he possesses all rights of the opus, and transfers all rights to the AWI, including those associated with the co-authors. The non-exclusive right of use (einfaches Nutzungsrecht) remains with the author unless stated otherwise. The AWI reserves the right to publish the submitted articles in its repository ePIC (electronic Publication Information Center, see inside page of verso) with the option to "print-on-demand".

Titel: RV Akademik Fedorov and RV Polarstern Seite an Seite im Eis, kurz vor Begin der MOSAiC Expedition (Foto: Jan Rohde, AWI)

Title: RV Akademik Fedorov and RV Polarstern side by side in the ice, shortly before the start of the MOSAiC expedition (Photo: Jan Rohde, AWI)

The Expedition AF122/1
Setting up the MOSAiC Distributed Network in October 2019 with Research Vessel AKADEMIK FEDOROV

Edited by
Thomas Krumpen and Vladimir Sokolov
with contributions of the participants

Please cite or link this publication using the identifiers

https://hdl.handle.net/10013/epic.16bc0ab7-fe46-4fb5-ae69-3edc93a72356
https://doi.org/10.2312/BzPM_0744_2020

ISSN 1866-3192

Akademik Fedorov

AF122/1

20 September 2019 – 31 October 2019

Tromsø - Tromsø

Chief Scientists

Vladimir Sokolov (AARI)

Thomas Krumpen (AWI)

Contents

1. ÜBERBLICK UND FAHRTVERLAUF

Thomas Krumpen[1] and Vladimir Sokolov[2]

[1]AWI
[2]AARI

Im Frühherbst 2019 machte der deutsche Forschungseisbrecher *Polarstern* an einer Eisscholle in der nördlichen Laptewsee fest, um gemeinsam mit der Scholle eine einjährige Reise in Richtung Framstraße anzutreten. Ziel des internationalen Projekts MOSAiC (Multidisciplinary Drifting Observatory for the Study of Arctic Climate) ist es, relevante Prozesse innerhalb des Systems Atmosphäre-Eis-Ozean, die Einfluss auf die Meereismassen- und Energiebilanz haben, zu quantifizieren. Die so gewonnenen Daten dienen der Überprüfung von Klimamodellen und ein detaillierteres Prozessverständnis kann nachhaltig deren Genauigkeit verbessern. Das MOSAiC-Projekt stellt einen Versuch dar, sich an das “neue Normal” in der Arktis (wärmere Luftmassen und dünneres Meereis) anzupassen und das Schiff selbst als Beobachtungsplattform zu nutzen. Rund um das Schiff wurde ein Beobachtungsnetzwerk (Central Observatory, CO) mit umfangreicher Instrumentierung errichtet, um die Prozesse in Atmosphäre, Eis und Ozean entsprechend dokumentieren zu können. Zu diesem Zweck wurde das Schiff am 4. Oktober 2019 an einer vielversprechenden Eisscholle von etwa 2,8 x 3,8 km vertäut (siehe Abbildung 1.1 auf den Koordinaten 136°E, 85°N). Die Scholle war Teil einer losen, noch nicht ein Jahr alten Ansammlung von Packeis, welches die Sommerschmelze überlebt hatte (im Folgenden nach WMO 2017 als „Residual“-Eis bezeichnet). Mit Unterstützung des russischen Forschungsschiffs *Akademik Fedorov* wurde in einem Radius von 40 km um das CO ein Netzwerk (DN) bestehend aus autonomen Bojen auf 55 weiteren Eisschollen ähnlichen Alters installiert (roter Kreis in Abbildung 1.1 und Abbildung 1.3). Für weitere Informationen über die MOSAiC-Expedition verweisen wir auf www.mosaic-expedition.org.

In diesem Bericht geben wir zunächst einen Überblick über die Messungen, die von den Teilnehmern der *Akademik Fedorov* Expedition während der Aufbauphase des autonomen Beobachtungsnetzwerks durchgeführt wurden. Darüber hinaus gibt der Bericht einen Einblick in die anfänglichen Eisbedingungen vor Ort. Abbildung 1.2 fasst den Reiseablauf zusammen, während Abbildung 1.1 die Fahrtroute beider Schiffe, *Polarstern* und *Akademik Fedorov*, zeigt. Für eine detailliertere Beschreibung der anfänglichen Eisbedingungen vor Ort verweisen wir auf Kapitel 5.1 und Krumpen et al. (2020).

Kapitel 2 führt alle Aktivitäten auf, die auf L-Eisschollen durchgeführt wurden. Kapitel 3 beschreibt Messaktivitäten, die auf M- Eisschollen betrieben wurden. Kapitel 4 widmet sich den Gerätschaften, die auf P-Eisschollen ausgebracht wurden. Eine geografische Übersicht über die Einsätze an L-, M- und P-Standorten ist in Abbildung 1.3 dargestellt. Kapitel 5 listet zusätzliche Daten auf, die für die Entscheidungsfindung an Bord verwendet wurden (Satelliten- und Modelldaten, Wetterkarten usw.), sowie schiffs- und luftgestützte Messungen, die entlang der Fahrtroute durchgeführt wurden. Kapitel 6 gibt einen Überblick über die Projekte und beitragenden Partner.

References

Krumpen T, Birrien F, Kauker F, Rackow T, von Albedyll L, Angelopoulos M, Belter HJ, Bessonov V, Damm E, Dethloff K, Haapala J, Haas C, Hendricks S, Hoelemann J, Hoppmann M, Kaleschke L, Karcher M, Kolabutin N, Lenz J, Morgenstern A, Nicolaus M, Nixdorf U, Petrovsky T, Rabe B, Rabenstein L, Rex M, Ricker R, Rohde J, Shimanchuk E, Singha S, Smolyanitsky V, Sokolov V, Stanton T, Timofeeva A, Tsamados M (2020) The MOSAiC ice floe: Sediment-laden survivor from the Siberian shelf. The Cryosphere Discussion, tc-2020-64.

WMO (2017) Sea Ice Nomenclature, WMO/OMM/BMO - No.259, Edition 1970 – 2017, Terminology, Volume I.

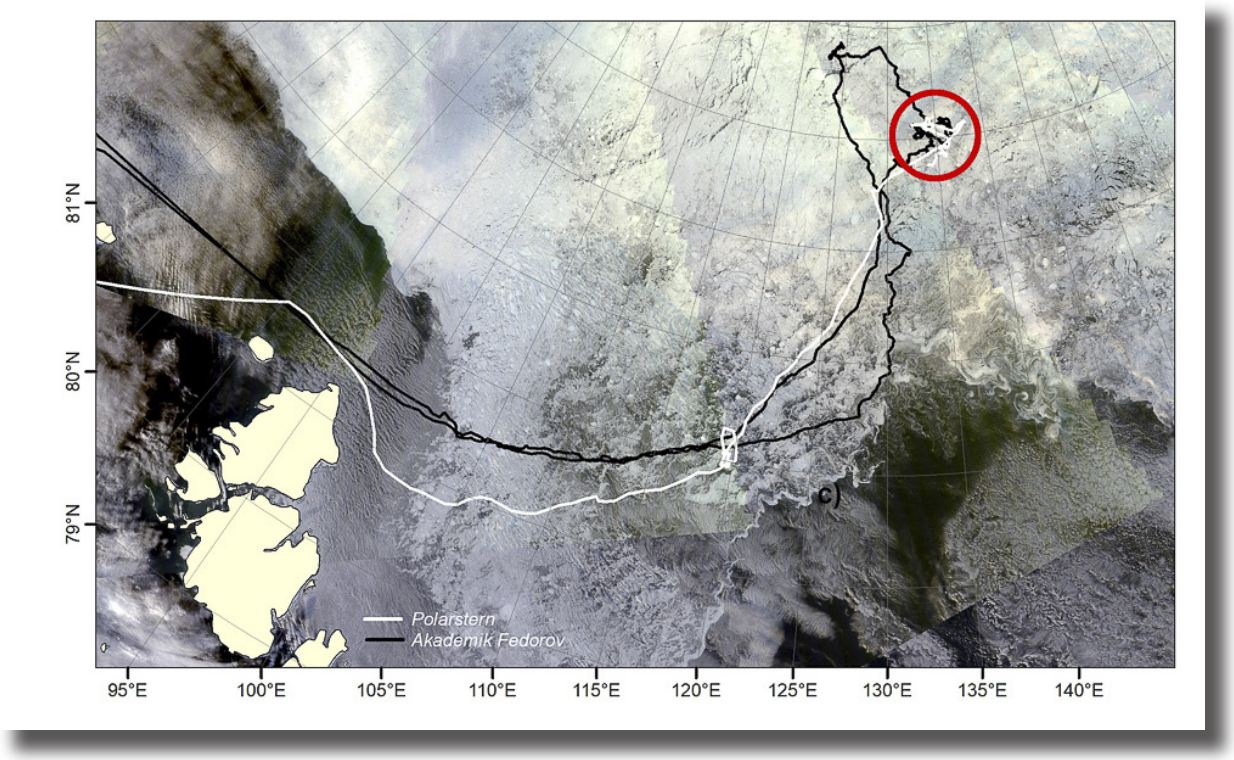

Fig. 1.1: Eisbedingungen in der MOSAiC-Startregion am 25. September 2019, kurz vor Verankerung des Schiffs an der MOSAiC-Scholle. Die Fahrtroute von Polarstern (weiß) und Akademik Fedorov (schwarz), werden gemeinsam mit einem am 22. September 2019 aufgenommenen MODIS-Bild (Quelle: NASA) dargestellt. Der rote Kreis (Radius von 40 km) verweist auf das Gebiet, in dem das autonome Netzwerk von der Akademik Fedorov ausgebracht wurde.

Fig. 1.1: Initial sea ice conditions in the MOSAiC study region on the September 25, 2019, shortly before anchoring at the MOSAiC floe. Ship tracks of Polarstern (white) and Akademik Fedorov (black) superimposed on a MODIS image (source: NASA) obtained on the 22 September 2019. The red circle with a radius of 40 km indicates the area where the Distributed Network was setup by the Akademik Fedorov.

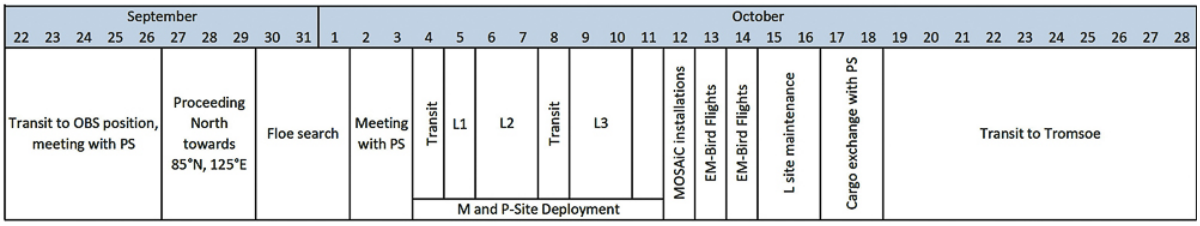

Fig. 1.2: Fahrtablauf der Akademik Fedorov Expedition
Fig. 1.2: Itinerary of the Akademik Fedorov expedition

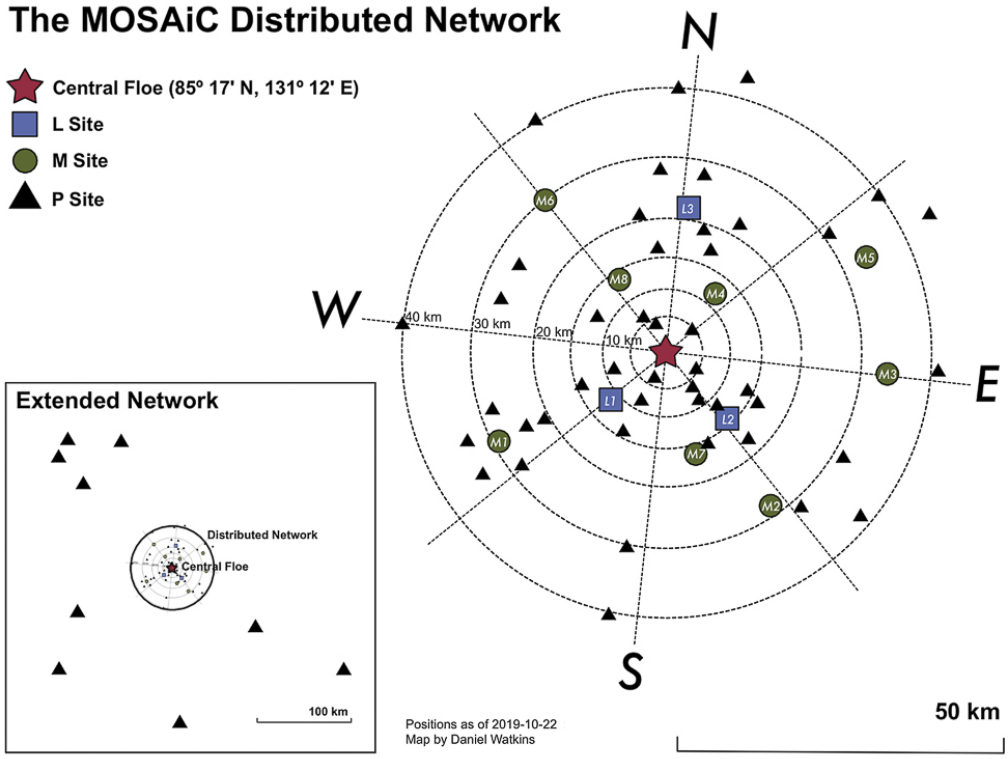

Abb. 1.3: Der Aufbau des autonomen Beobachtungsnetzwerks durch die Akademik Fedorov zwischen dem 4. und 11. Oktober (vgl. Abb. 1.2). Gezeigt werden die Positionen der einzelnen L- (blau), M- (grün) und P-Schollen (schwarz) relativ zur MOSAiC Eisscholle (roter Stern im Zentrum).

Fig. 1.3: The Distributed Network setup by the Akademik Fedorov between 4 and 11 October (compare Fig. 1.2). Shown are the positions of the individual L- (blue), M- (green), and P-site (black) deployments relative to the MOSAiC Central Observatory (CO, red star in the center).

SUMMARY AND ITINERARY

Thomas Krumpen[1] and Vladimir Sokolov[2]

[1]AWI
[2]AARI

In early autumn 2019 the German research icebreaker *Polarstern*, operated by the Alfred Wegener Institute (AWI), Helmholtz Centre for Polar and Marine Research, was moored to an ice floe north of the Laptev Sea in order to travel with the Transpolar Drift on a one-year long journey toward Fram Strait. The goal of the international Multidisciplinary drifting Observatory for the Study of Arctic Climate (MOSAiC) project is to better quantify relevant processes within the atmosphere-ice-ocean system that impact the sea ice mass and energy budget. Other main goals are a better understanding of available satellite data via ground-truthing and improved process understanding that can be implemented into climate models. The MOSAiC project represents an attempt to adapt to the “new normal” in the Arctic (warmer and thinner Arctic sea ice) and to use the ship itself as an observational platform. Around the ship, an ice camp (Central Observatory, CO) with comprehensive instrumentation was set up to intensively observe processes within the atmosphere, ice, and ocean. For this purpose, on October 4, 2019, the ship was moored to a promising ice floe measuring roughly 2.8 x 3.8 km (see Fig. 1.1 at coordinates 136°E, 85°N). The floe was part of a loose assembly of pack ice, not yet a year old, which had survived the summer melt (hereafter called residual ice according to WMO 2017). With the support of the Russian research vessel *Akademik Fedorov*, a Distributed Network (DN) of autonomous buoys was installed in a 40-km radius around the CO on 55 additional residual ice floes of similar age (red circle in Fig. 1.1 and Fig. 1.3). For more information about the MOSAiC expedition the reader is referred to www.mosaic-expedition.org.

In this report, we first provide an overview of measurements and deployments carried out by the participants of the *Akademik Fedorov* cruise during the setup phase of the Distributed Network. Moreover, the report provides insight into the initial ice conditions on-site and observations made on various additional floes visited by *Akademik Fedorov* during the search for a suitable MOSAiC CO. Fig. 1.2 summaries the itinerary of the cruise, while Fig. 1.1 provides the cruise track of both ships, *Polarstern* and *Akademik Fedorov*. For a more detailed description about the initial ice conditions encountered on site we refer to chapter 5.1 and Krumpen et al. (2020).

Chapter 2 lists all activities performed on L-site floes, chapter 3 describes deployments made on M-sites, while chapter 4 provides a summary of smaller installations carried out on P-sites. A geographical overview of L-, M-, and P-site deployments relative to the CO is given in Fig. 1.3. Chapter 5 lists additional data that was used for decision making on board (satellite and model data, weather charts, etc.) as well as ship- and airborne measurements carried out along the cruise track. Chapter 6 gives an overview of the projects and contributing partners related to education and outreach.

References

Krumpen T, Birrien F, Kauker F, Rackow T, von Albedyll L, Angelopoulos M, Belter HJ, Bessonov V, Damm E, Dethloff K, Haapala J, Haas C, Hendricks S, Hoelemann J, Hoppmann M, Kaleschke L, Karcher M, Kolabutin N, Lenz J, Morgenstern A, Nicolaus M, Nixdorf U, Petrovsky T, Rabe B, Rabenstein L, Rex M, Ricker R, Rohde J, Shimanchuk E, Singha S, Smolyanitsky V, Sokolov V, Stanton T, Timofeeva A, Tsamados M (2020) The MOSAiC ice floe: Sediment-laden survivor from the Siberian shelf. The Cryosphere Discussion, tc-2020-64.

WMO (2017) Sea Ice Nomenclature, WMO/OMM/BMO - No.259, Edition 1970 – 2017, Terminology, Volume I.

2. GENERAL SET-UP

2.1 Ice and snow surveys

Jakob Belter[1], Francesca Doglioni[1],
Jari Haapala[2], Anika Happe[3],
Nikolay Kolabutin[4], Ewa Korejwo[5],
Thomas Krumpen[1], Robbie Mallett[6],
Tatiana Matveeva[7], Alex Mavrovic[8],
Egor Shimanshuk[4], Vasiliy Smolyamitskiy[4]
and Michel Tsamados[6]

[1]AWI
[2]FMI
[3]U Oldenburg
[4]AARI
[5]IOPAN
[6]UCL
[7]LMSU
[8]UTR

Grant No. AF-MOSAiC-1_00

Objectives

The objective of this activity was to characterize sea ice and snow conditions of the MOSAiC distributed network floes. To do this we conducted ice and snow thickness surveys, ice drilling and photographic mapping in the vicinity of the buoy deployments (Tab. 2.1.1).

Work at sea

Sea ice thickness measurements were conducted in a regular manner using two complementing methods – drilling and ground electromagnetic survey (GEM). Drilling was made with the Kovacs 5 cm ice auger. In addition to ice thickness measurements, freeboard and snow thickness was also measured. Drilling provided also indirect information on a structure of sea ice. The GEM was used to obtain data on spatial variability of sea ice thickness in the deployment area. The GEM was mounted on sledge, pulled by the operator.

Snow thickness was measured by using the MagnaProbe instrument. It provides accurate point measurements. In these surveys, we conducted snow measurements with 10 meters spacing. *In-situ* measurements were complemented with ship radar images, panorama photos from the ship, field photos and satellite images.

All the deployment sites were located on the remnant ice floes which were easily detectable from the satellite images. The floes were surrounded by the brashed ice. According to the WMO sea ice terminology, the MOSAiC floes were initially classified as a remnant ice but can be called now as second year ice floes since they have survived until 1 January 2020.

Floes composed both level and deformed ice. The area of the measurements were restricted to the safety zone determined by polar bear guards,w around 300-500 meters distance from the *Akademik Fedorov*. The measurements cover both level and deformed ice areas, but the safety zone was not extended to the most ridged areas of the floes.

The modal sea ice thickness, which indicate thickness of level ice, was 0.3 – 0.4 meters. Mean thickness of the floes was 0.8 – 1.7 meters (Tab. 2.1.2). However, highest mean thickness was obtained at the M4 where measurements were mainly conducted over thick deformed ice. Due to the early season, mean snow thickness over the ice was only 10 cm on the average.

Tab. 2.1.1: Sea ice measurements at the L and M sites

	L1	L2	L3	M4	M7
Start date	5 Oct 2019	6 Oct 2019	9 Oct 2019	8 Oct 2019	11 Oct 2019
End date	5 Oct 2019	7 Oct 2019	10 Oct 2019	8 Oct 2019	11 Oct 2019
Number of drillings	13	15	12	9	-

Tab. 2.1.2: Sea ice characteristics of the floes

	L1	L2	L3	M4	M7
Ice type	remnant ice	remnant ice	remnant ice	remnant ice	remnant ice
Mean ice thickness (GEM)	1.1	0.8	1.4	1.7	1.3
Modal ice thickness (GEM)	0.4	0.4	0.3	NaN	0.3
Mean lev. ice thick. (drill.)	0.36	0.34	0.35	0.31	-
Min. lev. ice thick. (drill.)	0.23	0.25	0.28	0.27	-
Mean snow thickness	0.1	0.1	0.1	0.1	0.1
Mean level ice freeboard	0.017	0.027	0.027	0.03	-

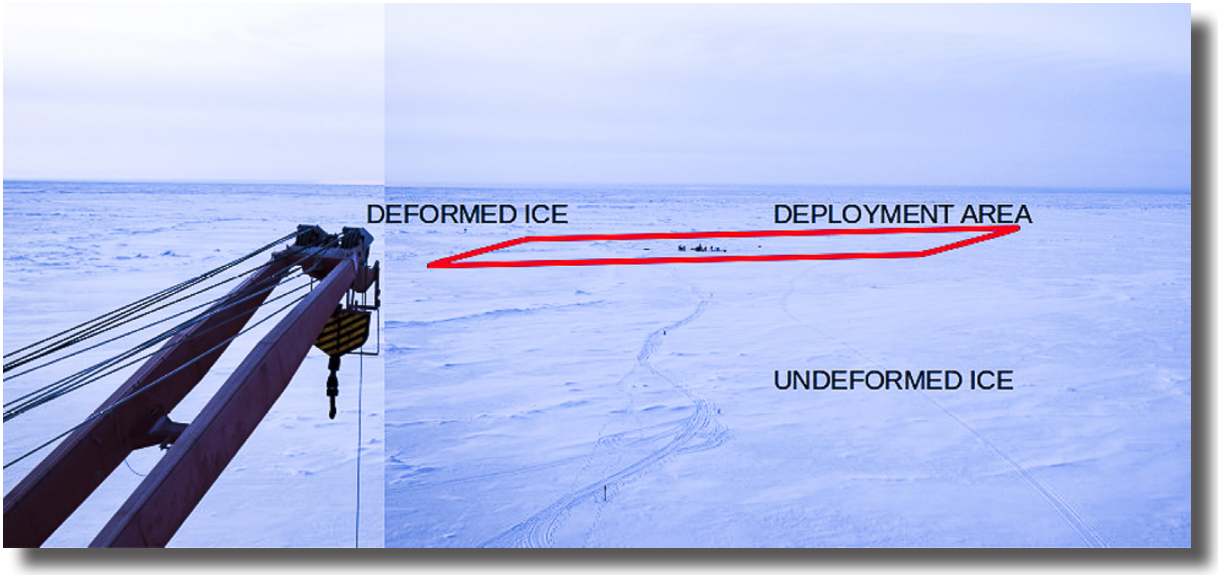

Fig. 2.1.1: Panorama of site L1 on October 5. The deployment area is highlighted by red lines.

Preliminary results

Site L1, 5 October 2019 (Fig. 2.1.1 - 2.1.5)

The L1 was established to a relatively round ice floe of 2 km x 2.5 km size. It was composed of both undeformed and deformed ice. The deployment area was around 500 meters from floe edge and in the boundary of undeformed and deformed ice. An atmospheric flux station, an

Autonomous Ocean Flux Buoys, an Ice Tethered Platform, two sea ice mass balance buoys, a bio-optical buoy and a snow buoy were installed in that location.

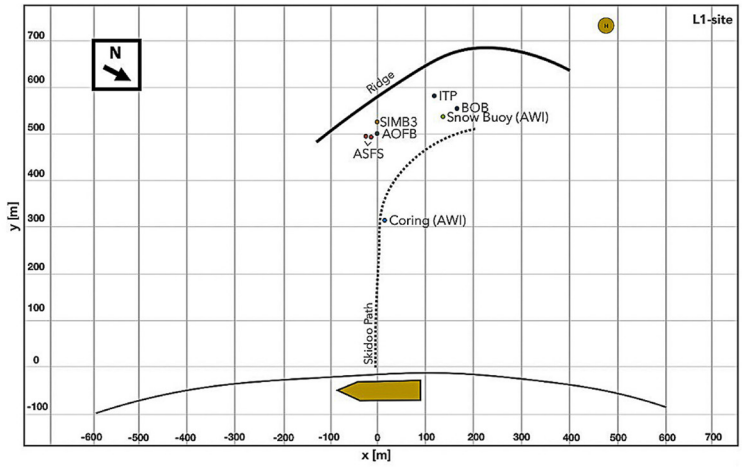

Fig. 2.1.2: Schematic map of the deployment at the L1. 'H' denotes the location of the helipad.

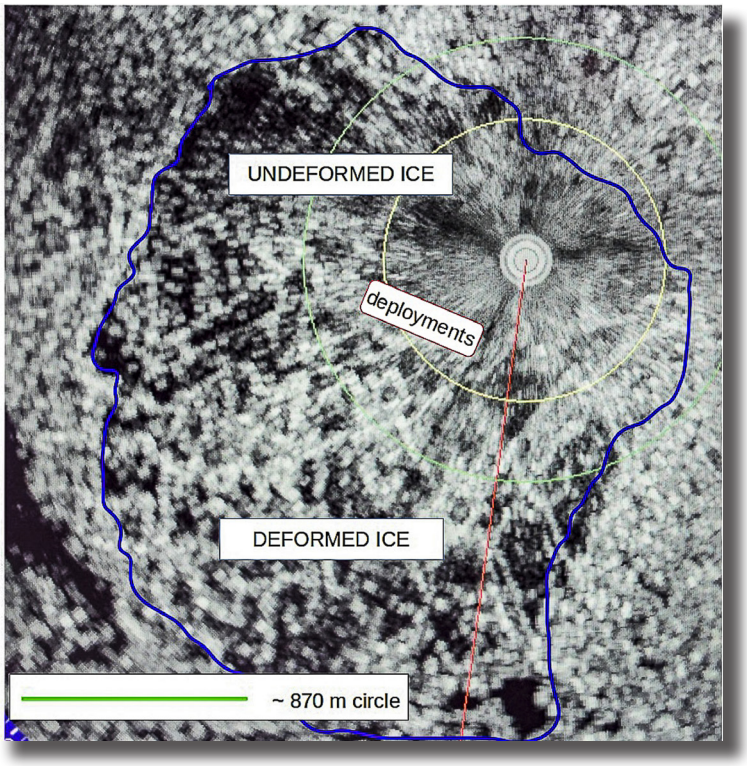

Fig. 2.1.3: Ship radar image at the L1 site

The mean ice thickness of the deployment area was 1.1 m (Tab. 2.1.2) with a relatively uniform central part between 0.6 and 1.2 m thick ice while some thicker parts can be found on the ridged area south of the stations with a maximum ice thickness of 3.0 m. The mean snow thickness is 0.1 m and is rather uniform. Only some spots around the ridges exceed a snow thickness of 0.2 m. According to drilling data, mean thickness of the undeformed ice was 0.36 m. Minimum and maximum thicknesses were 0.23 m and 0.57 m, respectively.

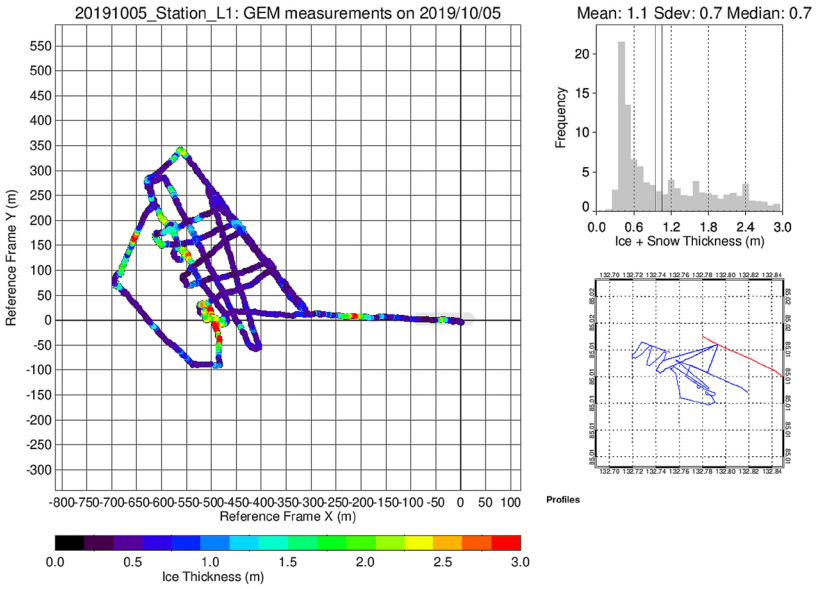

Fig. 2.1.4: Spatial variability of sea ice thickness and its frequency distribution at the floe L1

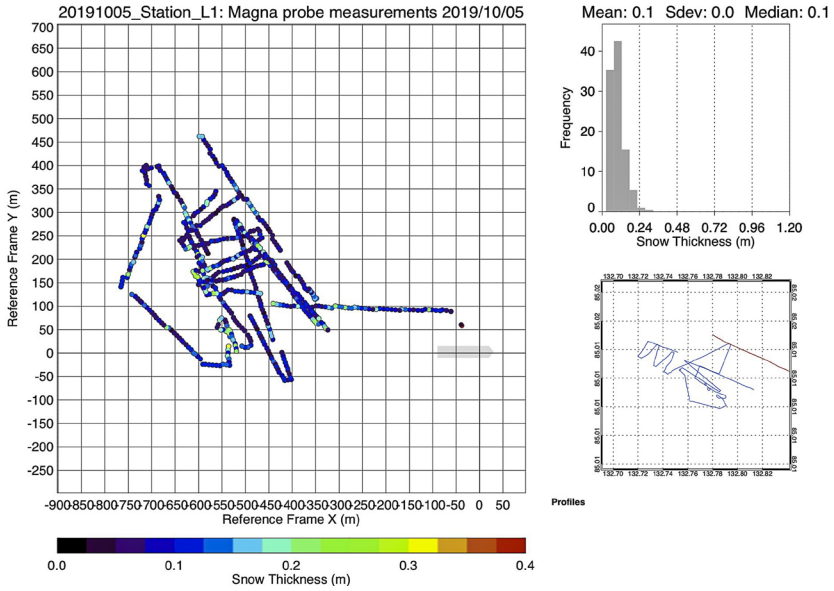

Fig. 2.1.5: Spatial variability of snow thickness and it's frequency distribution at the floe L1

However, there might be some errors in the GEM data measurements as it is a very sensitive object which may has been carried too close to metal objects during the survey. Near the deployed instruments, the GEM indicates rather thick ice. That can be due to impact of tripods on measurements. Another suspicious spot is at (-200,0). That might be due to a skidoo passing too closely to GEM device.

Site L2, 6 - 7 October 2019 (Fig. 2.1.6 - 2.1.10)

The L2 was established on a large remnant ice floe. Sea ice and snow surveys were conducted in two consecutive days. An atmospheric flux station, an Autonomous Ocean Flux Buoy, an Ice Tethered Platform, two sea ice mass balance buoys, a bio-optical buoy and a snow buoy were deployed on the floe.

Based on drilling measurements, level ice thickness varied between 0.28 m. to 0.48 meters. The mean, 0.35 m, compared well with the modal thickness of the GEM measurements (0.4 m). Mean ice thickness of the survey area was 0.7 m. Since the modal thicknesses of the L1 and L2 are practically but mean thickness of the L2 is considerably lower than in the L1, it indicates that the survey area of the L2 composes less deformed ice.

In the deployment area sea ice thickness varies from 0.4 m to 1.0 meters. This rather undeformed area is surrounded by deformed ice where thickness was from 1.5 to 3.0 m. Edges of the survey area mark also a boundary to a more deformed parts of the floe. Another ridge could be observed stretching parallel along the ship. It has not been measured but can be seen in the photos. That makes the whole deployment area surrounded by thick deformed ice.

The mean snow thickness was 0.1 m with a maximum of 0.23 m. These values correspond with those of the snow thickness measurements at the L1.

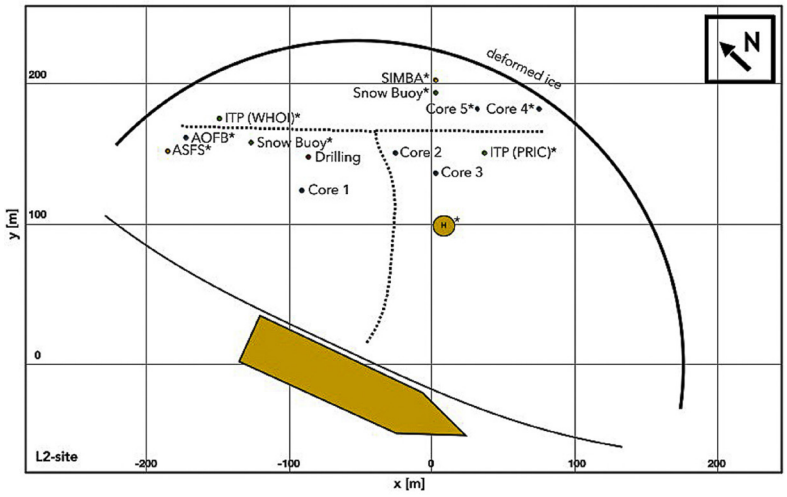

Fig. 2.1.6: Schematic map of the deployment at the L2. Stars indicate instruments for which the exact location were not established. 'H' denotes the location of the helipad.

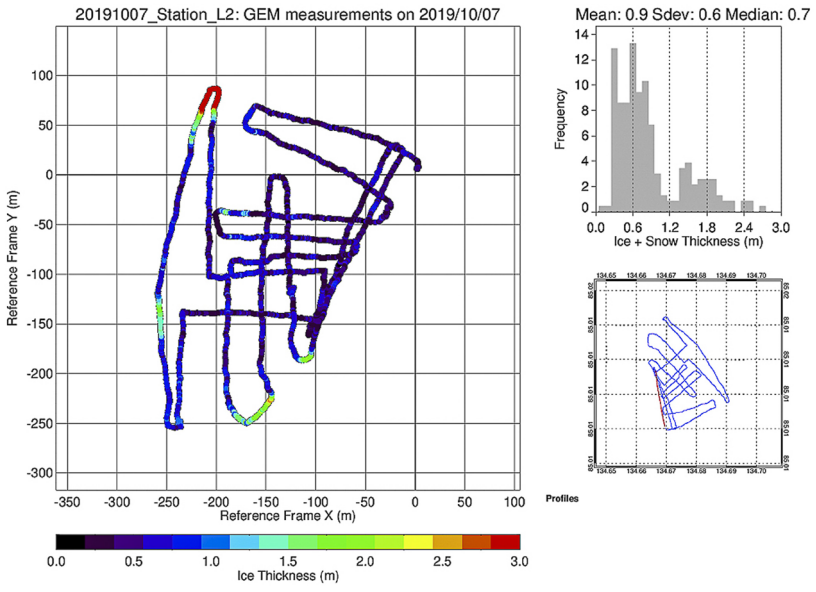

Fig. 2.1.7: Spatial variability of sea ice thickness and its frequency distribution as measured by the GEM at the floe L2 on 6 October 2019

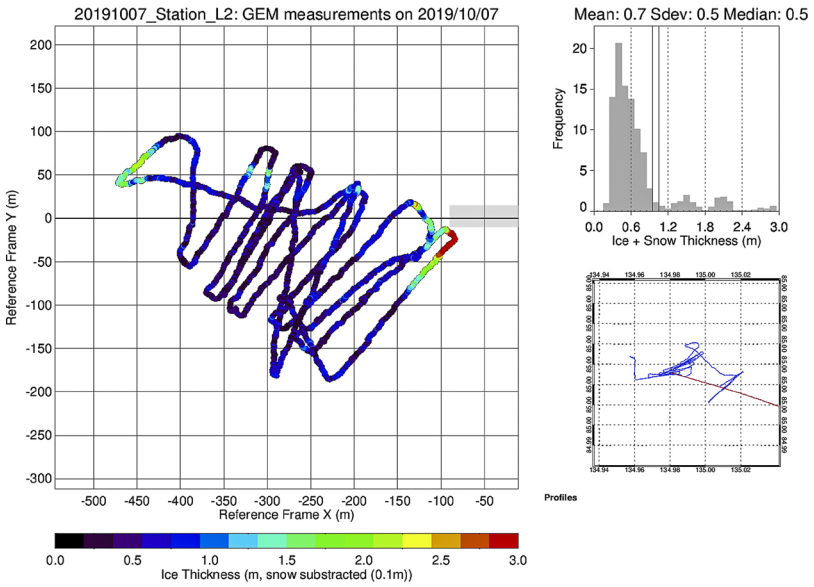

Fig. 2.1.8: Spatial variability of sea ice thickness and its frequency distribution as measured by the GEM at the floe L2 on 7 October 2019

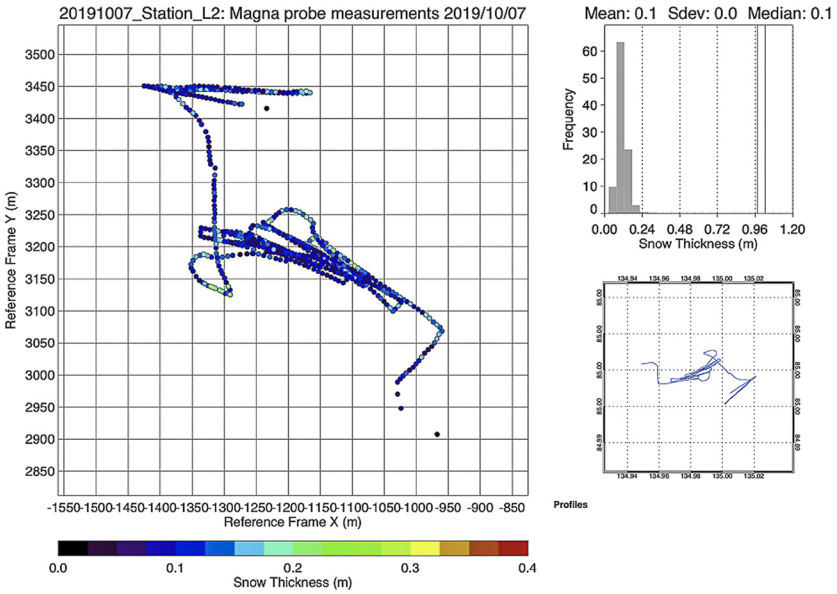

Fig. 2.1.9: Spatial variability of snow thickness and its frequency distribution as measured by the Magna probe at the floe L2 on 6 October 2019

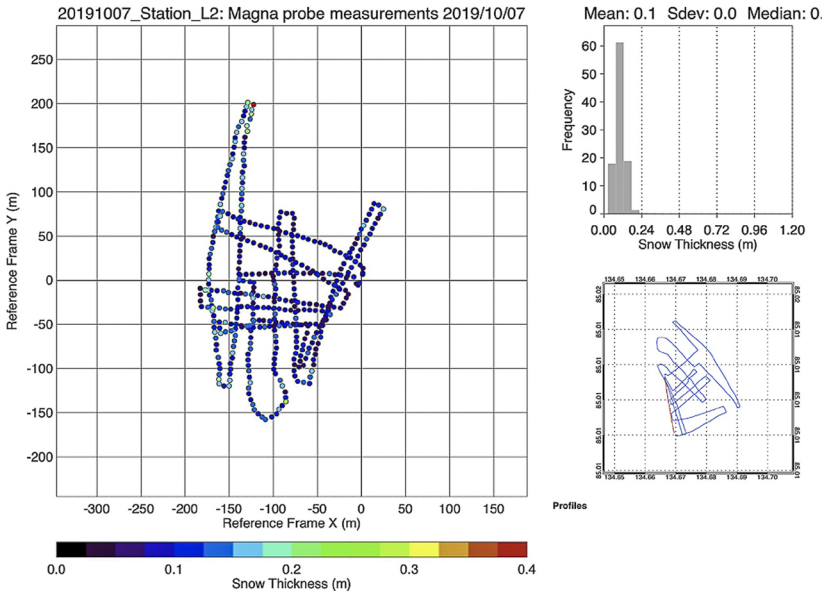

Fig. 2.1.10: Spatial variability of snow thickness and its frequency distribution as measured by the Magna probe at the floe L2 on 7 October 2019

Site L3 9 - 10 October 2019 (Fig. 2.1.11 - 2.1.12)

L3 was the third large floe on which instruments were deployed for the MOSAiC expedition distributed network. This floe was a medium size remnant floe surrounded mainly by a thin new ice. A 300 wide lead was detected at the opposite site of the landing area. The surveyed area covered level ice region where the buoys were deployed as well as the surrounded deformed ice part of the floe. An atmospheric flux station, an Autonomous Ocean Flux Buoys, an Ice Tethered Platform, two sea ice mass balance buoys, a bio-optical buoy and a snow buoy were installed on this site.

Ridges of up to 1.5 m were present near edge of the floe, one ridge was present crossing the floe ~1 m high. The thin, level ice had thin snow cover with a distinct wind slab and small (cm) wind-formed features semi-regularly spaced.

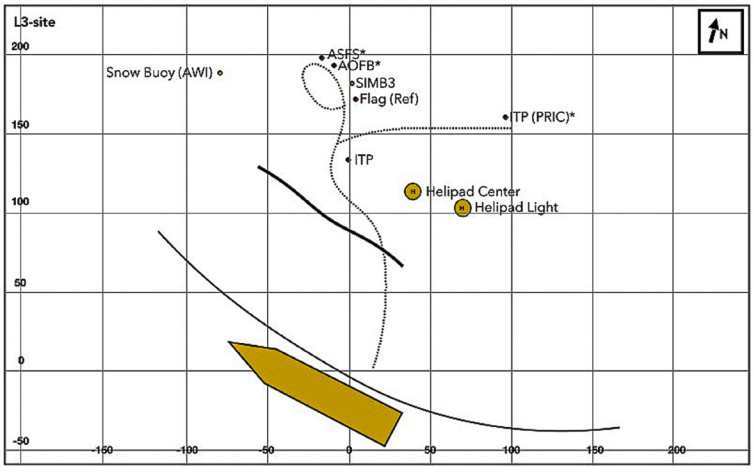

Fig. 2.1.11: Schematic map of the deployment at the L3. Stars indicate instruments for which the exact location were not established. 'H' denote the location of the helipad.

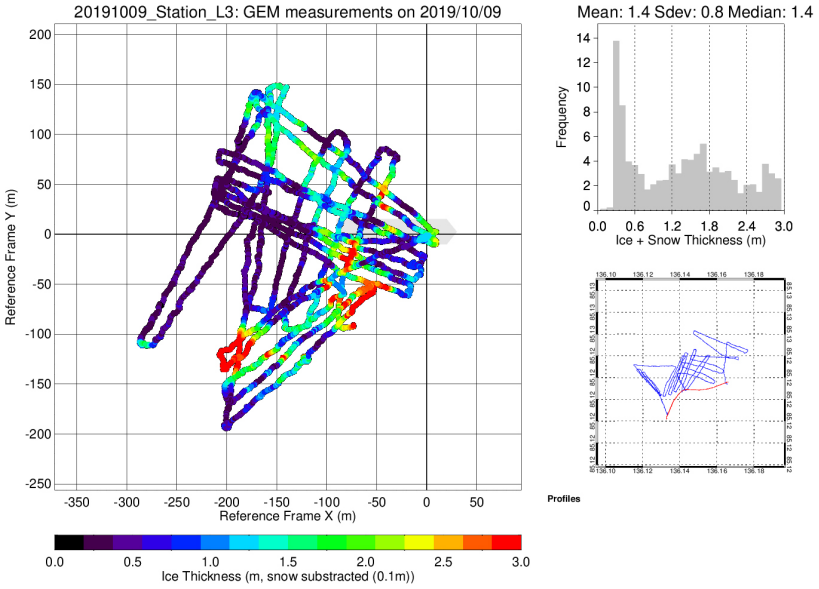

Fig. 2.1.12: Spatial variability of ice thickness and its frequency distribution as measured by the GEM at the floe L3 on 10 October 2019

Site M4 8 October 2019 (Fig. 2.1.13 - 2.1.14)

The M4 ice floe was rather small with less than 500 m^2 in size and an undefined shape. The ice floe survey had to interrupted due to a formation of a crack in the vicinity of measurement area. Consequently, observations covered only a fraction of the deployment area and cannot be regarded to represent ice thickness of the entire floe. Due to the cracking, ice coring wasn't conducted. The deployed network for the M-sites differs very much from the L-sites. On M4 a snow buoy, a SIMBA and a SAT have been deployed.

According to drilling measurements, level ice thickness was 0.27 – 0.35 m. The GEM surveys covered mainly thick ridged ice area where the deployments were made. There ice thickness was considerably larger, in many location larger than 2 meters. Mean thickness of this short survey was 1.7 m. The core of the ridge where ice thickness exceeded 3 meters was located at the center of the survey area. The snow thickness shows no significant differences to the L-site floes as the mean is also 0.1 m with a maximum of 0.27 m.

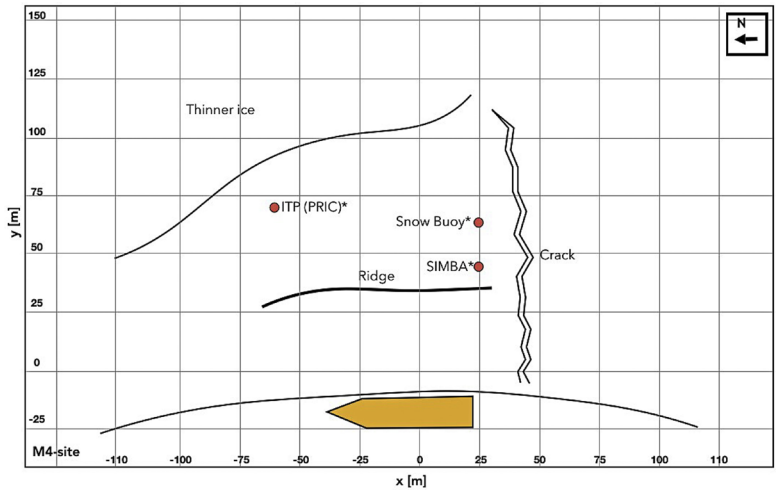

Fig. 2.1.13: Schematic map of the deployment at the M4. Stars indicate instruments for which the exact location were not established

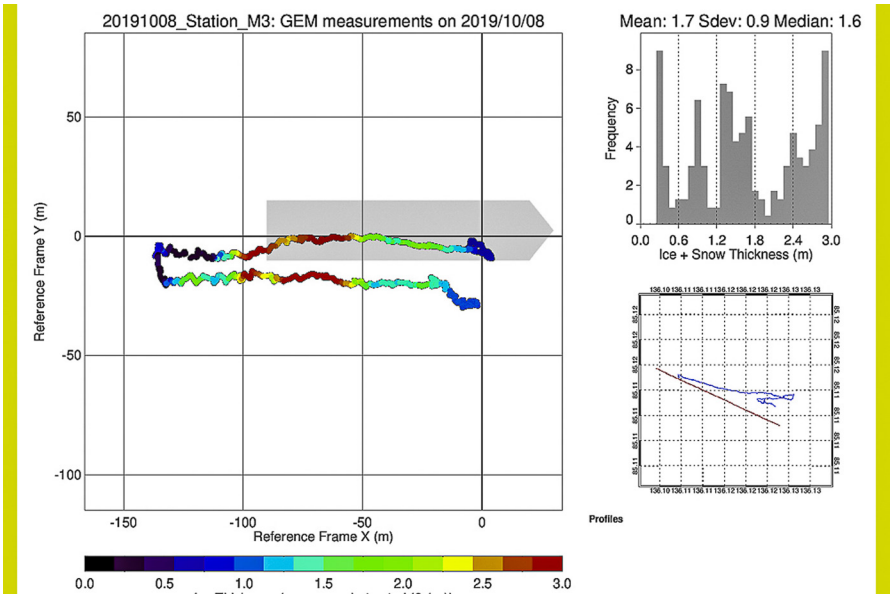

Fig. 2.1.14: Spatial variability of sea ice thickness and it's frequency distribution at the floe M4

Site M7 11 October 2019 (Fig. 2.1.15 - 2.1.17)

This floe was a small and an undefined shaped floe of remnant ice. The survey area included level ice area where the deployments took place and heavily deformed area close to the right edge of the deployment area. Ice coring was not conducted in this floe.

The modal GEM derived ice thickness was 0.3 m, but since the measurements included large fraction of the deformed ice, the mean ice thickness of the study area was 1.3 m. In the level ice areas, ice thickness varies from 0.3 to 0.5 meters, in the ridged areas ice thickness was 2 – 3 meters.

As in the previous measurement sites, the mean snow thickness was 0.1 meters but on the ridges snow thickness increased up to 0.24 meters.

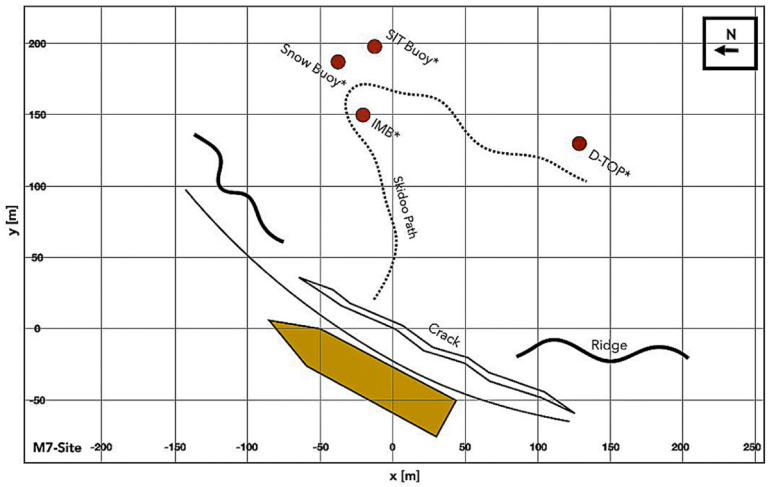

Fig. 2.1.15: Schematic map of the deployment at the M4

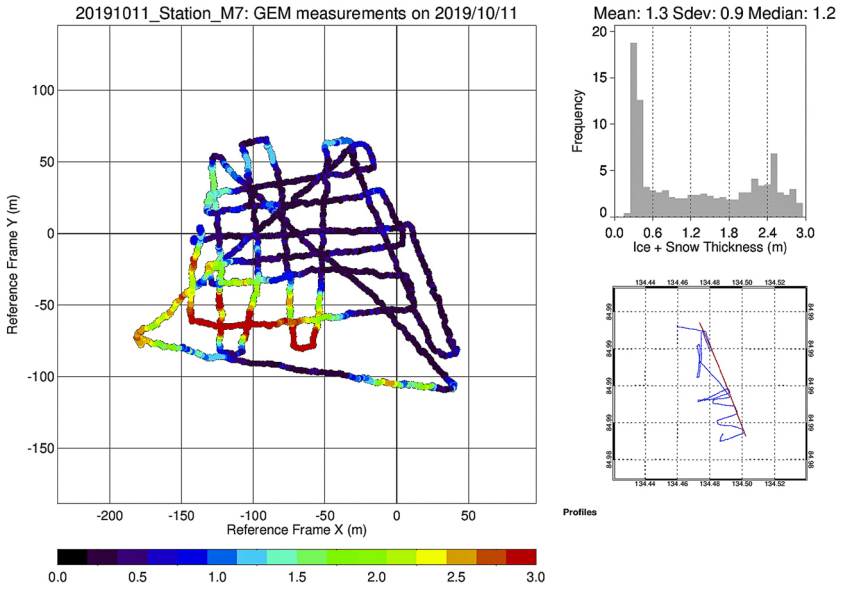

Fig. 2.1.16: Spatial variability of sea ice thickness and it's frequency distribution at the floe M7.

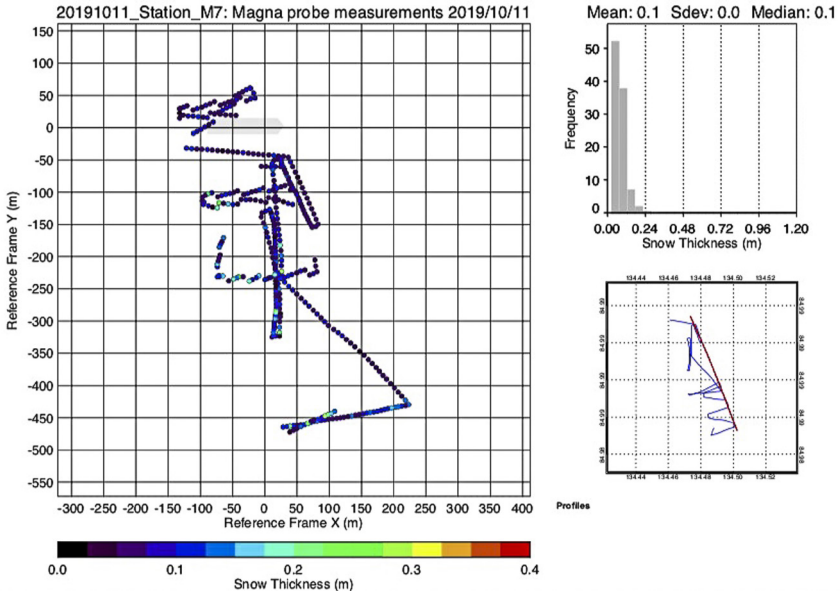

Fig. 2.1.17: Spatial variability of snow thickness and its frequency distribution as measured by the Magna probe at the floe M7 on 11 October 2019

Data management

Data will be stored at the PANGAEA data repository (World Data Center PANGAEA Data Publisher for Earth & Environmental Science (www.pangaea.de). All data are handled, documented, archived and published following the MOSAiC data policy.

2.2. Deployment of the automated surface flux stations at the MOSAiC distributed network L-sites

Christopher Cox[3], Ola Persson[1,2,3], Dave Costa[1,2,3], Anne Gold[1,2], Sean Horvath[2,4], Neil Aellen[5], Katie Gavenus[6,7], Mauro Hermann[5], Tatiana Mateeva[8], Alex Mavrovic[9], Julika Zinke[10]
not on board: Matthew Shupe[1,2,3], Thomas Ayers[3], Michael Gallagher[1,2,3], Jesse Leach[3], Sara Morris[3], Jackson Osborn[1,2,3], Sergio Pezoa[3], Taneil Uttal[3]

[1]CIRES
[2]U Colorado
[3]NOAA
[4]NSIDC
[5]ETH
[6]CACS
[7]PolarTREC
[8]LMSU
[9]UTR
[10]Stockholm University

Grant-No. AF-MOSAiC-1_00
NSF Award #OPP1724551

Objectives

As the Arctic becomes increasingly dominated by seasonal ice coverage, it is correspondingly incumbent upon the scientific community to collect the observations needed to develop forecast and climate modeling capabilities that realistically represent the dynamic and thermodynamic physics in the changing system. The experimental design of MOSAiC targets this problem and the Distributed Network (DN) component of MOSAiC provides the spatially-resolved observations needed to link the dynamic and thermodynamic drivers. The Automated Surface Flux Stations (ASFS) contribute to the DN by making continuous, high temporal resolution surface property and atmospheric boundary layer measurements for the purposes of enhancing process-oriented understanding of the exchanges of energy that modulate the sea ice mass balance in the central Arctic Ocean. ASFS measures variables relevant to both thermodynamic processes (e.g., radiative, sensible and latent turbulent fluxes, snow surface conductive fluxes and meteorology) and ice dynamical processes (e.g., positioning, surface stress, and winds). The observations complement similar measurements being made at the central MOSAiC observatory, as well as analogous observations made within the ice and ocean columns by collaborating DN buoy programs. Collectively, these observations support a full accounting of the vertical fluxes of energy and momentum across the coupled atmosphere-ice-ocean system.

Work at sea

ASFS were deployed at each of the three L-sites, positioned nearby the Autonomous Ocean Flux Buoy (AOFB) on the floe-edge side of the L-site. For each installation, the ASFS frame was anchored to the ice and positioned on top of a ~1.2 m x 2.4 m section of white-painted plywood (for ablation control) and grounded to salt water. Mounted to the frame is a vertical mast and a horizontal boom to which instruments are attached. The boom protrudes approximately 3 meters from the main frame over undisturbed snow and the vertical mast elevates measurements related to turbulence to between 3 and 3.5 m height. Details of the on-board scientific instrumentation can be found in Table 2.1. A localized (4 m x 10 m) snow survey was conducted to initialize the snow depth measurements. Conductive flux plates were buried beneath the boom to either side of the centerline at 3 cm depth, 4-5 m from the frame. Additionally, a limited set of collocated broadband radiometric measurements (~3 hours) were made using an experimental Mobile Atmospheric Radiation Comparison (MARC) station that is intended for use as a baseline for transferring radiometric inter-comparison data across the MOSAiC array. Images of the stations and surrounding areas shortly after deployment are shown in Fig. 2.1.

- The first station (named “ASFS 40”) was installed at the L1 site on 5 October 2019 (UTC) on ~1.7 m thick ice, composed of rafted ice layers, with salt water observed at a depth of 40-50 cm. The local snow depth was an average of 9.1 cm.
- The second station (“ASFS 30”) was installed at the L2 site on 7 October 2019 (UTC) approximately 60 m from the floe edge on a small meltpond, frozen-over but not melted-through, and composed of an 8.3 cm layer of snow, and a vertical ice profile of ~30 cm of ice, ~30 cm of water and an additional ~40 cm of ice.
- The third station (“ASFS 50”) was installed at the L3 site on 9-10 October 2019 (UTC) on a flat pan composed of ~30 cm of ice, ~200 m from the floe edge. The local snow depth was an average of 6.5 cm.

The ASFS consists of a Direct Methanol Fuel Cell (DFMC), which generates the 65-70 W of power used to operate the instrumentation; collect, record and transmit data; and to provide the heating and ventilation necessary to mitigate the formation of ice on sensors. When distance and transfer rate requirements of the radio connections permit, data is collected remotely from a base station at *Polarstern* via 2400 MHz radio. When separation between *Polarstern* and an L-site is beyond the range of the radio, the system provides limited status and scientific information by Iridium. Data is also stored locally on both an internal hard drive and removable microSD card for manual retrieval. Approximately 140 Mb of data (camera images excluded) are generated each day. Raw 20 Hz data for eddy covariance calculations are archived and account for approximately 98 % of the data volume. Generally, visits to retrieve data, refuel and perform routine maintenance are planned once per month, but the station can operate autonomously for 2-3 months.

Data (1 min averages and 5 second samples) were being retrieved at *Polarstern* in near real time from L1 and L2 (~12 km from *Polarstern*) shortly following installation in October 2019. L3 (~23 km from *Polarstern*) was deployed on a floe that was out of range for the radios at *Polarstern* and therefore only limited amounts of data became immediately available. During installation, the frame was leveled to within 1.5º, as recorded by an inclinometer integrated into the sonic anemometer. The level of the radiometer assembly was further refined to within several tenths of a degree of level on an independent leveling platform, using the upward facing pyranometer as a guide. Settling of the frame over the next 7-10 days at L1 and L2 changed the level by less than 0.2º.

Preliminary (expected) results

The principle questions that will be addressed by using ASFS data in conjunction with collocated measurements supported by collaborators and complementary data at the main observatory are as follows:

- How do sea-ice energy and momentum budget terms covary across the MOSAiC domain as functions of space (20-40 km), time and ice-type?
- What are the relative contributions of thermodynamic and dynamic drivers of energy transfer across the atmospheric-ice-ocean system?
- What are the biases in thermodynamic and dynamic processes as a function of forecast time in numerical weather prediction models?

To illustrate atmosphere-ice-ocean coupling, Fig. 2.2.1 shows an example time series of a sampling of data streams collected from the L1, L2 and L3 ASFS during the DN deployment period. The figure shows periods of increased horizontal wind speed (Fig. 2.2.2a) corresponding to enhanced mixing in the atmospheric boundary layer (Fig. 2.2.2b), occurring during periods of increased LWD (largely due to cloud cover, Fig. 2.2.2c) and associated warmth (Fig. 2.2.2d), as well as the response in the ice of damped conduction of oceanic heat toward the snow surface (Fig. 2.2.2e).

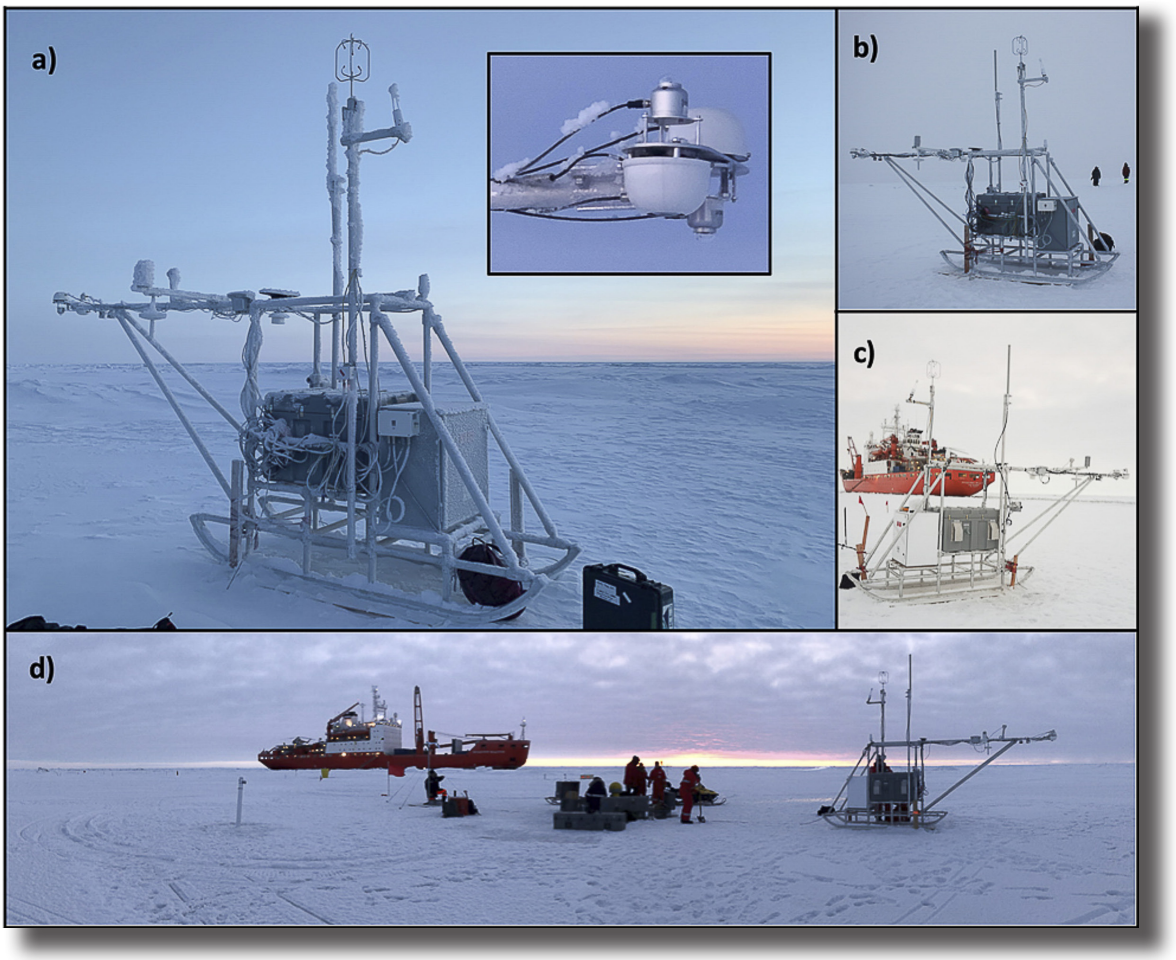

Fig. 2.2.1: (a) ASFS at L1 on October 15, 10 days in after installation, showing heavy frost and rime development on the frame and highlighting successful ice mitigation on sonic anemometer (photo A. Gold) and radiometer assembly (inset, photo C. Cox). (b) ASFS at L1 during installation, October 5 (photo O. Persson). (c) ASFS at L2 during installation, October 7 (photo A. Gold). (d) ASFS at L3 during installation showing also deployment site of nearby AOFB at the red flag at photo center (photo C. Cox).

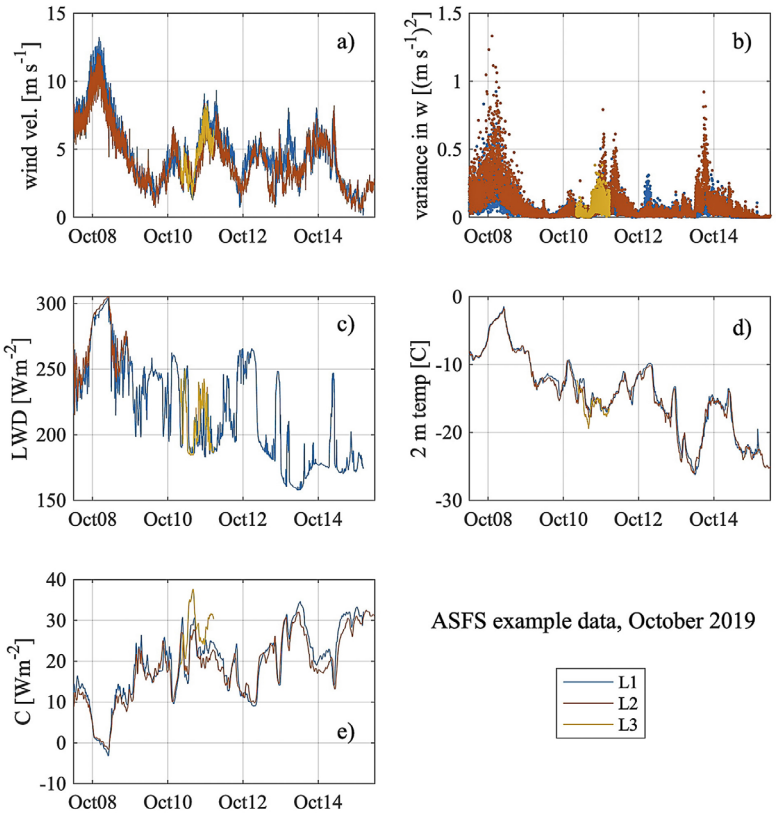

Fig. 2.2.2: Sample of data (1 min avg) collected from ASFS at L1 (blue), L2 (red) and L3 (yellow) between 12 UTC on 7 October 2019 and 12 UTC on 15 October 2019. (a) Wind velocity at ~3.5 m; (b) 1 min variance in the vertical wind component [w], a proxy for the relative amount of atmospheric mixing at measurement height; (c) downwelling longwave radiation [LWD]; (d) air temperature at 2 m height; and (e) conductive flux [C] at 3 cm depth where positive values are defined as warming the surface.

Tab. 2.2.1: List of instrumentation installed on ASFS

Instrument	Variable	Location	Collection Interval
Hukseflux IR20 pyrgeometer	downwelling logwave radiation	boom, 2 m height	1 min avg
Hukseflux IR20 pyrgeometer	upwelling longave radiation	boom, 2 m height	1 min avg
Hukseflux SR30 pyranometer	downwelling shortwave radiation	boom, 2 m height	1 min avg
Hukseflux SR30 pyranometer	upwelling shortwave radiation	boom, 2 m height	1 min avg
Metek uSonic-3 sonic anemometer	3-d (u,v,w) wind	mast, 3.5 m height	20 Hz, 1 min avg
Licor 7500DS open-path gas analyzer	H2O/CO2 gas concentration	mast, 3 m height	20 Hz, 1 min avg
Apogee SI-411 infrared thermometer	8-14 µm surface brightness temp	boom, 2 m height	1 min avg
Campbell SR50A acoustic ranger	surface height (snow depth)	boom, 2 m height	1 min avg
Vaisala PTU300 meteorology	temperature, pressure, relative humidity	boom, 2 m height	5 sec, 1 min avg
Hemisphere v102 GPS	position, heading, altitude	boom, 2 m height	5 sec, 1 min avg
Hukseflux HFP01 flux plate	conductive flux at 5 cm depth (2 places)	surface, 3 cm depth	1 min avg
Webcam	hemispheric images (2 views)	boom, frame	30 min

Data management

Data from the ASFS will be accessible from PANGAEA data repository (World Data Center PANGAEA Data Publisher for Earth & Environmental Science (www.pangaea.de) and archived at the Arctic Data Center (arcticdata.io), which is supported by the National Science Foundation (NSF) and DOIs provided to PANGAEA according to the agreement between Arctic Data Centre and PANGAEA. The data will be provided in netCDF format and archived within 6 months of the completion of the MOSAiC field campaign. All data are handled, documented, archived and published following the MOSAiC data policy.

2.3 Ice Tethered Profiler

Chris Basque[1], Andrew Davies[1], Sam Cornish[2,6], Francesca Dogliono[3,6], Rosalie McKay[4,6], Pierre Priou[5,6]
not on board: John Toole[1], Richard Krishfield[1], Jeff O'Brien[1], Silvia Cole[1], Ben Rabe[3], Mario Hoppmann[3]

[1]WHOI
[2]U Oxford
[3]AWI
[4]NTNU
[5]MUN
[6]MOSAiC School

Grant-No. AF-MOSAiC-1_00
NSF PLR-1303644 & ONR N000141612381

Objectives

The Ice-Tethered Profiler (ITP) system is designed to obtain automated near real-time measurements of salinity and temperature relative to depth in the upper ocean layer down to 750 m multiple times per day. More information on the ITP technology and ITP project are given in Krishfield et al. (2008) and Toole et al. (2011). All three of the profilers deployed during the cruise are equipped with Sea-Bird CTD sensor packages, while one was also equipped with a MAVS current meter and another with a Bio-optical package (PAR, Fluorometer and DO). Each of the profilers was programmed specifically to ensure optimal data retrieval for the ITP system while also recording its GPS position (and engineering data) throughout the day to track movement of the ice that supports it. The systems autonomously profile the upper ocean as the sea ice drifts, allowing hydrographic measurements to be acquired in remote locations in all seasons. All data is transmitted and made available in near real time at www.whoi.edu/itp.

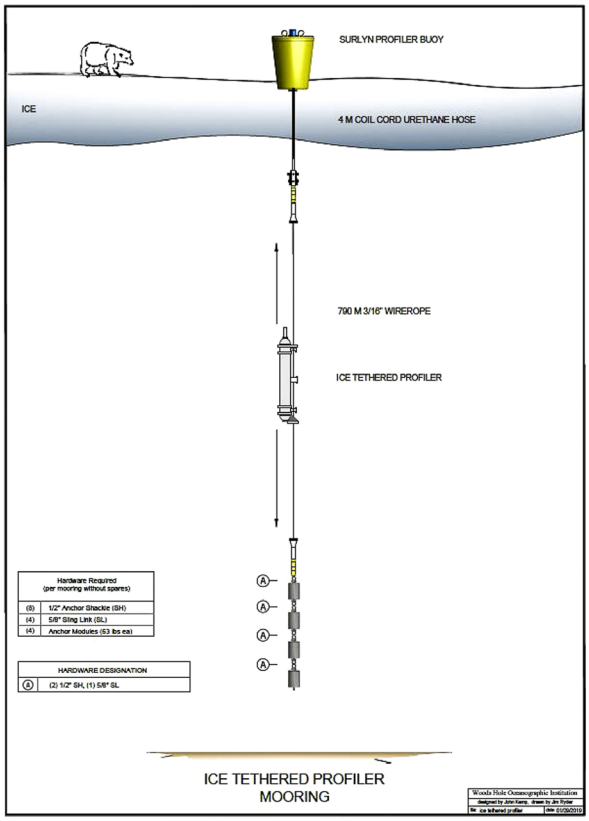

Fig. 2.3.1: Mooring Drawing of an ITP

The ITP (Fig. 2.3.1) is one of the many instruments deployed as a part of the MOSAiC Expedition Distributed Network. One was deployed at each L-site alongside other systems such as an AOFB, Seasonal IMBs, and a MET Station to return a complementary set of data above, within, and below the ice.

Work at sea

At each L-site, one ITP was deployed at a distance determined to minimize the possibility of entanglement with the other tethered mooring systems (Tab. 2.3.1). During transit of the ship to the ice pack (and outside the limit of the Russian EEZ), the surface packages to the ITPs were powered on and placed outside on deck to verify that their Iridium communication and GPS performed correctly. Bench testing was conducted on the three ITP profilers to confirm

that no damage occurred during shipping and that they would operate properly once deployed. Once the date was confirmed for each deployment, the start times for the instruments were entered and preparations began preparing the required deployment apparatus for the field operations.

At each L-site, drilling gear (10.5” gas powered and 14” and 24” hydraulic augers) was offloaded first, either the day before, or early on the deployment day to allow our team to drill the necessary amount of holes for the ITPs and other buoy systems. Next the equipment to deploy the system was delivered, and finally the ITP profiler to keep it warm for as long as possible to ensure that it did not freeze before being deployed in the water. Deployment of each ITP took around 4 hours. This time varied with offloading time, transit for snowmobiles and when the holes were envisaged. A detailed description of the operations for deploying ITPs on ice is provided in WHOI Technical Report 2007-05 (Newhall et al., 2007; Figs. 2.3.2 and 2.3.3).

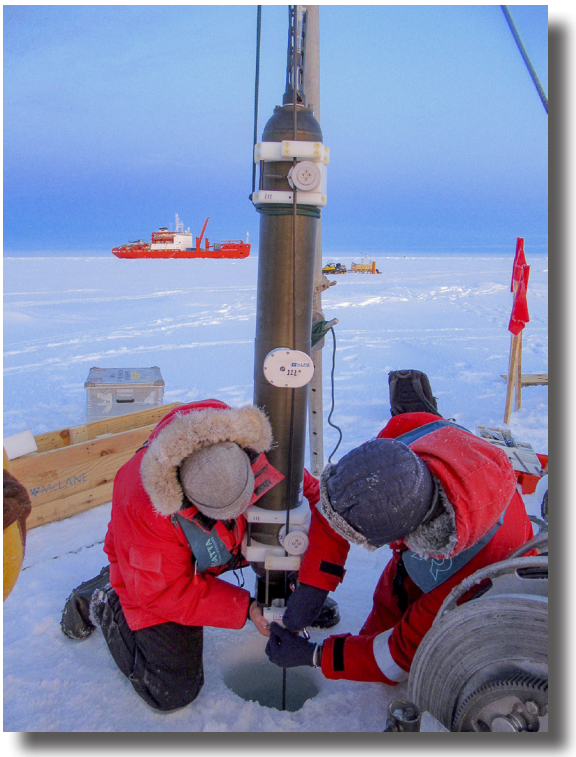

Fig. 2.3.2: Attaching profiler onto the jacketed wire prior to lowering the system through the ice hole (ITP 111 system).

Fig. 2.3.3: ITP 102 as deployed at the L3 site

Tab. 2.3.1: Basic ITP information at the three L sites

L-Site #	ITP #	Instruments Attached	Ice thickness
L 1	ITP 111	CTD	2.8 meters
L 2	ITP 94	CTD, Bio Package	0.9 meters
L 3	ITP 102	CTD, MAVS Current Meter	0.7 meters

Preliminary (expected) results

All three ITPs started their programmed profiles after they were deployed on schedule. All sent data to the ITP data server at WHOI and the graphs below show the first CTD profiles for each ITP (as of mid-October 2019, Figs. 2.3.4 - 2.3.6).

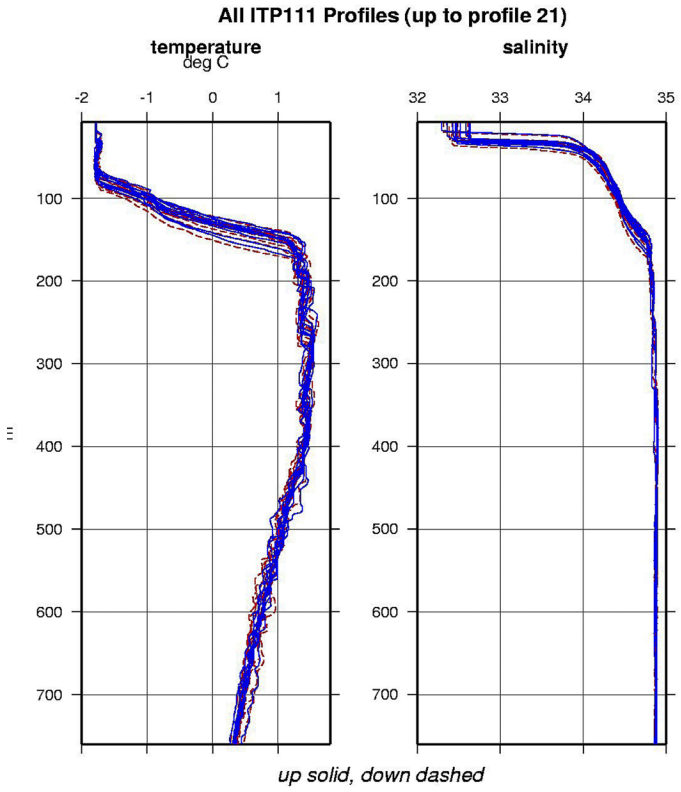

Fig. 2.3.4: CTD data from ITP 94 at the L2 site

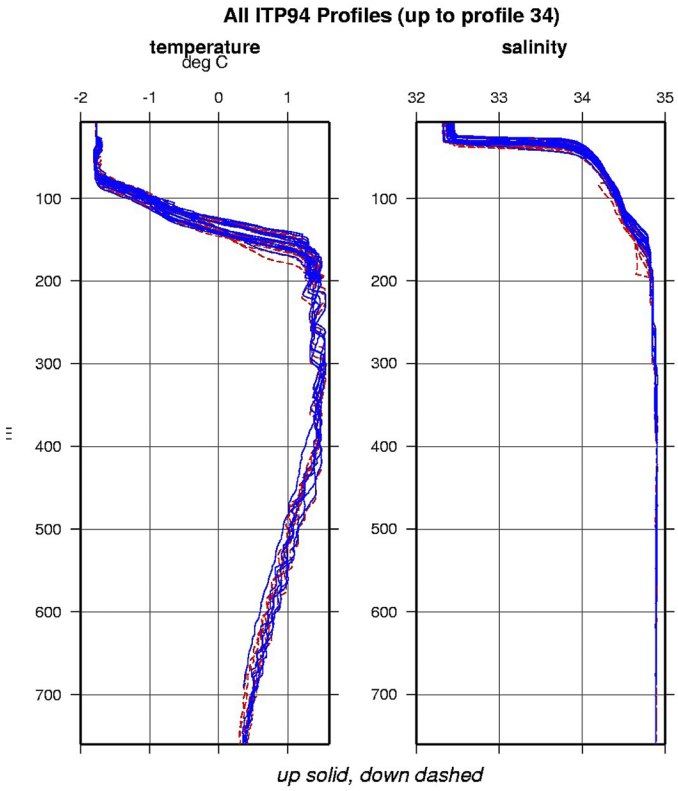

Fig. 2.3.5: CTD data from ITP 111 at the L1 site

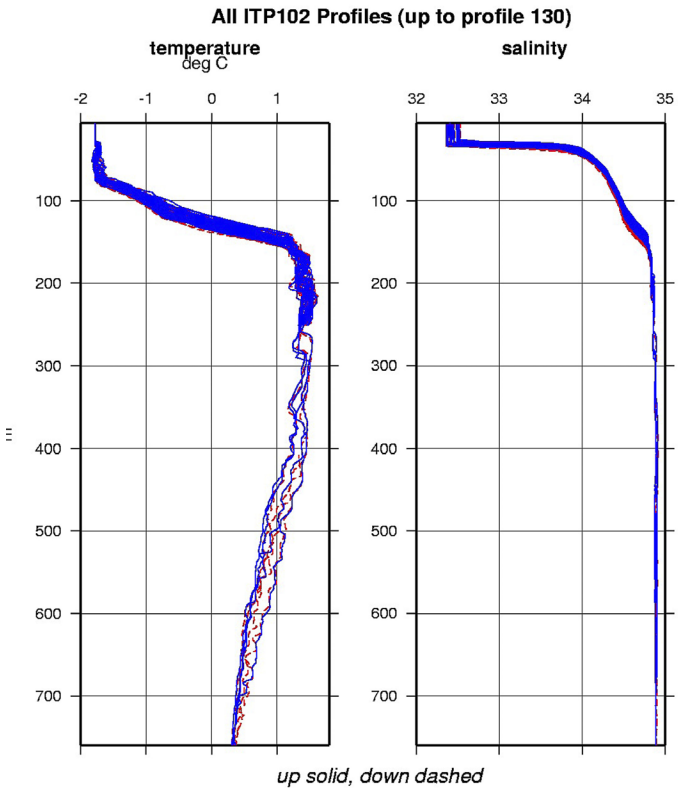

Fig. 2.3.6: CTD data from ITP 102 at L3 site

Data management

All data retrieved by the systems is sent to the Woods Hole Oceanographic Institution, where it is available to the public within hours of acquisition at the ITP website, www.whoi.edu/itp. Along with the three deployed on this trip, the data from all other ITPs can also be accessed.

Data will be stored at either at the PANGAEA data repository (World Data Center PANGAEA Data Publisher for Earth & Environmental Science www.pangaea.de or at the Arctic Data Center (arcticdata.io), which is supported by the National Science Foundation (NSF) and DOIs provided to PANGAEA according to the agreement between Arctic Data Centre and PANGAEA. All data are handled, documented, archived and published following the MOSAiC data policy.

References

Krishfield R, Toole JM, Proshutinsky A and Timmermans ML (2008) Automated Ice-Tethered Profilers for seawater observations under pack ice in all seasons. Journal of Atmospheric and Oceanic Technology, Vol. 25, doi:10.1175/2008JTECHO587.1.

Newhall K, Krishfield R, Peters D and Kemp J (2007) Deployment Operation Procedures for the WHOI Ice-Tethered Profiler. Technical Report of the Woods Hole Oceanographic Institution, WHOI-2007-05, 41 pp.

Toole JM, Krishfield R, Timmermans ML and Proshutinsky A (2011) The Ice-Tethered Profiler: Argo of the Arctic. *Oceanography,* 24 (3):126–135, http://dx.doi.org/10.5670/oceanog.2011.64.

2.4 Autonomous ocean flux buoys in the MOSAiC distributed network

Tim Stanton[1,2], William Shaw[2]

[1]MLML
[2]NPS

Grant-No.: AF-MOSAiC-1_00
NSF Award #1723400

Objectives

Sophisticated coupled regional ocean-ice-atmosphere models continue to under-predict late summer ice pack area and volume in the central Arctic. There is a clear need to identify small scale processes that are contributing to rapid melt-out of ice floes, particularly ones that have strong positive feedbacks in the coupled ocean-ice-atmosphere system. Manned observation systems at the central MOSAiC ice floe and autonomous systems deployed at ranges from 5 to 40 km within the MOSAiC Distributed Network have been designed to measure forcing and response of the coupled system. These observation systems have been designed to operate over a year-long period as the whole instrument network drifts out of the central Arctic as part of the Transpolar Drift.

Approach

The NPS contribution to the MOSAiC Network is four Autonomous Ocean Flux Buoys (AOFBs) developed in our Ocean Turbulence Group. The AOFB instrument system (Fig. 2.4.1) supports an integrated ocean flux package consisting of a very low noise 3D current sensor with co-located precision temperature and conductivity sensors, allowing direct, eddy correlation measurements of heat, salt and momentum fluxes. This flux sensor is attached to a 3 m long carriage device that permits the flux measurement depth to be remotely chosen, allowing, for example, late summer fresh layer fluxes to be captured. The carriage also supports upward and downwelling solar radiation sensors, Chlorophyll A, Dissolved Organic Matter, and turbidity sensors to better understand solar radiation absorption in the water column just below the ice. A typical two hour sample cycle starts with a 40 minute eddy correlation time series 3 m below the ice, followed by a 5 cm resolution upward profile of T, S, and optical properties, and in late summer, another 30 minute eddy correlation flux measurement 1 m below the ice. An Acoustic Doppler Current Profiler measures current profiles every 2 m to 80 m depth, well within the pycncoline, while an upward-looking acoustic altimeter measures local, basal ice melt/growth rates adjacent to the surface buoy.

The turbulent diffusivity of the placid, strongly stratified pycnocline is important to characterize in order to improve diffusivity parameterizations in numerical models and to quantify fluxes of heat trapped within the pycncocline (like the deep Atlantic warm layer) up to the ocean mixed layer where the heat can melt ice. The AOFB supports three, 2 m-high, pycnocline spars (Fig. 2.4.1b) at 50 m depth that continuously measure thermal diffusivity and heat fluxes. Each spar has eight 25 cm-spaced precision temperature sensors that measure the background thermal gradients and thermal finestructure, while a 200 Hz sampled micro-thermistor measures the thermal micro-gradients within the water column advecting past the spar frame allowing the thermal dissipation rate χ to be estimated. These two measurements allow the thermal turbulent diffusivity and heat flux to be measured within the strongly stratified pycnocline.

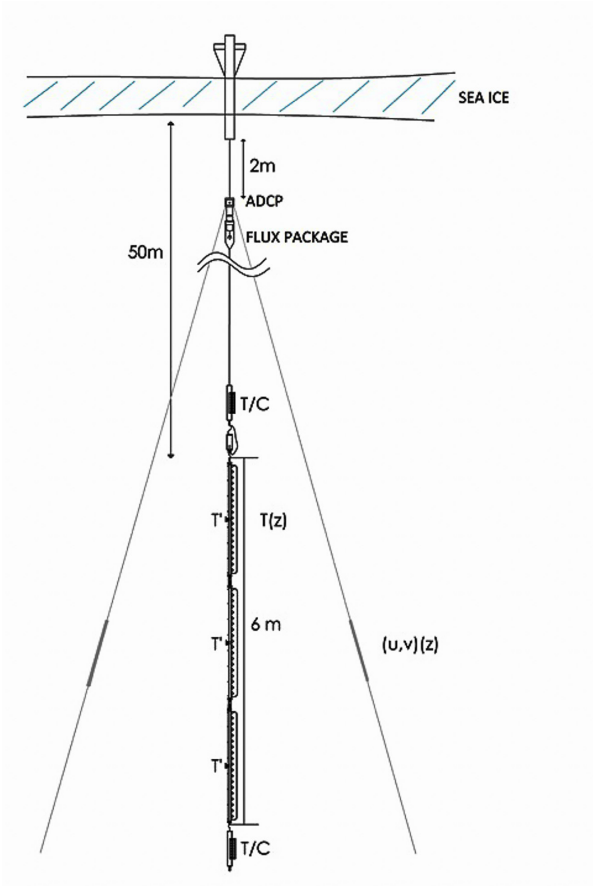

A B

Fig. 2.4.1: A) A schematic of the AOFB instrument system with a pycnocline spar deployed at 50 m. In the MOsAiC version, the eddy-correlation flux package is mounted on a 3 m long carriage allowing near surface T, S and optics profiles to be made, and flux measurement depths to be controlled. B) A detail of the 2 m long spar sections with the 8 temperature gradient sensors and fast microthermistor to resolve the thermal dissipation rate in the center.

Work at sea

The MLML/NPS contribution to the MOSAiC network is four AOFBs, with one at each of the three L sites, and one at 'MET City' on the central floe (Tab. 2.4.1).

During the transit to the deployment area, an intensive, carefully-coordinated plan was evolved to enable deployment of the many instruments in the three L, eight M and 40 P sites that comprise the Distributed Network, with very limited ship time available. After a suitable L site floe was identified, the *Academic Fedorov* nudged in by the floe, a safety survey was conducted, and the instrument sites staked. During this time a carefully ordered offload of equipment from the #3 forward hold to the ice was started, and people moved to the ice using the gangway to begin 4 – 6 independent, concurrent instrument installations. Where possible, the floe survey, site layout and ice hole drilling by the WHOI team began on the afternoon before the instrument deployment day, maximizing daylight time needed for the more complex MET, AOFB and ITP systems. While this operation was underway, helicopter flights to M and P sites began and ran while flying conditions permitted operations. The MOSAiC School students played an important role in each science activity as well as logistic support roles like freight

unloading, snowmobile driving and bear watch, significantly increasing their field experience in these tough Arctic conditions.

On October 5, 2019, at Site L1, AOFB 43 was deployed near the edge of a first-year ice floe, within 8 m of the MET tower. Significant ridging was present on the south and southeast of the MET/AOFB deployment area, leading to a wide range of ice thickness in the area. Chris Basque and Andy Davies (the WHOI ITP team) drilled a 24" hole for the deployment. AOFB 43 was deployed with a solar panel array and an Air-X wind generator atop an 8-ft tall pole for supplemental power. AOFB 43 did not include the pycnocline spar subsystem. For L1 the entire deployment operation was largely completed in a single day. Student assistants for this deployment included Natalia Ribeira Santos and Marylou Athanase. The ship stayed at the flow overnight, and we briefly returned to the site the next morning to complete the installation of the wind generator system. Total time for installation (excluding surveying and drilling) was about 7 hours.

On October 7, 2019, at Site L2, AOFB 44 was deployed near the edge of a first-year ice floe, within 8 m of the MET tower. On day 1 of the deployment, the installation sites were located and ice holes for all systems were drilled, including a 24" hole for AOFB 44 by the WHOI team. On day 2, a complete AOFB system (including pycnocline spars, solar array and wind generator) was deployed in about 8 hours. Student assistants for this deployment included Marylou Athanase and Robbie Mallett.

On October 10, 2019, at Site L3, AOFB 45 was deployed near the edge of a large, flat first-year ice floe, within 8 m of the MET tower. On day 1 of the deployment, the installation sites were located and ice holes for all systems were drilled including a 24" hole for AOFB 44 by the WHOI team. Somewhat alarmingly, at the hole for AOFB 45, the ice thickness was only 35 cm. On day 2, the AOFB system was deployed in less than 6 hours. Like AOFB 43, it was deployed with solar array and wind generator, but without the pycnocline spar subsystem. Student assistants for this deployment included Natalia Ribeira Santos and Sam Cornish.

With the 3 L-site AOFB installations complete, AOFB 46 was transported to the main floe helicopter landing site around noon on October 12, 2019 with the AOFB and WHOI teams. Sam Cornish was our student assistant. The next morning the two teams returned to deploy a special version of the pycnocline spar subsystem that sends full bandwidth data to a laptop in the MET City hut. The AOFB deployment followed, but had a delay swapping to another hydrohole due to a discovery of a deep, sloping slab of ice around 3 m depth. Late in the day, a fourth hole was drilled on 1 m thick ice, and an ice base mapper system was installed. The AOFB was successfully deployed. This resulted in a challenging day for all but with a good outcome. Alex Mavrovic was our student assistant. The following morning the pycnocline spar and mapper system were connected to the MET hut laptop, and a very quick system check performed before returning to the *Academic Fedorov* around noon.

Tab. 2.4.1: List of AOFB deployments

Site	AOFB Number	Station Book Entry
L1	43	L1_AOFB_NPS_20191005
L2	44	L2_AOFB_1_NPS_20191007
L3	45	L3_AOFB_1_NPS_20191010
'MET City' (central floe)	46	n/a

Preliminary results

An example of the high resolution finescale thermal structure within the pycncoline resolved by the pycnocline spar at MET City in Fig. 2.4.2 shows a blob of warm water advecting past the spar.

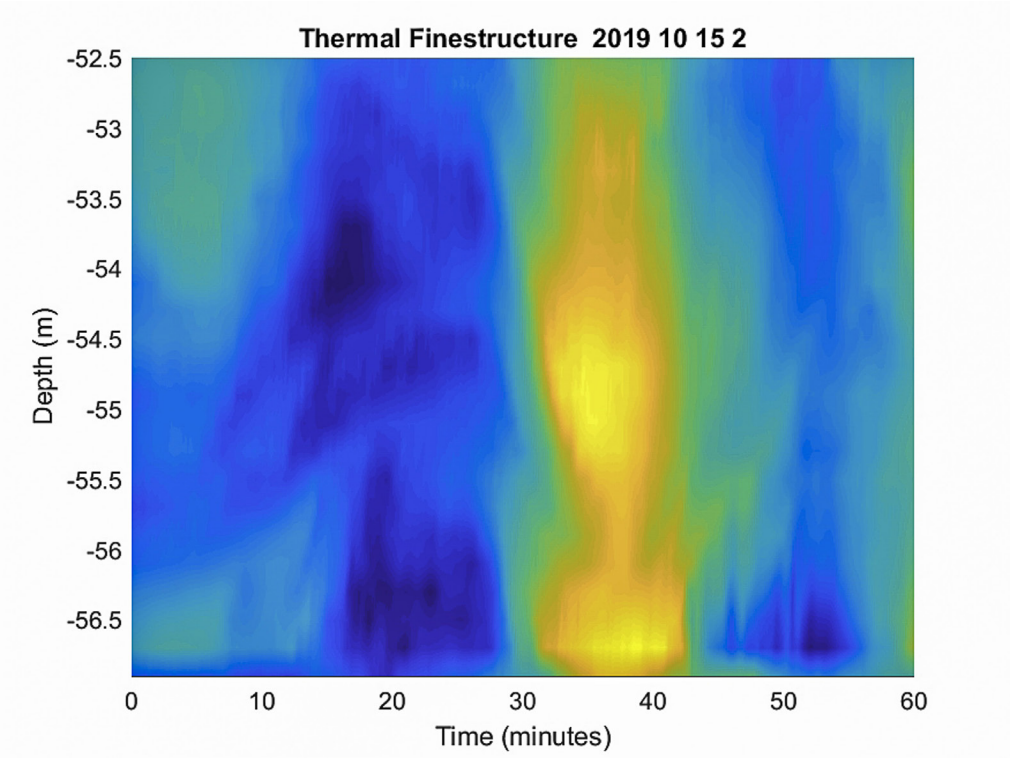

Fig. 2.4.2: A one hour timeseries of thermal finestructure advecting past the pycnocline spar at MET City on the main MOASiC floe. The resulting thermal gradients are used with the thermal dissipation rate measured at three depths to calculate vertical heat fluxes associated with turbulent mixing within the pycnocline.

Data management

Data from each AOFB is transmitted twice a day via a Rudics Iridium satellite link to a server at NPS. In near real time, raw data are processed into an archival format, and a subset of data are made available on the NPS AOFB website https://www.oc.nps.edu/~stanton/fluxbuoy/. On a quarterly basis, preliminary, processed data sets will uploaded to the MOSAiC Central Storage.

Data will be stored at either at the PANGAEA data repository (World Data Center PANGAEA Data Publisher for Earth & Environmental Science www.pangaea.de or at the Arctic Data Center (arcticdata.io), which is supported by the National Science Foundation (NSF) and DOIs provided to PANGAEA according to the agreement between Arctic Data Centre and PANGAEA.

All data are handled, documented, archived and published following the MOSAiC data policy.

2.5 Seasonal ice mass balance (SIMB3) buoys

Ryleigh Moore[1], Michel Tsamados[2], Igor Vasilevich[3], Thea Schneider[4], Lisa Craw[5],Ian Raphael[6]
not on board: Don Perovich[6]

[1]U Utah
[2]UCL
[3]AARI
[4]U Potsdam
[5]U Tasmania
[6]Dartmouth College

Grant-No. AF-MOSAiC-1_00
NSF Award #1724424

Objectives

The purpose of this study is to improve the representation of sea ice cover and surface albedo feedback in climate models through the integration of climate model experiments and field measurements. This work is funded by NSF Award #1724424.

The SIMB3 buoy (Fig. 2.5.1) is capable of autonomously capturing and reporting a variety of different measurements including snow depth, ice thickness, vertical temperature profile, GPS location, air temperature, and barometric pressure (Planck et al., 2019). The spatial and temporal measurements from the buoy can be used to approximate heat fluxes through the ice as well as the growth and decline of ice mass balance throughout the year.

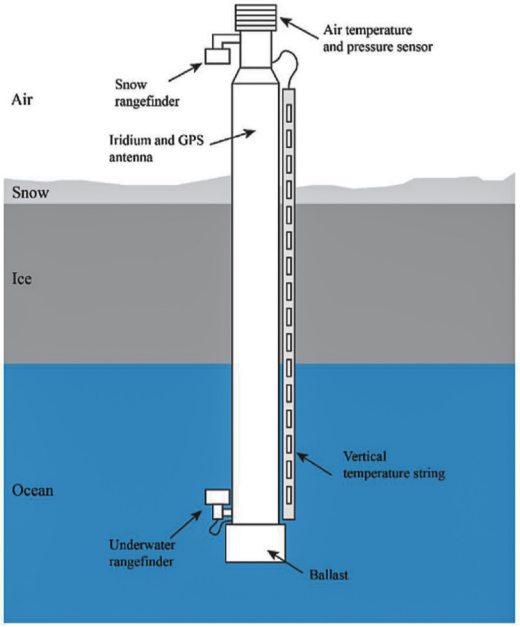

Fig. 2.5.1: A schematic of a SIMB buoy (Planck et al., 2019)

Work at sea

During the first weeks of the expedition, the buoys were assembled and unassembled in the hold in order to prepare for deployment. During this time, Ryleigh Moore, Michel Tsamados, Igor Valisevich, and Lisa Craw were taught by Ian Raphael how to put the SIMB3 buoys together.

Since Ian Raphael transferred to the *Polarstern* before the L site operations, Ryleigh Moore led the SIMB3 buoy deployment at L1, L2, and L3 (Fig. 2.5.2). At each L site, the hole necessary for deployment was drilled with the help of Andy Davies (WHOI) and Chris Basque (WHOI). Ian Raphael will install a fourth SIMB3 at the *Polarstern* floe.

At the L1 site, team lead Ryleigh Moore was assisted by Michel Tsamados and Igor Vasilevich in the deployment of the SIMB3 buoy.

At the L2 site, team lead Ryleigh Moore was assisted by Michel Tsamados and Thea Schneider in the deployment of the SIMB3 buoy.

At the L3 site, team lead Ryleigh Moore was assisted by Lisa Craw in the deployment of the SIMB3 buoy. A few observers on the ice also assisted in the deployment at the L3 site – Chelsea Harvey, Katie Gavenus, Natalia Ribeira Santos, and Sam Cornish.

The sample identification numbers in the Station Book for the buoys are denoted as L1_SIMB3_1_Dartmouth_20191005, L2_SIMB3_1_Dartmouth_20191007, and L3_SIMB3_1_Dartmouth_20191010 for L1, L2, and L3 respectively. Photos and videos of installation can be accessed by contacting Ryleigh Moore at RMoore@math.utah.edu.

Fig. 2.5.2: Photos taken of SIMB3 buoy at L1 (left), L2 (middle), and L3 (right)

At each L site, the following measurements and observations were taken: buoy location (at a specified time), the time the buoy was activated, snow depth, ice thickness, distance from top sensor housing to the ice, distance from the top temperature string housing to the ice, and floe characteristics (see Tab. 2.5.1 and Tab. 2.5.2).

Tab.: 2.5.1: Deployment details (L1-L3)

Site	Buoy Number	Ice Thickness	Snow Thickness	Freeboard
L1	MOSAiC #1	94-108 cm	6.5 cm	2-3 cm
L2	MOSAiC #3	77-83 cm	7 cm	5 cm
L3	MOSAiC #2	18 – 30 cm	6 - 6.5 cm	5 cm

Ice thickness varied because measurements were taken in different areas around the hole since the final buoy orientation after freezing in is not known. The range of ice thickness for each site is listed in Tab. 2.5.1. Specifically at L3, Ryleigh Moore was able to stay until the buoy was mostly frozen in. The ice thickness under the sensor was about 28 cm at that time.

Note also that the buoy number doesn't match the L-Site number for L2 and L3.

More in-depth information about the individual floes can be found in the ice floe survey section of the cruise report.

Tab.: 2.5.2: Deployment measurements at L1-L3

Site	Distance from the bottom of the top sounder housing to the ice	Distance from bottom of the top temperature string housing to the ice
L1	120 cm	105 cm
L2	116 cm	102 cm
L3	122 cm	108 cm

Preliminary (expected) results

It is expected to find that thinner ice over the past several decades has led to lower albedo, higher light transmittance, and a positive feedback loop of lower ice coverage in the Arctic.

All three SIMB3 buoys are transmitting properly but data access for the buoys is not available on the *Akademik Fedorov*.

Data management

Data will be stored at either at the PANGAEA data repository (World Data Center PANGAEA Data Publisher for Earth & Environmental Science www.pangaea.de or at the Arctic Data Center (arcticdata.io), which is supported by the National Science Foundation (NSF) and DOIs provided to PANGAEA according to the agreement between Arctic Data Centre and PANGAEA.

All data are handled, documented, archived and published following the MOSAiC data policy.

References

Planck CJ, Whitlocka J, Polashenski C, Perovich D (2019) The evolution of the seasonal ice mass balance buoy. Cold Regions Science and Technology, 165.

2.6 Deployment of fixed layer ocean buoy and the ocean profiler buoy

Xiaoming Ma[1], Youcheng Bai[2], Jian Ren[2],
Long Lin[2], Hangzhou Wang[3], Ruibo Lei[4],
Musheng Lan[4], Lei Wang[4]

[1]FIO
[2]SIO
[3]ZJU
[4]PRIC

Grant No. AF-MOSAiC-1_00

Objectives

In recent years, the environment of the Arctic has experienced unprecedented rapid changes, such as the rising air temperature, decreasing sea ice extent, decline and recovery of the cold halocline, increasing fresh water flux, etc. (Lang et. al., 2017; Parkinson and Digirolamo, 2016; Björk et. al., 2016; Köhl and Serra, 2014). The change in the Arctic Ocean mainly occurs in the upper layer which participates in air-ice-sea interaction and has direct impact on the Arctic climate. With the retreat of Arctic sea ice, the Arctic Ocean changes dramatically (Toole et al., 2010). Due to the ice-albedo feedback, more solar radiation enters the upper ocean, and then more ice melts, which will further facilitate the entry of solar radiation into the ocean. As a result, the upper ocean becomes warmer and stronger stratification (Jackson et al., 2010). The change of the upper ocean also has a remarkable impact on sea ice. The stored heat and stratification play a vital role in sea ice melting and freezing. So we deployed one fixed layer ocean buoy and one ocean profiler buoy to focus on the changes in the upper ocean environment and their effects on Arctic water masses, stratification, heat content and sea ice evolution.

Work at sea

The fixed layer ocean buoy consisted of two parts: an ice surface unit (Fig. 2.6.1) and ocean sensors. The surface unit includes GPS, Iridium communication, SD card, power, and foam float. The ocean sensors extend 200 m below the ice, with 5 layers at depths of 5 m, 10 m, 50 m, 100 m, and 200 m, respectively. The upper 4 layers are equipped with CTs, and the deepest layer is CTD.

The ocean profiler buoy has a surface unit (Fig. 2.6.2) and an ocean profiler as well. The surface unit is designed by Chinese National Ocean Technology Center, which includes GPS, Iridium modular, power, and foam float. The ocean profiler is bought from McLane Company. Inductive coupling technology is applied to data communication between the profiler and the surface unit, and finally the data acquisition unit transfers the real-time observations via iridium satellites.

The fixed layer ocean buoy was deployed in L1 Site, at 85º00’40“N, 132º45’34“E. While the ocean profiler buoy was deployed in L2 Site, at 84º59’21“N, 135º11’39“E

Preliminary (expected) results

Since the data communication problem, data derived from the fixed layer ocean buoy and the ocean profiler buoy are not transferred in real-time. However, sensors and the profiler both have self-contained function that can automatically store data so we could get data after the buoys’ recovery.

Data management

The fixed layer ocean buoy and the ocean profiler buoy have been added into the system of SENSOR.awi.de.The data coordination PI is Na Liu from the First Institute of Oceanography,

MNR, China (liun@fio.org.cn). The state of buoy will be updated weekly to the group leader of sea ice of MOSAiC, which provides the basic information to consider if it is necessary to maintain the buoy.

Data will be stored at the PANGAEA data repository (World Data Center PANGAEA Data Publisher for Earth & Environmental Science (www.pangaea.de)).

All data are handled, documented, archived and published following the MOSAiC data policy.

Fig.2.6.1: Fixed layer ocean buoy

Fig.2.6.2: Ocean profiler buoy

References

Björk G, Söderkvist J, Winsor P et al. (2016) Return of the cold halocline layer to the Amundsen Basin of the Arctic Ocean: Implications for the sea ice mass balance. *Geophysical Research Letters*, 29(11):8-1.

Itoh M, Shimada K, Kamoshida T et al. (2012) Interannual variability of PWW inflow through Barrow Canyon from 2000 to 2006. Journal of Oceanography, 68(4).

Jackson JM, Carmack EC, McLaughlin FA, Allen SE and Ingram RG (2010) Identification, characterization, and change of the near-surface temperature maximum in the Canada Basin, 1993-2008, Journal of Geophysical Research: Oceans, 115, C05021, doi: 10.1029/2009JC005265.

Köhl A, Serra N (2014) Causes of Decadal Changes of the Freshwater Content in the Arctic Ocean. *Journal of Climate*, 27(9):3461–3475.

Lang A, Yang S, Kaas E (2017) Sea ice thickness and recent Arctic warming. Geophysical Research Letters, 44.

Parkinson C, Digirolamo N (2016) New visualizations highlight new information on the contrasting Arctic and Antarctic sea-ice trends since the late 1970s. Remote Sensing of Environment, 183:198-204.

Toole JM, Timmermans ML, Perovich DK, Krishfield RA, Proshutinsky A and Richter-Menge JA (2010) Influence of the ocean surface mixed layer and thermohaline straitfication on Arctic ice in the central Canada Basin, Journal of Geophysical Research: Oceans, 115, C10018, doi: 10.1029/2019JC005660..

2.7 Direct flux measurement of trace gas exchange between ice and atmosphere

Stephen Archer[1], Vera Schlindwein[2]
not on board: Kevin Posman[1], Jaques Huber[3], Detlev Helmig[3], Byron Blomquist[3]

[1]BLOS
[2]AWI
[3]U Colorado

Grant No. AF-MOSAiC-1_00

Objectives

This study addresses the exchange of four climate-active trace gases, carbon dioxide (CO_2), methane (CH_4), dimethylsulfide (DMS) and ozone (O_3), between the Arctic ocean and polar atmosphere over an entire annual cycle during the Multidisciplinary drifting Observatory for the Study of Arctic Climate (MOSAiC) field campaign in 2019-2020.

Observations of gas transfer in sea ice were identified as a key requirement for improving sea ice biogeochemical models in a recent review. Physical descriptions of air-sea gas transfer have made significant progress. A gas transfer extension to the NOAA COARE bulk flux model is one such example, applicable to open ocean conditions. The physical mechanisms of gas transfer in the presence of sea ice are different from the open ocean, notably by the general absence of breaking waves and by near-surface thermohaline stratification related to the freeze-melt cycle, terrestrial freshwater input, and heat fluxes.

The footprint for flux measurements from towers can extend to more than 1 km depending on wind speed, atmospheric stability and measurement height, covering a variety of sea ice surfaces and open water leads. It is therefore desirable to obtain statistically robust estimates for gas flux directly at the sea ice or snow surface in undisturbed conditions with a small footprint, closely linking observed fluxes to environmental controls and biogeochemical processes in sea ice. As a component of our larger project we aimed to develop portable dynamic-chamber systems for short-term measurements of surface fluxes on undisturbed snow and ice.

Work at sea

Equipment was transferred from *Polarstern* on 06.10.2019, allowing the dynamic flux chamber to be assembled and tested over the next ~10 days. This included two sessions of on-ice tests at the L3 site on, 09.10.2019 and 10.10.2019. Only the systems used to determine CH_4 and CO_2 fluxes were assembled.

Preliminary results

Not applicable

Data management

Data will be stored at the Arctic Data Centre (arcticdata.io) following the agreement between ADC and the MOSAiC Project lead. DOIs will be communicated to PANGAEA data repository (World Data Center PANGAEA Data Publisher for Earth & Environmental Science www.pangaea.de for later access via the future MOSAiC Data Portal.

All data are handled, documented, archived and published following the MOSAiC data policy.

2.8 Deployment of unmanned ice stations

Ruibo Lei[1], Guangyu Zuo[2], Hangzhou Wang[3], Musheng Lan[1]

[1]PRIC
[2]TUT
[3]ZJU

Grant No. AF-MOSAiC-1_00

Objectives

As the loss and thinning of sea ice, more solar radiation will be absorbed by the ice-ocean system, which may stimulate the ice-albedo feedback (Nicolaus et al., 2012) and make a remarkable impact on the biological activities within and under the ice. The heat stored under the oceanic mixed layer under the ice will release and delay the ice growth during autumn and early winter. Based on the traditional sea ice mass balance buoy, we decided a new concept of the buoy to measure snow and sea ice mass balance, and reflection, absorption and transmittance of spectral solar radiation for the snow-covered ice. Thus, the feedback regime among radiation, snow, ice, ocean and biology can be quantified.

Work at sea

The unmanned ice station includes two parts, with the ice part for the measurement of snow and ice mass balance, as well as the spectral solar radiation, and the ocean part for the measurement of oceanic mixed layer. For the ice part, two sonars are used to measure the snow depth and ice thickness, which are similar with the traditional CRREL IMB (Richter-Menge et al., 2006). The 4.5-m thermistor chain with the vertical resolution of 0.03 m is used measured the temperature profile of snow and ice. The meteorological sensors to measure air temperature, pressure and relative humidity at the altitude of 1.5 m.

The irradiance measurement system has 8 fiber probes. Two probes were placed at ~1 m above the snow surface with one pointing upward and another pointing downward, to measure the down welling and upwelling irradiance separately. Four probes were fixed along a 6-mm-diameter fiberglass pole at intervals of 50 cm. The fiberglass pole with four probes was inserted into an auger hole of diameter 5 cm and tilt angle 45°. These four probes were fixed at at the interface between snow and ice, as well as 0.12, 0.25 and 0.37 under the ice surface. The two remaining probes were placed 1.2 m and 1.7 m below the water lever through a 10-cm-diameter auger hole, together with the corresponding antifouling device. The measurement of irradiance covers the wavelength between 350 and 1,000 nm, and the data at 29 wavelengths were recorded.

The unmanned ice station was deployed at L3 site (85ºN7.99'N, 135º40.738'E), with the ice and ocean parts deployed 10 m apart. The deployment site and the site for one SIMBA buoy (FMI0603) are located at two sides across one ice ridge, where the ice at the unmanned ice station site is relatively thick compared to SIMBA site. The initial ice thickness for the holes of setup of sonar, chain and optical sensor were close, with the values of 1.28, 140, and 1.20 m, respectively. The snow depth for all sites are 0.07 m.

The ocean part is assembled with five CT sensors (at the depth from the sea surface level of 5.4, 10.4, 15.4, 20.4, and 25.4 m), one CTD sensor (at the depth of 40.4 m), and sensors to measure dissolved oxygen and Chlorophyll a were fixed at two depths of 5.4 and 15.4 m, respectively. A weight of about 10 kg was fixed at the bottom of the CT-sensor chain.

Preliminary (expected) results

There are five CT sensors within the mixed layer of ocean under the ice, and one CTD under the mixed layer (Fig. 2.8.1). Thus, the ocean part of unmanned ice station covers the whole mixed layer. The air temperature ranged from -10ºC to -25ºC, which means the onset of ice freezing season.

As shown in Fig. 2.8.2, about 43 % solar radiation at the wavelength of 350-1,000 nm was reflected back to the air from the snow surface, which was relatively small compared to previous observation (e.g., Nicolaus et al., 2010). This is because the snow cover is destroyed during drilling to deploy the sensor. This issue is expected to be solved soon when snow falls and/or snow will be blowing. About 29 % of the solar radiation was transmitted through the snow cover into the top of ice layer, and about 3 % solar radiation was transmitted through the snow-covered ice. The data looks reasonable. We expected to obtain the data through the year to analyze the impacts of snow and ice mass balance on solar radiation partition among air, snow, ice and ocean.

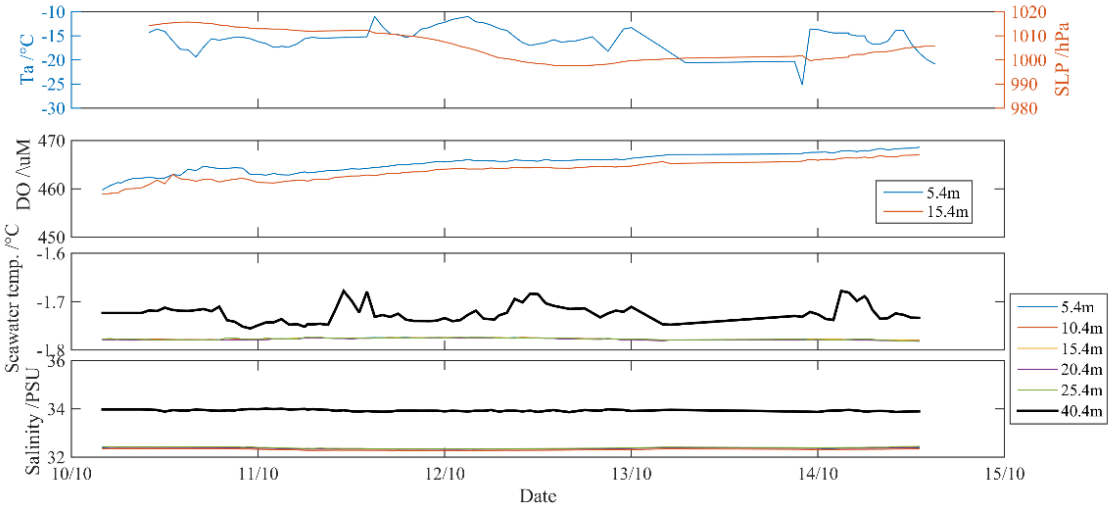

Fig.2.8.1: (a) Air temperature and sea level air pressure, (b) concentration of oxygen in the water, (c) seawater temperature and (d) salinity from 5.4 m to 40.4 m under the sea level

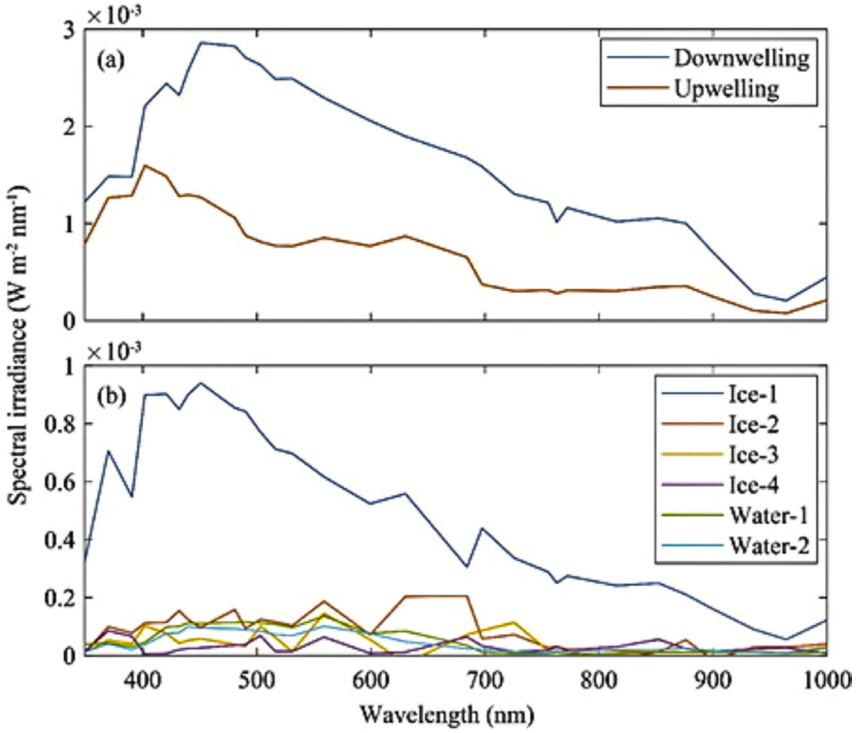

Fig.2.8.2: Spectral irradiance measured by the fibre optical probes at various depth

Data management

The unmanned ice station has been added into the system of SENSOR.awi.de. The data coordination PI is Ruibo Lei from the Polar Research Institute of China (leiruibo@pric.org.cn). Data will be stored at the PANGAEA data repository (World Data Center PANGAEA Data Publisher for Earth & Environmental Science (www.pangaea.de)).

All data are handled, documented, archived and published following the MOSAiC data policy.

References

Nicolaus M, Hudson SR, Gerland S, and Munderloh K (2010) A modern concept for autonomous and continuous measurements of spectral albedo and transmittance of sea ice. Cold Regions Science and Technology, 62, 14-28.

Nicolaus M, Katlein C, Maslanik J, and Hendricks S (2012) Changes in Arctic sea ice result in increasing light transmittance and absorption, Geophysical Research Letters, 39, L24501, doi:10.1029/2012GL053738.

Richter-Menge JA, Perovich DK, Elder BC, Claffey K, Rigor I, and Ortmeyer M (2006) Ice mass balance buoys: a tool for measuring and attributing changes in the thickness of the Arctic sea-ice cover, Annuals of Glaciology, 44, 205–210.

3. M-SITE DEPLOYMENTS

3.1 Deployment of snow buoys

Mario Hoppmann[1], Ying-Chih Fang[1] [1]AWI
not on board: Marcel Nicolaus[1]

Grant-No. AF-MOSAiC-1_00

Objectives

The Arctic Ocean has been undergoing drastic changes in recent decades. A major challenge to understand this evolution is the lack of *in-situ* observational data due to its remoteness and harsh environmental conditions. One key knowledge gap is the seasonal cycle of the snow cover on the pack ice of the Arctic Transpolar Drift. Snow on sea ice influences the sea ice energy- and mass balance via its optical and thermodynamic properties, impacts the freshwater budget of the ocean, and is of critical importance for biological processes and biogeochemical cycles.

The main aim of the MOSAiC drift experiment is to document the properties and processes related to the central Arctic climate- and ecosystem in unprecedented detail. An integral part of this undertaking is the extension of the MOSAiC central ice floe observations in time and space by using a suite of autonomous instruments. One of those platforms, the Snow Buoy (SB), is specialized in the measurement of snow depth on sea ice and its temporal evolution over the course of at least one year. Through the deployment of many such instruments within the MOSAiC Distributed Network (DN), we expect to obtain new knowledge in the spatial and temporal variability of the Arctic snow pack. Co-deployments with other specialized instruments such as for example Ice Mass balance Buoys (IMBs) and (bio-optical) ice and ocean buoys is expected to increase our understanding of the linkages between atmospheric, snow, ice and ocean properties and processes.

Work at sea

The Snow Buoy is a platform that measures changes in snow depth on sea ice using four ultrasonic pingers that are attached to a square frame on a mast at a height of 1.5 m above the ice surface (Fig. 3.1.1). The unit is also equipped with sensors to record basic atmospheric parameters: barometric pressure, surface- and air temperature, as well as GPS position. A dataset is reported back every hour via the iridium satellite network.

Each buoy was tested on deck a few days prior to deployment (Fig. 3.1.2a). After transport of instrument and gear to a deployment site (Fig. 3.1.2b), a 10-inch hole is carefully drilled into the ice using a motor drill. After the placement of an ablation plate on the ice surface, the main cylinder containing the batteries is lowered into the hole, and 4 ropes are anchored in the ice to stabilize the mast against the wind. The snow cover is carefully restored after deployment (Fig. 3.1.2c). Calibration of relative changes to absolute values is achieved by recording the initial snow depth below the individual pingers during deployment. GPS position and time is documented during deployment. The instrument is manufactured by MetOcean Telematics (Halifax, Canada) and was developed as a cooperation with the AWI.

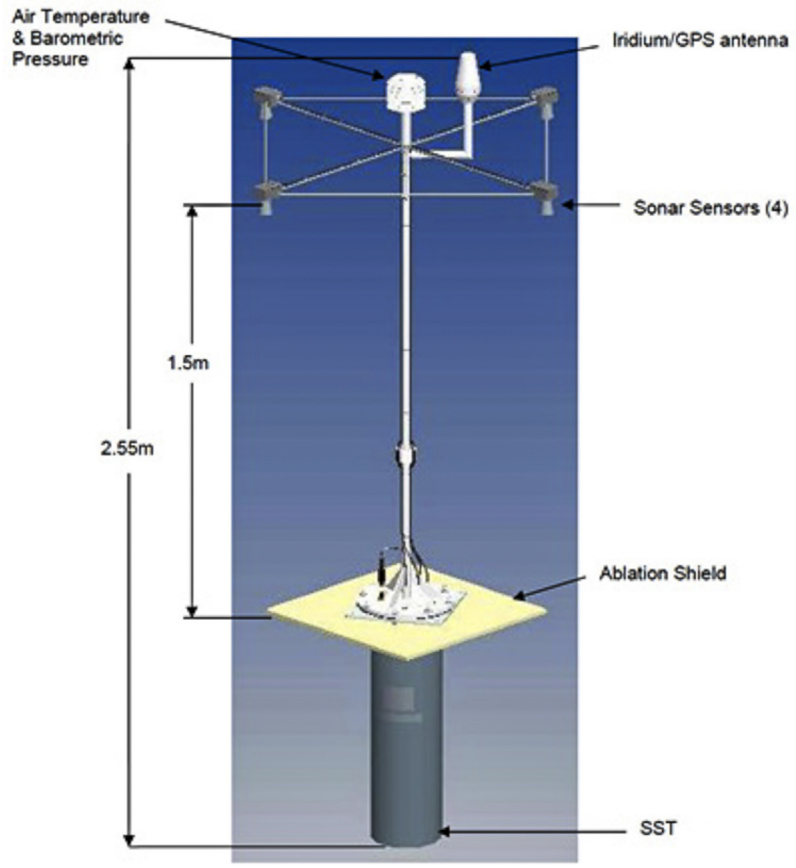

Fig. 3.1.1: Technical drawing of Snow Buoy (MetOcean Telematics)

During the DN installation, one Snow Buoy was installed on each of the 8 M-sites that were deployed either via ship (M4 and M8) or helicopter (all other sites). The buoys were co-located with IMBs and Salinity Ice Tethers within a radius of 20 m. A D-TOP free floating profiler buoy was co-located in 100 m distance. These deployments were complementing the three main L-sites.

Preliminary results

Tab. 3.1.1: Overview of snow buoy deployments on M-sites, including initial snow depths below the 4 snow pingers for calibration.

Station log ID	IMEI	z_ice	SH1	SH2	SH3	SH4
M1_SB04_AWI_20191005	300234066080170	180	15	15	18	10
M2_SB05_AWI_20191007	300234066344810		12	14	13	12
M3_SB06_AWI_20191007	300234066444880	70	16	9	14	11
M4_SB07_AWI_20191008	300234066346540		20	9	17	21
M5_SB08_AWI_20191009	300234067009210		13	10	8	11
M6_SB09_AWI_20191010	300234066995900	200	22	22	25	24
M7_SB10_AWI_20191011	300234066081180		11	12	10	13
M8_SB11_AWI_20191011	300234062788470		10	3	6	9

Data management

Snow Buoy data are available in near real time on www.meereisportal.de. The positions and selected data are automatically uploaded to the database of the International Arctic Buoy Program (IABP), which is publicly accessible. The Snow Buoys also contribute to the Global Telecommunication System (GTS).

Data will be stored at the PANGAEA data repository (World Data Center PANGAEA Data Publisher for Earth & Environmental Science (www.pangaea.de)).

All data are handled, documented, archived and published following the MOSAiC data policy.

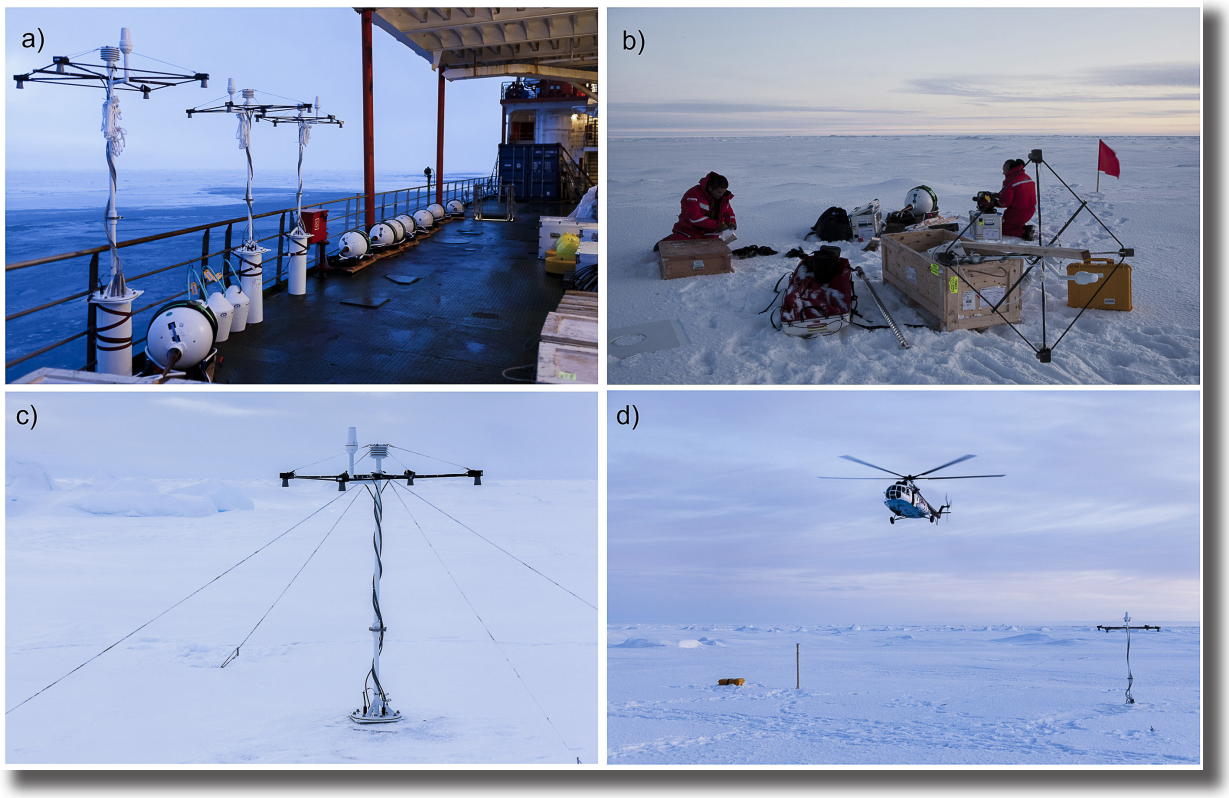

Fig. 3.1.2: a) Snow Buoy testing on deck, b) M-site deployment operation, c) exemplary Snow Buoy after deployment, d) IMB (left) and Snow Buoy (right) as part of an M-site deployment via MI-8 helicopter.

3.2 Deployment of thermistor chain ice mass balance buoys (SIMBA)

Ruibo Lei[1], Mario Hoppmann[2]
not on board: Bin Cheng[3]

[1]PRIC
[2]AWI
[3] FMI

Grant-No. AF-MOSAiC-1_00

Objectives

We deployed a number of SAMS-type thermistor chain Ice Mass balance Buoys (IMBs) within the MOSAiC Distributed Network. These so-called SIMBA buoys (Snow and Ice Mass Balance Array) were designed by the Scottish Association for Marine Science (SAMS) and were provided for MOSAiC by the Polar Research Institute of China and the Finnish Meteorological Institute. The SIMBA measures air-snow-ice-ocean temperature profiles using Maxim Integrated DS28EA00 thermistors at a vertical spatial resolution of 0.02 m (Jackson et al., 2013). An additional feature of these platforms is the application of heat to each sensor in order to measure the temperature response, which depends on the medium the thermistor is currently residing in. Using the measurements of the vertical temperature profile of atmosphere, snow, ice and ocean and the measurements of temperatures before and after the pulsed heating, the interfaces between air, snow, sea ice and ocean can be derived, which enables a calculation of the mass balance of snow and sea ice. We can then explore the point to point difference of the accumulation and melt of snow, as well as the growth and decay of sea ice within the MOSAiC DN. Conditions on the initial deployment sites were snow depths ranging from 0.05 to 0.15 m, and ice thicknesses ranging from 0.35 to 1.80 m. Thus, the influence of initial snow and ice thickness on the seasonality of snow and ice mass balance and the associated energy balance among atmosphere, snow, ice and ocean can be determined. Some positive feedbacks, e.g., the ice-albedo feedback, and negative feedbacks, e.g., the climate warming-ice freezing feedback, can be addressed. Some special processes related to sea ice thermodynamics, such as the freezing of water within the cavities of a ridge or the refreezing of the melt pond, can also be potentially observed. By comparing with the historic data (e.g., Perovich et al., 2014 and Lei et al., 2018), we can obtain the interannual variations of sea ice mass balance from the Central Arctic to the Fram Strait, and its responses to the changes in atmospheric circulation and oceanic heat flux.

Work at sea

In total, 13 SIMBA buoys were deployed during the DN setup, including 8 M-site deployments, 4 L-site deployments and 1 other deployment (see Table 3.2.1).

Tab. 3.2.1: Deployment information of SIMBA buoys

Station	Deployment date	Location	Buoy ref. number	IMEI number	Sea ice thick-ness [m]	Snow depth [m]	Description of the deployment site
L1	2019-10-05	85º 0.6759‘N; 132º 46.6864‘E	PRIC 0906	300234068704730	1.44	0.13	The floe diameter is about 3 km, the deployment site is level ice and surrounding some ice ridge
L2	2019-10-07	84º 59.454‘N; 135º 0.10071‘E	PRIC 0902	300234068709320	1.06	0.10	The floe diameter is about 1.5 km. The floe is basically level at the side with all buoys deployments, very ridged at the other site. The deployment site is level ice, but very close to the ridge.
L2	2019-10-07	84º 59.44698‘N; 135º 0.0996‘E	PRIC 0904	300234068705730	1.31	0.15	This site is much closer to the ridge that the PRIC 0902 site. To the top of ridge sail, just about 10 m ahead, the ice thickness > 4m.
L3	2019-10-09	85º 7.69 ‘N; 135º 40.681‘E	FMI 0603	300234068705280	0.45	0.06	Floe diameter is about 1.5 km, most level ice is very thin with thickness less than 0.5 m. The deployment site is over the level ice and close to the ridge. The level ice at the other side of ridge is relative thick with thickness ranging 1.0 to 1.8 m. The unmanned ice station was deployed over that side.
M1	2019-10-05	84º55.14’N, 131º15.672’E	FMI0603	300234068705280	1.80	0.15	Floe diameter of 1-2 km, melt ponds over frozen 25 cm, some ridges, buoy site in centre, DTOP in 100 m
M2	2019-10-07	84º42.4776’N, 136º48.216’E	FMI0508	300234065177750	0.81	0.14	Not available
M3	2019-10-07	85º3.1032’N, 137º50.076’E	FMI0509	300234065170760	0.80	0.10	Not available
M4	2019-10-08	85º6.6677’N, 136º11.7588’E	FMI 0510	300234065171790	1.57	0.10	The floe, with a diameter of about 1.5 km, was rafted with some gaps between the layers. Most part of the floe with ice thickness larger than 3 m (including the gap).
M5	2019-10-09	85º3.2112’N, 139º1.722’E	FMI0605	300234068700290	0.97	0.13	Not available

Station	Deployment date	Location	Buoy ref. number	IMEI number	Sea ice thick-ness [m]	Snow depth [m]	Description of the deployment site
M6	2019-10-10	85°7.665'N, 133°13.002'E	PRIC0903	300234068701300	1.74	0.14	Not available
M7	2019-10-11	84°58.844'N, 134°29537'E	FMI 0602	300234068700320	0.75	0.05	The floe, with a diameter about 3 km. The deployment site is over the level ice.
M8	2019-10-11	84°44.3682'N, 135°50.46'E	FMI0604	300234068706760	0.70	0.10	Not available
Ak01	2019-10-13	84°53.5996'N, 133°13.5580'E	FMI0406	300234064817930	0.35	0.05	The floe, with a diameter of about 2km, was aggregated new ice and old ice ridge. Most level ice is new ice. The deployment site is over the new ice.

Preliminary (expected) results

SIMBA buoys were deployed on all L- and M-sites, at the scale of about 50 km × 50 km (Fig. 3.2.1). Thus, the thermodynamic processes of snow and sea ice measured by the SIMBA buoys were highly representative for the regional ice conditions. As shown in Fig. 3.2.2, the vertical temperature gradient through the snow was much higher than that within air and water. By 11 Oct. 2019, the vertical temperature gradient was established only for the top part of ice because the drill hole for deployment needed some time to refreeze. The data is valid only from the point where the hole has refrozen, which depends on the snow and ice thickness, as well as the air temperature. The daily circle was only observed for the temperature within air and snow, which highlights the thermodynamic insulation of a snow cover as a result of its low heat conductivity.

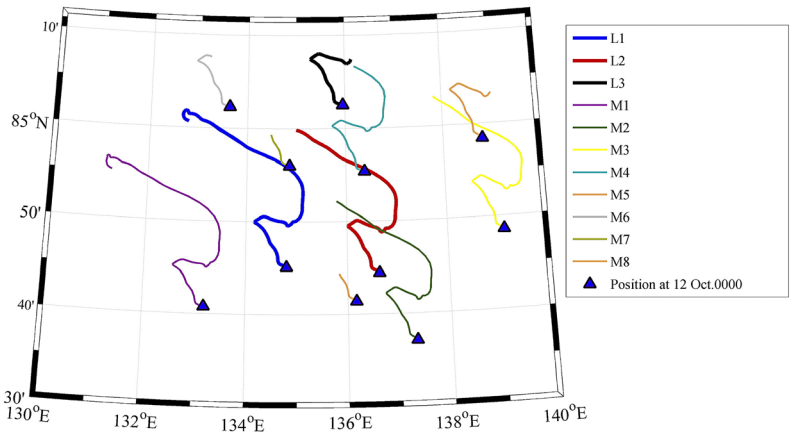

Fig. 3.2.1: The trajectories of SIMBA buoys deployed at L and M sites

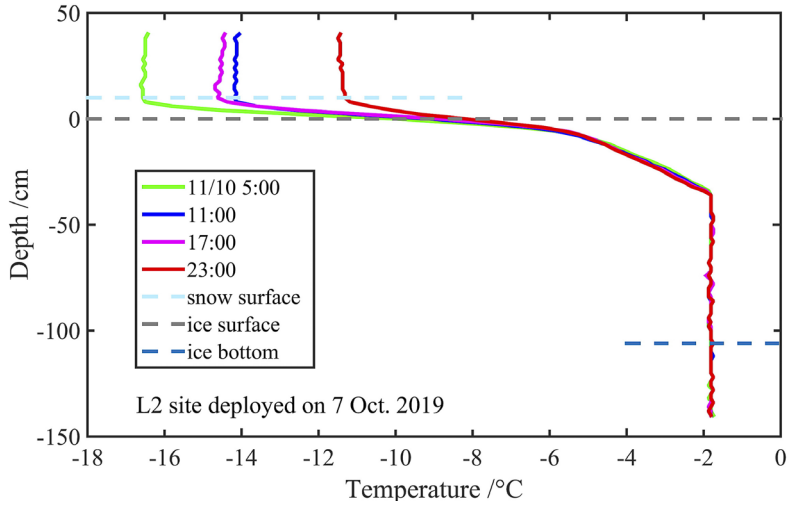

Fig. 3.2.2: Temperature profile from air through snow and ice cover into the water at the L2 site

Data management

All SIMBA buoy data are made available on meereisportal.de on a daily basis.

Data will be stored at the PANGAEA data repository (World Data Center PANGAEA Data Publisher for Earth & Environmental Science (www.pangaea.de)).

All data are handled, documented, archived and published following the MOSAiC data policy.

References

Jackson K, Wilkinson J, Maksym T, Meldrum D, Beckers J, Haas C., Mackenzie D (2013) A novel and low cost sea ice mass balance buoy, J. atmos. oceanic Technol., 30(11):13825, http://dx.doi.org/10.1175/JTECH-D-13-00058.1.

Lei R, Cheng B, Heil P, Vihma T, Wang J, Ji Q (2018) Seasonal and interannual variations of sea ice mass balance from the Central Arctic to the Greenland Sea. Journal of Geophysical Research: Oceans, 123. https://doi.org/10.1002/2017JC013548.

Perovich D, Richter-Menge J., Polashenski C, Elder B, Arbetter T, Brennick O (2014) Sea ice mass balance observations from the North Pole Environmental Observatory, Geophys. Res. Lett., 41, 2019–2025, https://doi.org/10.1002/2014GL059356.

3.3 Deployment of the salinity ice tether (SIT) ocean buoys

Ying-Chih Fang[1], Mario Hoppmann[1], Francesca Doglioni[1], Tao Li[2], Jialiang Zhu[2], Robbie Mallett[3], Lisa Craw[4], Natalia Ribeira Santos[4], Sam Cornish[5], Marylou Athanase[6], Falk Ebert[7]

[1]AWI
[2]OUC
[3]UCL
[4]U Tasmania
[5]U Oxford
[6]LOCEAN-IPSL
[7]HU Berlin

Grant-No. AF-MOSAiC-1_00

Background and objectives

The deployment of eight SIT ocean buoys during MOSAiC is part of the NERC/BMBF project "*Investigation and parameterization of the seasonally-evolving ice-ocean boundary layer system and its response to (sub) mesoscale variability*". (Sub) mesoscale variability is capable of inducing substantial vertical velocity (several meters per day) from below the ocean mixed layer. In the seasonally ice-covered ocean, this process is more complicated by modulation of sea ice within the evolving ice-ocean boundary layer. This ocean-ice coupled system has been investigated near marginal ice zones, where (sub) mesoscale currents interact with ambient mesoscale field and result in sea ice aggregation and advection (Manucharyan and Thompson 2017). However, little is known about how (sub) mesoscale variability influence the upper ocean in the central Arctic. Moreover, an appropriate parameterization of such features in a general circulation model (GCM) is still challenging. Our objectives are to observe the evolution of the upper ~100 m thermohaline field within a semi-Lagrangian framework. We expect to observe ubiquitous horizontal density gradients that accompanying with (sub) mesoscale currents due to baroclinic instability, and footprints of (sub) mesoscale variability should be detected. This will be conducted by deploying Salinity Ice Tether (SIT) buoys radially in the MOSAiC Distributed Network (DN). These data, accompanied by velocity and turbulence measurements in the MOSAiC Central Observatory (CO), will be utilized for process and model studies. The modeling efforts will be in conjunction with *in-situ* data. Geographical and seasonal variability of (sub) mesoscale currents will be the focus of this project. Ultimately, we hope to obtain a better understanding of what potential effects, generating mechanisms, and roles of (sub) mesoscale features are in the central Arctic and link our results to provide an implication to the local biogeochemical activity.

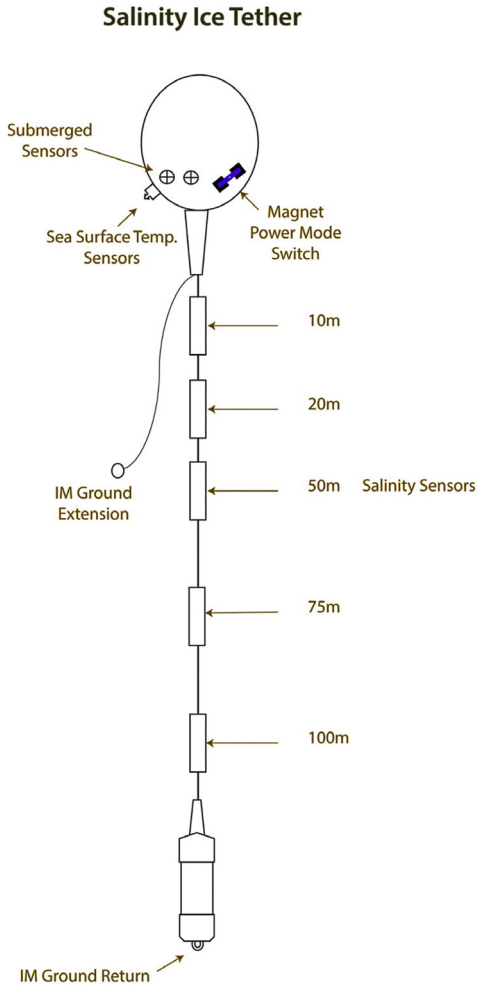

Fig. 3.3.1: Schematic diagram of the SIT buoy.

Work at sea

The SIT buoy (Pacific Gyre, California, USA) is comprised of a surface float that houses the main electronics and batteries, and a 100 m long inductive modem (IM) cable with an ~25 kg anchor attached to the end (Fig. 3.3.1). Along the tether, five inductive SBE37-IMP Microcat CTDs (SeaBird Scientific, California, USA) were mounted at pre-selected depths: 10 m, 20 m, 50 m, 75 m, and 100 m. The buoy also records surface temperature and GPS position, and carries a submergence indictor. The individual CTDs were configured to a 2 minute internal recording interval, while the buoy transmits GPS and CTD data every 10 minutes via the iridium network. During the MOSAiC Distributed Network deployment activities, eight such SIT buoys were deployed, one at each M-site.

The installation of batteries into the 40 SBE37 CTDs was performed between 23 and 25 September. Initial tests of IM communication for each of the SIT buoys was started afterwards. The IM tether was unspooled and the SBE37 CTDs were attached to the cable. Freshwater was inserted into the pumps and the buoy was switched on. The data files were retrieved and checked for the correct initialization. Sampling of a few CTDs was not triggered, but the problems could be fixed by restarting the buoys. All eight SIT buoys were successfully tested on deck and declared ready for deployment.

The first deployment at site M1 was performed on 5 October by helicopter. On the ice, the tether was unspooled and the CTDs were attached to their designated depth positions along the cable. They were covered with towels to avoid freezing of the conductivity cells. In the meantime, a 10-inch hole was drilled in an area of thicker ice. The cable was then manually lowered into the water by a team of 3 persons. After deployment of the tether, the surface float was placed on the hole and the magnet was removed to switch it on. Table 3.3.1 summarizes the deployments at each M site. Note that two M sites were deployed from the ship en route searching other suitable M-site floes. M7 and M8 were deployed in parallel.

Fig. 3.3.2: Deployment of the 100 m IM tether

Tab. 3.3.1: Summary of the SIT buoy deployments

Site	Date	Time (UTC)	Lon	Lat	Platform
M1	2019-10-05	04:40	131.28 °E	84.92 °N	Helicopter
M2	2019-10-07	02:30	135.75 °E	84.87 °N	Helicopter
M3	2019-10-07	07:10	137.82 °E	85.05 °N	Helicopter
M4	2019-10-08	01:30	136.24 °E	85.11 °N	Ship
M5	2019-10-09	01:20	134.47 °E	85.16 °N	Helicopter
M6	2019-10-10	03:10	133.23 °E	85.13 °N	Helicopter
M7	2019-10-11	02:20	135.83 °E	84.74 °N	Helicopter
M8	2019-10-11	01:10	134.49 °E	84.99 °N	Ship

Preliminary (expected) results

The SIT buoys were preconfigured to transmit data back to the server at the Pacific Gyre every 10 minutes. We briefly processed the data obtained between 02:00 UTC 11 Oct 2020 and 01:40 UTC 12 Oct 2020 (Fig. 3.3.4). This period was chosen so eight SIT buoys were in a contemporary period. The drifting trajectories for the eight M sites show a coherently southeastward pattern (Fig. 3.3.3). We estimated the drifting speed of ~7 km in a day, which corresponds to ~8 cm s^{-1}.

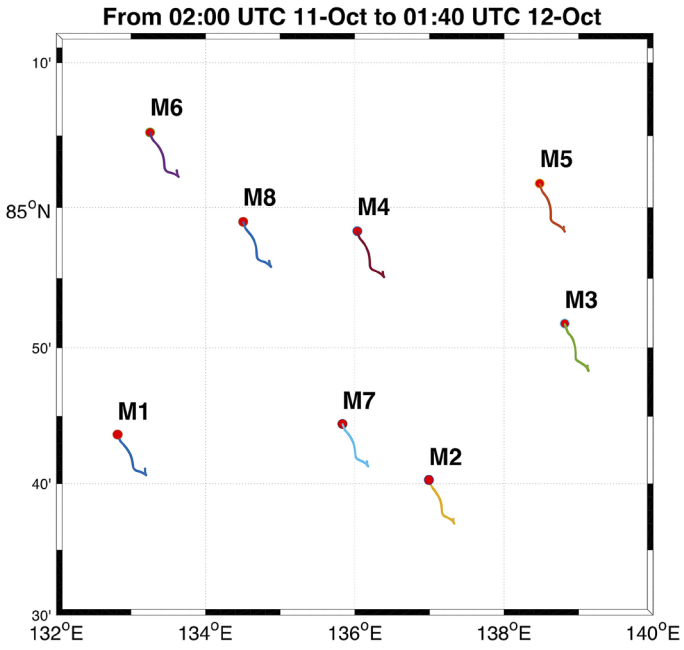

Fig. 3.3.3: SIT drift trajectories for the eight M-sites.

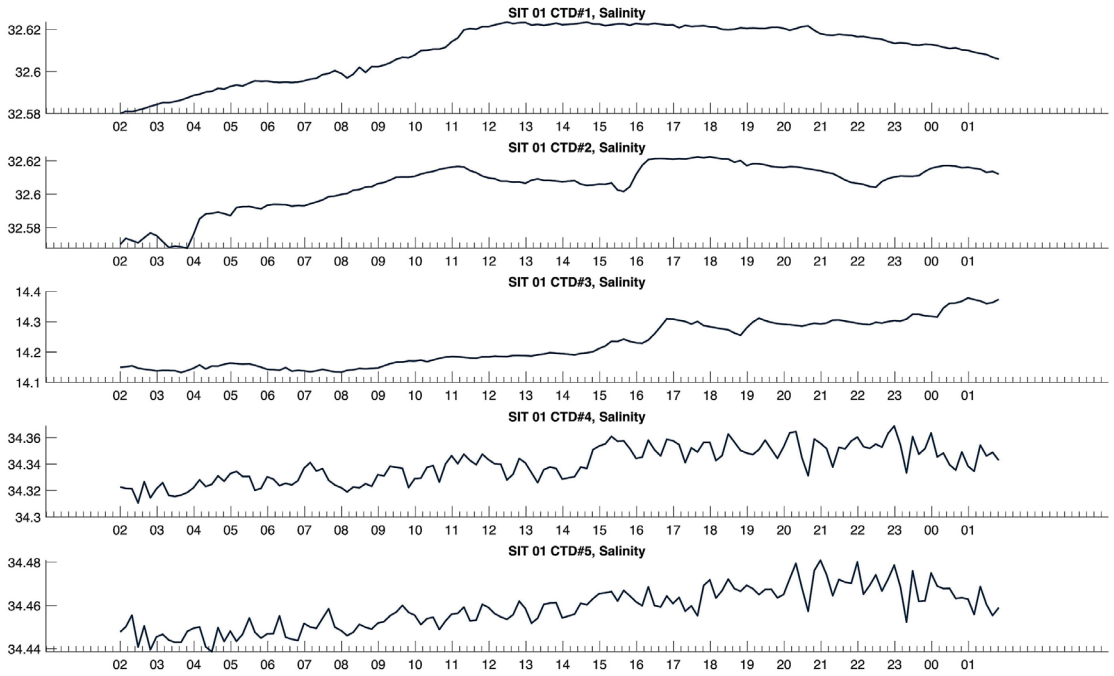

Fig. 3.3.4: Salinity time series from SIT #1. The panels show the CTD data at 10 m, 20 m, 50 m, 75 m, and 100 m, respectively. Note the salinity at 50 m was ~14, which indicates a clogged conductivity cell.

As of 17 October, three CTDs did not report their data back. Possible explanations are problems in the IM connection, or flooding of the sensors. Furthermore, five SBE37 exhibited too low salinities (<20) (Fig. 3.3.4), indicating ice within the conductivity cell. Based on our observation of the data, it appears that the salinity reading will slowly increase with time.

Data management

The transmitted data is publicly available in near-real time on meereisportal.de. The internally recorded 2 minute data will be available after recovery of the instruments. After a final quality check, the data will be stored at the PANGAEA data repository (World Data Center PANGAEA Data Publisher for Earth & Environmental Science (www.pangaea.de)).

All data are handled, documented, archived and published following the MOSAiC data policy.

References

Manucharyan GE, Thompson AF (2017) Submesoscale Sea Ice-Ocean Interactions in Marginal Ice Zones. J. Geophys. Res. Ocean., 122, 9455–9475.

3.4 Drift-towing ocean profiler (d-top)

Tao Li[1], Jialiang Zhu[1], Ying-Chih Fang[2], Mario Hoppmann[2], Ruibo Lei[3], Lei Wang[4]
not on board: Jinping Zhao[1]

[1]OUC
[2]AWI
[3]PRIC
[4]BNU

Grant-No. AF-MOSAiC-1_00

Grant-No. 2016YFC1400303. The National Key Research and Development Program of China

Objectives

With the extreme sea ice decline (Comiso, 2012), the energy balance and flux at the ice-ocean interface have become a hot spot in the Arctic climate study. Atlantic Water (AW) entering the Arctic Ocean provides the main source of heat and salt to the Arctic Basin (Schauer et al., 2008). The cold halocline and fresh mixed layer in the upper ocean, however, have prevented the AW up to the surface and hence sea ice melt (Koenig et al., 2016). The purpose of this study is to improve the understanding of the interaction of sea ice and upper water column in the Eurasian Basin of the Arctic Ocean, especially during the freezing season in autumn and winter. The scientific questions we are trying to answer here are: (1) how does the brine rejection due to the formation of sea ice affect the formation and evolution of the cold halocline layer in the Eurasian Basin; (2) how does the mixed layer vary seasonally in the Transpolar Drift.

Work at sea

A Drift-Towing Ocean Profiler (hereafter, D-TOP, Fig. 3.4.1) was deployed on 5 M-sites (Tab. 3.4.1) The D-TOP consists of three components: a surface package, a cable of 120 m length, and the main instrument, a CTD profiler. The sampling rate of the D-TOP is 12 hours for a CTD profile, and 1 hour for meteorological sensors. Ideally, the vertical range of a profile is from 0.2 m beneath the ice bottom to the maximum length of the tether.

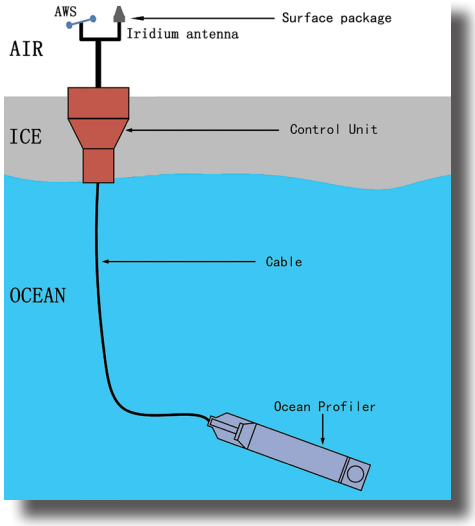

Fig. 3.4.1: A schematic of D-TOP system

Onboard Test

After a long trip from China to Norway, the D-TOPs were tested onboard before the deployment. The onboard test included hardware connection and control unit operation. Once the three parts of D-TOP had been connected as a functional system, the control unit started to sample

and then sent the data to the shore-based server (see Fig. 3.4.2 (left)). Although we obtained the confirmation of data receipt from the server side, an on-board test procedure of 3 days was also successfully performed, and all nits were cleared for deployment.

Deployment

Five D-TOPs were successfully deployed at M-sitesFour units were deployed using the helicopter, whileone was deployed from the Fedorov. The summary of ice thickness and snow depth at the deployment sites are shown in Table 3.4.1. Average deployment duration at each site was about 2.5 hours, depending on the ice thickness and weather condition. It should be noticed that a D-TOP deployment attemptat M4 was unsuccessful due to an unexpected ice thickness of over 2.8 m and harsh weather conditions. The final distribution of the M-sites can be found in the ice floe survey section of the cruise report.

All five D-TOPs were sampling and transmitting data properly upon deployment. The D-TOP201908, however, has sent some unreasonable CTD data to the shore-based server since Oct. 11 2019. After six days, the sensors of depth and temperature in the D-TOP201908 started to collect reasonable data again. However, the salinity sensor is still not working well up to now. The possible causes are unclear.

Fig. 3.4.2. Onboard test and in situ deployment of D-TOPs

Table 3.4.1: Summary of the ice conditions at M sites with D-TOPs

Site	Buoy Number	Ice Thickness (cm)	Snow Depth (cm)
M1	201904	114	25
M2	201905	124	12
M3	201906	145	10
M5	201908	154	15
M8	201907	105	8

Preliminary (expected) results

All five D-TOPs have been reporting back their locations and meteorological data from each site every hour, revealing south-east movements for all D-TOPs as shown in Fig. 3.4.3 (right). Taking the D-TOP201907 as an example, the air temperature ranged from -10°C to -25°C with the minima on October 14 and 16 while a similar trend of relative humidity occurred during the same period (Fig. 3.4.4, left). Meanwhile, the average speed of the floe ice the D-TOP201907 sits on was about 0.09 m/s.

The water properties such as temperature, salinity, dissolved oxygen and chlorophyll in the upper ocean on the D-TOP201907's trajectory are shown in Fig. 3.4.4. Main characteristics of the water column are an increased trend of the temperature and salinity with depth and the opposite variations in DO and Chl, which means that the phytoplankton is mainly relying on the light radiation and nutrient in the upper mixed layer. The strong cold halocline occurred within 25 ~ 40m and further deepened in last few days, while the week thermocline was significantly affected by the underlying warm Atlantic Water. The seasonal variations of the mixed layer and cold halocline will be deeply analyzed with the continuous sampling by five D-TOPs and other in situ measurements in the MOSAiC floe ice.

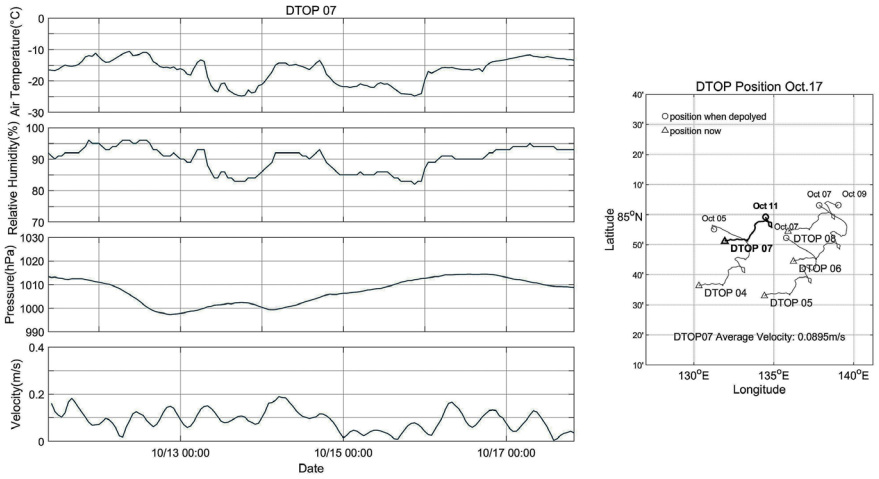

Fig. 3.4.3: Time series of air temperature, relative humidity, air pressure and ice velocity of the D-TOP201907 (left), and trajectories of five D-TOPs (right) from October 12th to 17th, 2019.

Data management

Processed data and final results will be stored at the PANGAEA data repository (World Data Center PANGAEA Data Publisher for Earth & Environmental Science (www.pangaea.de)).

All data are handled, documented, archived and published following the MOSAiC data policy.

References

Comiso JC (2012) Large decadal decline of the Arctic multiyear ice cover. Journal of Climate, 25(4), 1176-1193.

Koenig Z, Provost C, Villacieros- Robineau N, Sennechael N, Meyer A (2016) Winter ocean-ice interactions under thin sea ice observed by IAOOS platforms during N-ICE2015: Salty surface mixed layer and active basal melt. Journal of Geophysical Research: Oceans, 121, 7898-7916.

Schauer U, Beszczynska-Moeller A, Walczowski W, Fahrbach E, Piechura J, Hansen E (2008) Variations of measured heat flow through the Fram Strait between 1997 and 2006. In: Dickson RR, Meincke J, Rhines P eds. Arctic-Subarctic Ocean Fluxes: Defining the Role of the Northern Seas in Climate, Springer Sci, Amsterdam, Netherlands, pp. 65-85.

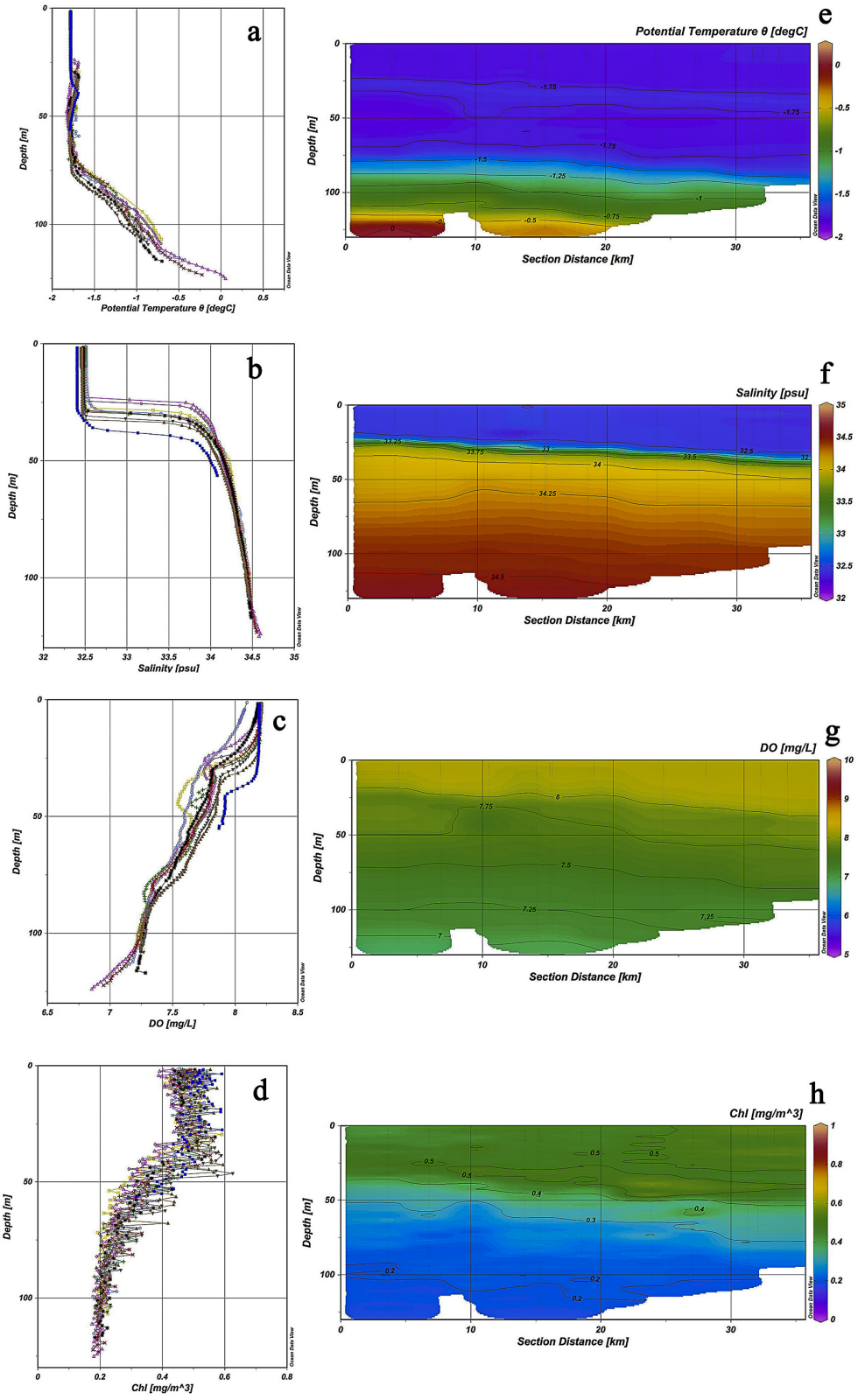

Fig. 3.4.4: Profiles (a~d) and sections (e~h) of the potential temperature, salinity, dissolved oxygen (DO) and chlorophyll (Chl) of D-TOP201907 from October 12th to 17th, 2019

4. DEPLOYMENT OF THE P-BUOY ARRAY

Daniel Watkins[1], Ruibo Lei[2], Mario Hoppmann[3], Vasily Smolianitsky[4]
not on board: Jennifer Hutchings[1]

[1]Oregon State University
[2]PRIC
[3]AWI
[4]AARI

Grant-No. AF-MOSAiC-1_00

Objectives

The goal of the P-buoy array is to track the motion and deformation of sea ice at multiple scales across its first year of existence. The P-sites of the MOSAiC Distributed Network consist of drifting buoys reporting at minimum GPS positions. Alongside observations based around the *Polarstern*, the P-site array aims to enable concurrent measurement of sea ice deformation across a range of temporal and spatial scales from local (1 meter, 1 second) to large scale (1,000 km, 1 month) in a nested manner (Fig. 4.1). Arranging buoys at distances from 5 km to 50 km away from the central floe and along 5 km-radius circles centered at L sites allows for scaling relationships for deformation to be extended to scales and physical regimes that have not previously been measured. Additional buoys will be placed at distance of 100+ km from the central floe to capture large-scale motion.

By collecting position data at P-sites throughout the MOSAiC year, it is anticipated that transitions in the physical mechanisms controlling sea ice deformation and floe size will be identifiable. Hypothesized transitions include (a) when sea ice becomes contiguous with the coast, (b) the transition between freezing and melt season, when leads and cracks no longer freeze over or break up, (c) floe disintegration when vertical melt becomes the dominant term for transition in the floe size distribution, and (d) when waves break floes.

High temporal and spatial resolution position data from the P-sites will be used in coordination with other MOSAiC teams to build time-evolving maps of sea ice, complementing for example synthetic aperture radar satellite imagery, visual observations, and radar observations near *Polarstern*. This will allow investigation into the spatial and temporal lead distributions, the limits of SAR-based detection sea ice deformation, and the relative contributions of atmospheric and oceanic forcings to deformation-based changes in the sea ice thickness distribution.

Work at sea

Deployment of the P-site buoys was carried out primarily using a polar-equipped Mi-8 helicopter. Communication with the Russian pilots and expert guidance for selection of suitable floes was provided by Vasily Smolyamitskiy and Anna Timofeeva of the Arctic and Antarctic Research Institute (AARI). Deployment was carried out concurrently with the deployment of the M-site stations. 8-12 GPS drifting buoys were loaded in the helicopter alongside the M-site equipment. The AARI team used satellite imagery to identify potential M-site floes, and a flight path was chosen to allow multiple floes to be tested prior to unloading the M-site equipment and team. Following the M-site unloading, the helicopter proceeded to the coordinates of ideal P-sites and to potential M-sites. At floes appearing to be good candidates for M- or L-sites, P-buoys

were left to serve either as a P-node, or if needed, as a guide back to the floe for M- or L-site deployment. Where possible, P-buoys serving as markers were recovered. In some cases this was not possible, so a P-node is closer to some L-sites than initially planned. This is the case, for example, with TUT 137, which was placed on the L3 floe during site selection and used to track the flow; however when the AK *Fedorov* moored to the floe, it was on the opposite side of a large floe and time constraints prohibited using a helicopter flight to retrieve the buoy from the other side. After candidate M-sites were visited the remainder of the flight was used to deploy buoys. In total. 52 GPS buoys were deployed over the course of 8 flights.

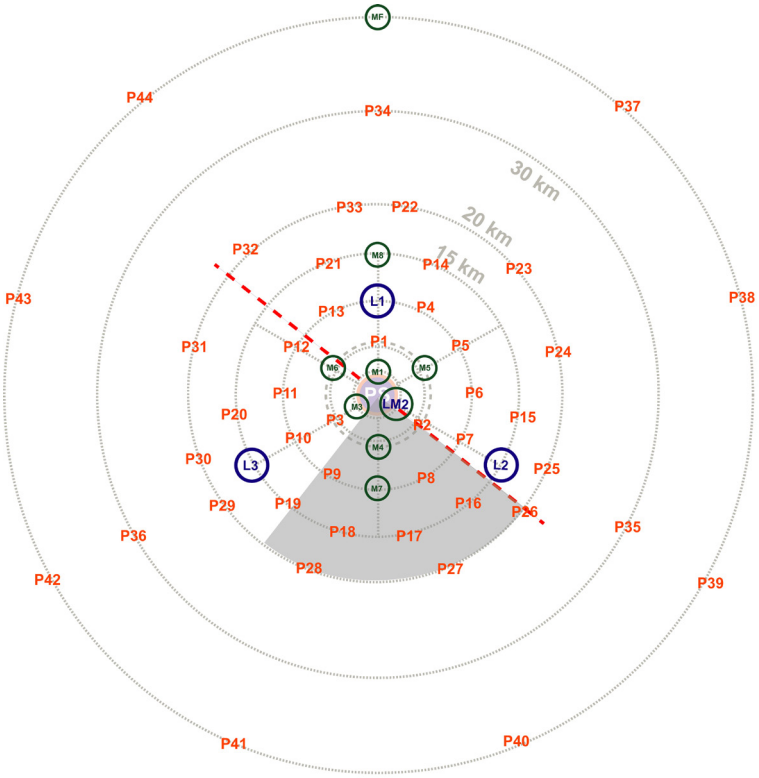

Fig. 4.1: Proposed layout of the Distributed Network

Tab. 4.1: Quantity and Type of buoys deployed by different institutions.

Quantity	Type	Institution
22	PacificGyre air-droppable IceTracker	OSU
7	MetOcean SVP with pressure and temperature sensors	AWI/EUMETNET
4	PacificGyre IceTracker B	AWI
2	PacificGyre IceTracker	AWI
13	TUT-GPS	PRIC
3	PacificGyre UniversalTracker	OSU

Air-droppable buoys were favored for the closely-spaced rings of buoys around the L-sites and central floes, and for shipside deployed as they could be tossed onto floes near the ship. EUMETNET meteorological buoys and AWI IceTracker B buoys were placed along the 40 km

ring at sites. Additional EUMETNET buoys were placed at a few “wide-P” sites to the southwest in a gap in IABP buoy coverage. The TUT-GPS, AWI IceTracker, and OSU UniversalTracker buoys were placed opportunistically throughout the P-array.

Buoys withheld for deployment during the MOSAiC year

It is expected that ice deformation throughout the year will result in some areas having insufficient buoy coverage. In addition, it is expected that some buoys will fail, for example if buried in a ridge or visited by inquisitive wildlife. For this reason 26 buoys were witheld for deployment later in the year. In addition to the 20 buoys initially stowed on *Polarstern* (6 from the Finnish Meteorological Institute, 6 from PRIC, and 6 from OSU), the following 6 buoys were transferred from the *Federov* to the *Polarstern*.

Tab. 4.2: List of buoys withheld for deployment during the MOSAiC year.

Name	IMEI	Institution
AWI-UTA-0009	300234067705760	AWI
AWI-UTA-0012	300234067707750	AWI
OSU-UT-0005	300234066415350	OSU
OSU-UT-0002	300234066253880	OSU
OSU-UT-0004	300234066412350	OSU
MO_SVP-B (P16)	300234062881930	AWI/EUMETNET

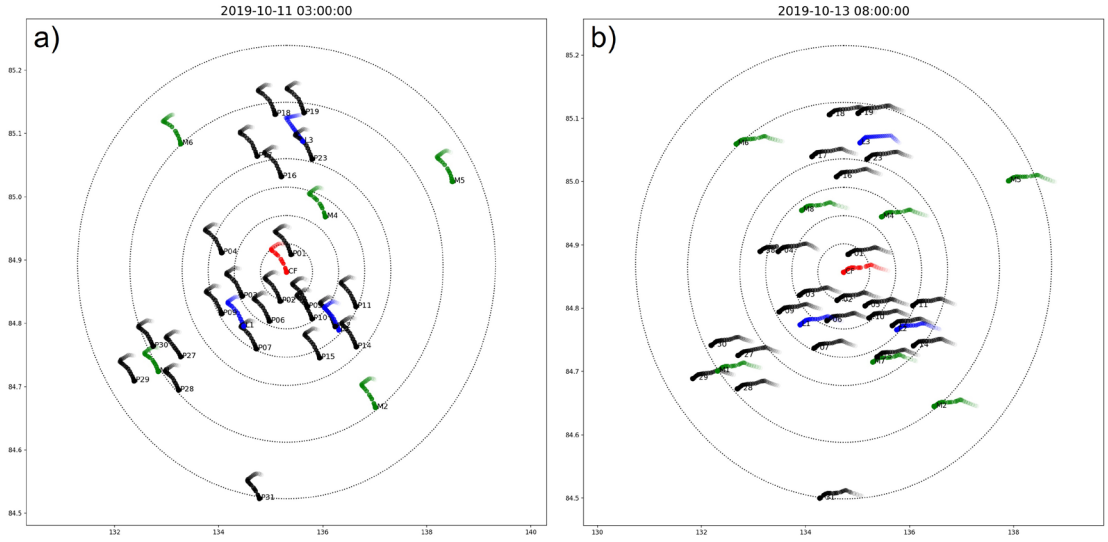

Fig. 4.2: “24-hour buoy motion tracks for (a) 03:00 UTC on 11. October 2019 and (b) 08:00 UTC on 13. October 2019. Concentric rings represent distances of 5, 10, 15, 20, 30, and 40 kilometers from the central MOSAiC floe.

*

Preliminary results

Initial observation of motion in the buoy array reveals the buoys in the distributed network moving together due synoptic motion.

Data management

Data will be uploaded onto the MOSAiC Central Storage throughout the year. In addition, in collaboration with the International Arctic Buoy Program, data from the P-sites will be collected and made available to MOSAiC participants via FTP.

Data will be stored at either at the PANGAEA data repository (World Data Center PANGAEA Data Publisher for Earth & Environmental Science (www.pangaea.de) or at the Arctic Data Center (arcticdata.io), which is supported by the National Science Foundation (NSF) and DOIs provided to PANGAEA according to the agreement between Arctic Data Centre and PANGAEA.

All data are handled, documented, archived and published following the MOSAiC data policy.

5. ADDITIONAL DATA

5.1 Ice observation and routing

Vasily Smolianitsky[1], Anna Timofeeva[1], [1]AARI
Vladimir Bessonov[1], Tomash Petrovsky[1], [2]AWI
Thomas Krumpen[2]

Grant No. AF-MOSAiC-1_00

Objectives

With exception of the periods 21-23 September and 23-28 October 2019, cruise of the *Akademik Fedorov* was conducted within the northmost parts of the Barents and Kara Seas and part of the Arctic Ocean adjacent to the Laptev Sea (Fig. 5.1.1). Permanent floating ice (sea ice and ice of land origin) is characteristic for all the above areas, hence the ice routing and regular ice observations were obligatory for most of the cruise time. Specified work onboard *Akademik Fedorov* was executed by the group of ice experts from Arctic and Antarctic Research Institute (AARI) in Sankt Petersburg, Russia.

Objective of the ice routing was to assist and optimize the navigation of the vessel while advancing and departing the area of work and the interior maneuvering inside the area during deployment of the distributed network. Subsequent tasks included collection and processing of satellite tactical and regional information on the state of ice cover and its presentation and interpretation. The only type of information was microwave - AMSR2 passive (GCOM-W1) and C and X-bands SAR (Sentinel-1and TerraSAR- X) obtained in a form of daily mosaics with medium (70-100 m) and low (1 – 3 km) resolutions. Processing of the imagery included georeference (if applicable) and reprojection. Presentation of information was done within DKart Navigator ENC system installed on the bridge and GIS (QGIS and ESRI ArcMap). Interpretation of the imagery was done in a form of an expert analysis of the features on, if available, co-located C- and X-band and AMSR2 imagery and included identification of the easier navigation areas (weaker new and young ice, openings and leads) and an opposite task – maximum solid ice for deploying L and M sites (big and medium floes with well-defined edges, preferably containing some ridges inside).

Objective of ice observations was the definition of the state of sea ice cover during the cruise. Subsequent tasks included recording of sea ice parameters following AARI methodology and verification of satellite data. Methodology of observations is described in the “Manual on conduction of ice air reconnaissance” (1981). Special feature of the methodology is a continuous estimation of sea ice parameters along the track of navigation simultaneously “on the route” (within the area around the ship of 2-3 widths of the hull) and “in the region” (within the range of eye visibility), with separation of recording into the zones with homogeneous ice characteristics. Besides sea ice total and partial concentrations, stages of ice development and forms of ice, a lot of other ice characteristics are determined following AARI methodology. These are ice thickness(es), hummocks and ridges concentration, stage of melting, snow

height and concentration, ice pressure, width of leads, fractures and cracks. All coding strictly follows the WMO “Sea Ice Nomenclature (2017). Observations were executed permanently for the whole area and time of sea ice present by 4 ice observers from a left side of the bridge by round the clock watches: 3 hours after 8 hours. Special measuring-rod, fixed on the left board of the ship was used for the estimation of ice thickness. For the iceberg risk waters, positions of the icebergs were recorded following observations done by navigators on the bridge.

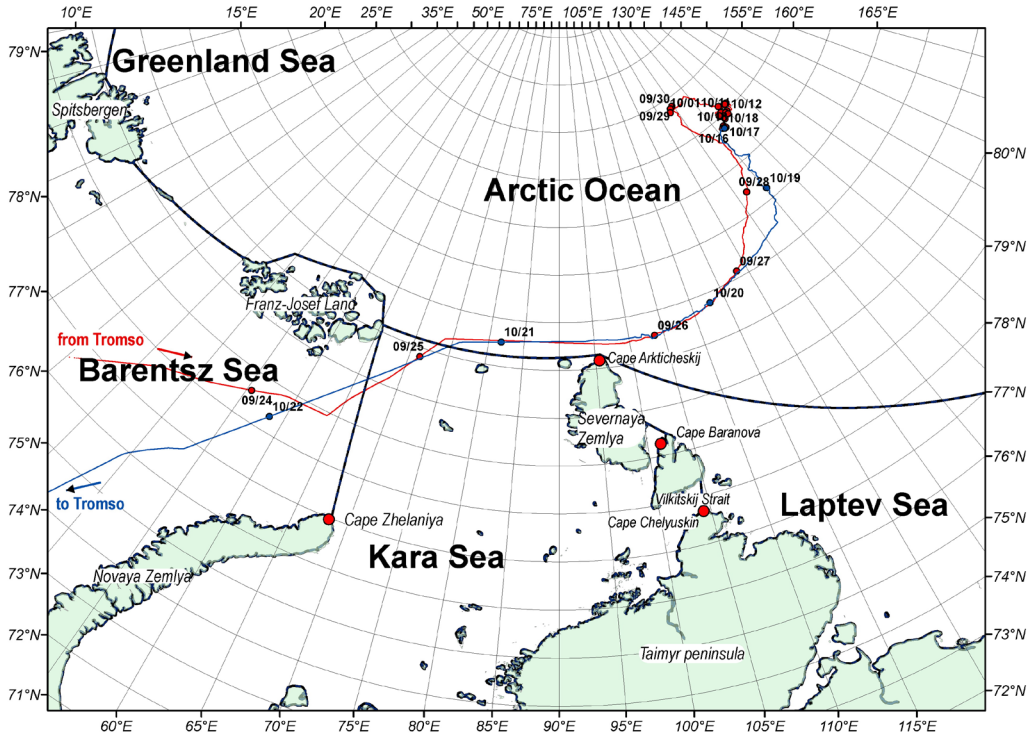

Fig. 5.1.1: Navigation area of Akademik Fedorov. IHO sea boundaries are shown (Flanders Marine Institute (2018)).

Work at sea

The entire period of ice routing and observations can be divided into three segments:

- vessel transit from Tromse to the area of the MOSAiC main ice floe search during 21-30 September;
- vessel navigation within the area of search in search of suitable ice floes for installation of the main MOSAiC observatory the distributed network (DN) with subsequent deployment of the DN during 30 September – 17 October;
- vessel transit from the working area to the port of Troms during 17 – 28 October.

Ice situation for the first segment of the voyage is shown on Fig. 5.1.2 in a form of the AARI ice analysis chart for 24 September in SIGRID-3 format (WMO/TD-No.1214) from the AARI WDC Sea-Ice archive. Applied color scheme corresponds to the WMO color standard for ice charts (WMO/TD-No.1215).

With an exception of a small area in the NW part of the Barents Sea adjacent to Spitsbergen archipelago where ice conditions were close to decadal normal, northern parts of the Barents,

Kara and Laptev Seas were characterized by extreme northernmost position of the ice edge and absence of the sea ice older than residual. That allowed to choose the route through the ice free and occasional open water areas northward of Novaya Zemlya and Severnaya Zemlya archipelagos with entering the ice of Arctic Basin NE of Cape Arkticheskij, which radically differs from the previously recommended ice navigation routes (Buzuev et al., 1988). Due to dark time and rough sea only several bergy bits and small icebergs were recorded for this iceberg risk area.

The vessel crossed the compacted ice edge on 26 September at 1:24:00 MSK at 81°29'N 102°04'°E, which was also a starting point for the permanent ice observations on the bridge. As navigation was conducted during the already started period of freeze-up, the first encountered ice had total concentration 9/10 with 4/10 of residual ice and 5/10 of new ice, predominantly as dark nilas.

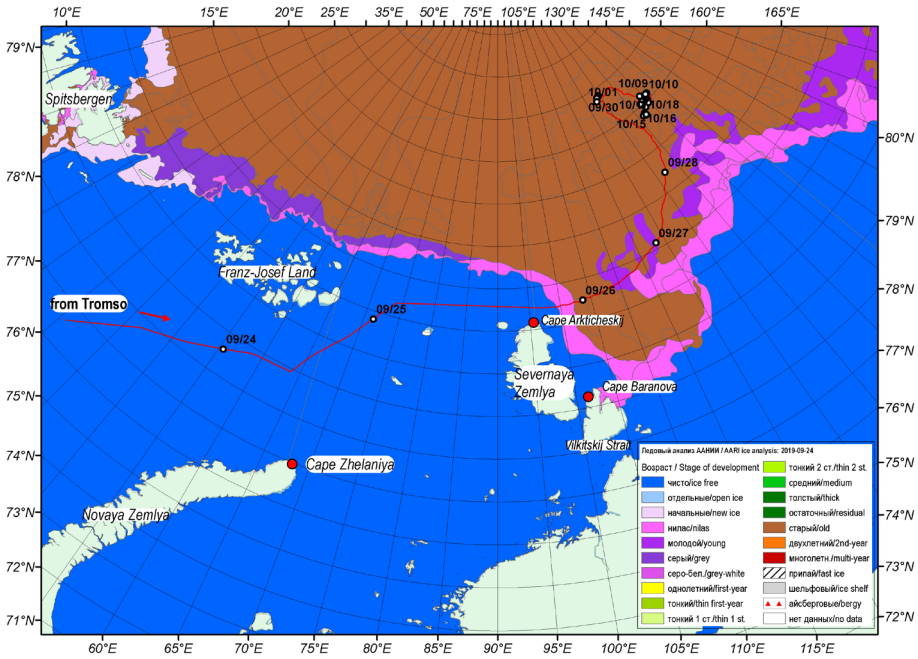

Fig. 5.1.2: Route of Akadimik Fedorov to the area of MOSAiC experiment. Background image – AARI ice analysis chart for 24 September 2019, colouring based on predominent stage of ice development

Typical ice conditions observed in the NW part of the Laptev after crossing the ice edge were 8-9/10 total concentration with 4-5/10 (occasionally up to 7/10) residual ice (3/10 of 30-70 cm thick, 1-2/10 of 70-120 cm thick) in a form of small floes and ice cakes 30-70 cm thick with 1-2/10 of grey ice and 4/10 (occasionally up to 6/10) of nilas (refer to Fig. 5.1.2). Further navigation to NE was conducted through a fracture zone with average total concentration 7-8/10 with 3/10 of residual ice (mainly 30-50 cm thick, occasionally to 100 cm and more), 2/10 of gray ice and 2-3/10 of nilas. Forms of new ice as pancake and grease ice were occasionally observed.

At 82°12'N 119°18'E on 27 September 5:07 MSK the vessel laid down in drift for reception of the German colleagues from the *Polarstern* who arrived by helicopter for discussion of the following action plan for *Akademik Fedorov*. Point at 85°20'N 125°20'E was chosen as a start of search for MOSAiC floe due to its equidistant position (within the 100 km range) from several potential ice floes candidates chosen earlier by the AARI specialist on a basis of the satellite imagery analysis.

Regional ice routing for the above segment was provided on a basis of the low resolution (2,500 m) passive microwave AMSR2 daily mosaics (YYYYMMDD.amsr2.n.cmb.gif) downloaded from the sea ice portal of the Danish Technical University (DTU) - seaice.dk. Processing of the imagery included reprojection to polar stereographic projection and conversion from GIF to GeoJPEG2000 (or GeoJP2) for further presentation inside the DKart Navigator ENC. Example of such regional information is given on Fig. 5.1.3. The AMSR2 daily data provided sufficient information on the position of the ice edge in the Kara and Laptev Seas and displacement of open, close and very close ice areas NE of Severnaya Zemlya. It should be also noted that the AMSR2 mosaics were the only source of satellite data for the latter region as the Sentinels 1A & 1B orbits are planned exceptionally rare for the Laptev Sea region and the optical data (e.g. MODIS or AVHRR) were not available due to dark time/cloudiness.

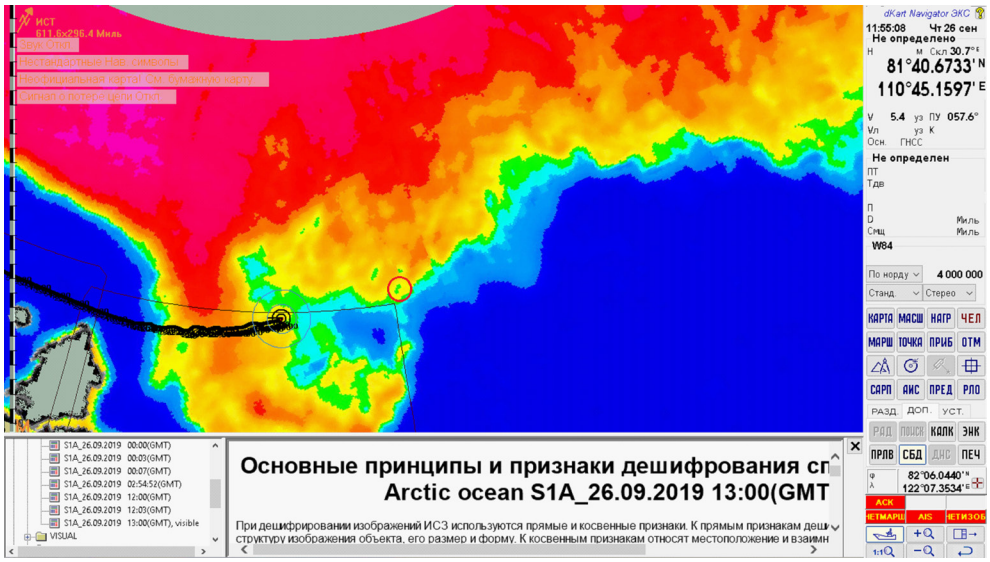

Fig. 5.1.3: AMSR2 passive microwave mosaic for 26.09.2019 in Dkart Navigator ENC

Further regional and tactical ice routing for the area northward of 82°N up to area of search for MOSAiC floe was supported by the Sentinel-1 AB products including: low resolution (1,000 m) DTU routine daily pan-Arctic mosaics (YYYYMMDD.s1ab.1km.n.mos.jpg), medium resolution (300 m) regional mosaics kindly produced by the DTU (YYYYMMDDhhmmss. S1. AkademikFedorov.jpg) for MOSAiC expedition and medium-high resolution (50-100 m) regional mosaics produced by Drift+Noise Polar Services GmbH in GeoTIFF format. The first two types of information were obtained from the DTU seaice.dk portal while the third one was obtained through the customized Drift+Noise portal (framsat.driftnoise.com). Use of advanced Iridium Next Internet communication terminal allowed smooth download of JPEG and GeoTIFF imagery up to a size of 30 Mb.

Interpretation of the Sentinel-1 imagery included search for fracture zones, individual fractures and leads, areas with new and young ice predominance or lowest concentration of ridged ice. Due to the fact that orbits passed the area of navigations once a day only (between 02 and 06UTC) with further additional 2-3 hours for processing the imagery at ESA / DTU / Drift+Noise sides, difference between the acquisition and actual time of navigation could be more than 24 hours which in most of the cases resulted in significant displacement of the potential navigational areas due to ice drift. Corrections to actual positions were obtained by comparing information on the shipborne radar and satellite imagery with further decision on the choice of a route. Examples of such decision makings are shown on Figs. 5.1.4 and 5.1.5.

Fig. 5.1.4 also provides a view of the first ice floe candidate; which properties were checked by breaking a small part of it by the vessel hull. The vast floe was approached 27 September at coordinates 84°33'N 128°15'E. Resulted observed thicknesses were: 20-30 cm – 10 %, 30-70 cm – 40 %, 70-100 cm – 40 %, >110 cm – 10 %. Bottom layer of the floe was significantly contaminated by algae and possibly mineral sediments.

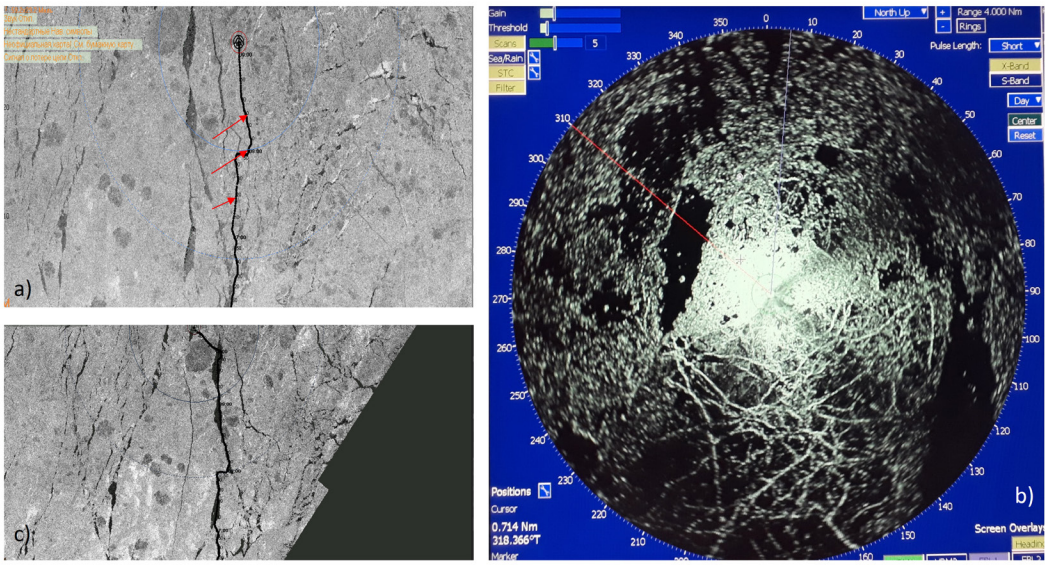

Fig. 5.1.4: Example of using satellite Information on the bridge during ice routing on 28.09.2019: a) Sentinel-1 image for previous date 27.09.2019 with actual track of Akademik Fedorov displayed in Dkart Navigator ENC system; b) actual image of fractures on shipborne ice radar; c) Sentinel-1 imagery for 28.09.2019 obtained next day.

After examination of the first candidate floe, the vessel routed using a system of leads (as shown on Fig. 5.1.5) toward the next candidate – a vast floe at 85°49'N 124°00'E which was reached 29 September at 03:06 MSK. Upon approach *Akademik Fedorov* penetrated through the edge of the floe which allowed to estimate predominate thickness of the edge area of floe close to 50 cm and note distinctive absence of algae and sediments in the ice eversions, i.e. opposite to previous candidate.

From September 29 to October 1 *Akademik Fedorov* was in drift, moored to the vast ice floe for conduction of surveys. Further, on 1 October *Akademik Fedorov* moved towards *Polarstern*. The meeting was dedicated to the final choice of the main floe for MOSAiC observatory and took place on October 2 at 85°15'N 134°46'E.

Further routing of *Akademik Fedorov* was carried out in a homogenous area of sea ice conditions within a 15-20 km radius from *Polarstern*, moored to the main ice floe. Track of *Akademik Fedorov* for 30 September – 17 October is shown on Fig. 5.1.6.

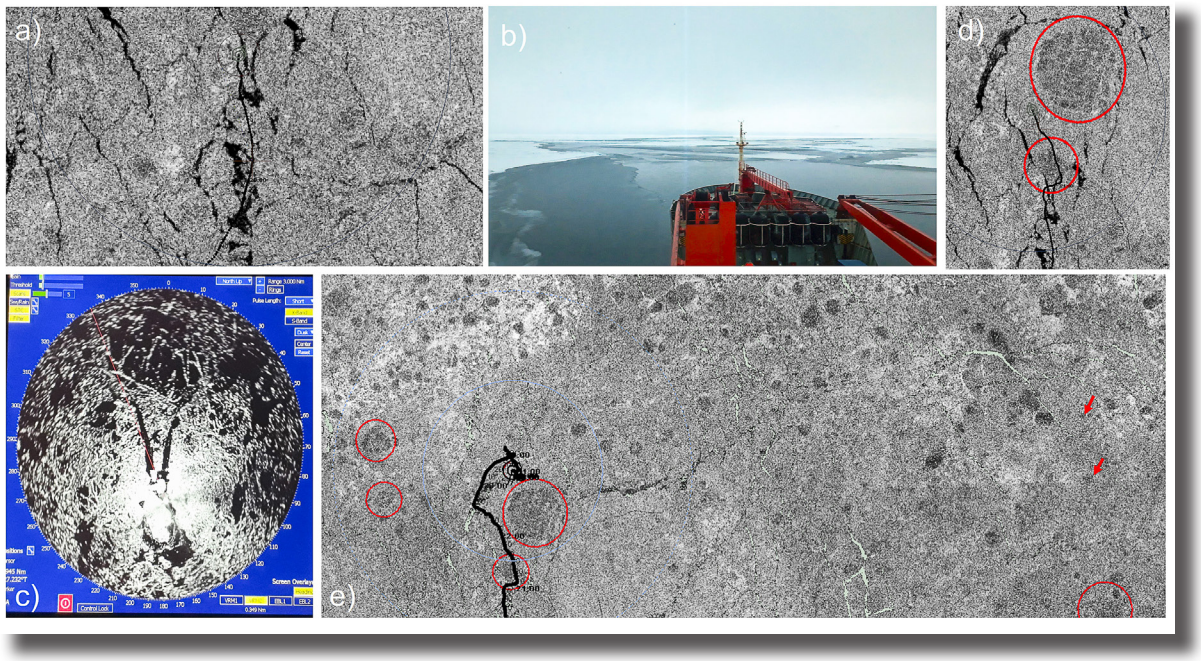

Fig. 5.1.5: Example of using of satellite Information on the bridge during ice routing: a) Sentinel-1 image for 28.09.2019 with actual track of Akademik Fedorov; b) photo of observed ice condition; c) fractures in the ice cover on shipborne ice radar; d) enlarged radar image with ship track in Dkart Navigator; e) the radar image of the Sentinel-1 for 28.09.2019.

Typical ice conditions for beginning of that period were characterized by 10/10 total concentration, 5/10 of residual ice with prevalent thicknesses 50-70cm (4/10) and 70-100 cm (1/10). Instead of previously observed gray ice, the next thicker stage of the young ice, the gray-white ice was observed with partial concentration 3-4/10. Remaining 1-2/10 belonged to nilas in the leads and fractures.

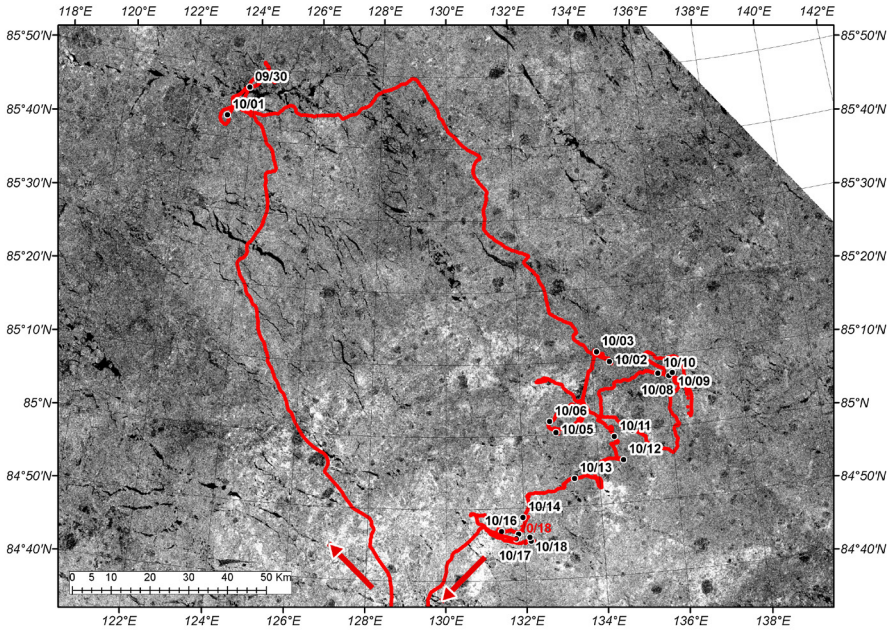

Fig. 5.1.6: Route of Akademik Fedorov within the area of MOSAiC experiment during 30 September – 17 October 2019. Background image – Sentinel-1 SAR for 2019-10-06 06:27UTC

During further research activity, between 6 and 17 October *Akademik Fedorov* repeatedly moored to big and vast ice floes, deploying three L-sites and two M-sites from a board. In general ice conditions in the working area did not undergo significant changes. An extensive anti-cyclone weather with frosts up to -25°C activated ice formation processes which resulted in higher up to 4/10 concentration of grey-white ice, appearance of some quantities of thin first stage first year ice and grey ice on fractures and leads.

Extended ice and helicopter routing for that period was mainly based on the fourth source of the microwave imagery – the DLR TerraSAR-X mosaics of high to medium resolution of 60-70 meters in georeferenced PNG format obtained by AWI. Processing of the imagery included similar reprojection from Mercator to polar stereographic projection and conversion from PNG to GeoJPEG2000 for further visualization in a GIS. In a total 17 scenes were used to support identification of the floes for potential L- and M-sites deployments, helicopter navigation to identified objects for further *in-situ* measurements, transit navigation of *Akademik Fedorov* within the area and lastly her safe escape from the area without damage to DN.

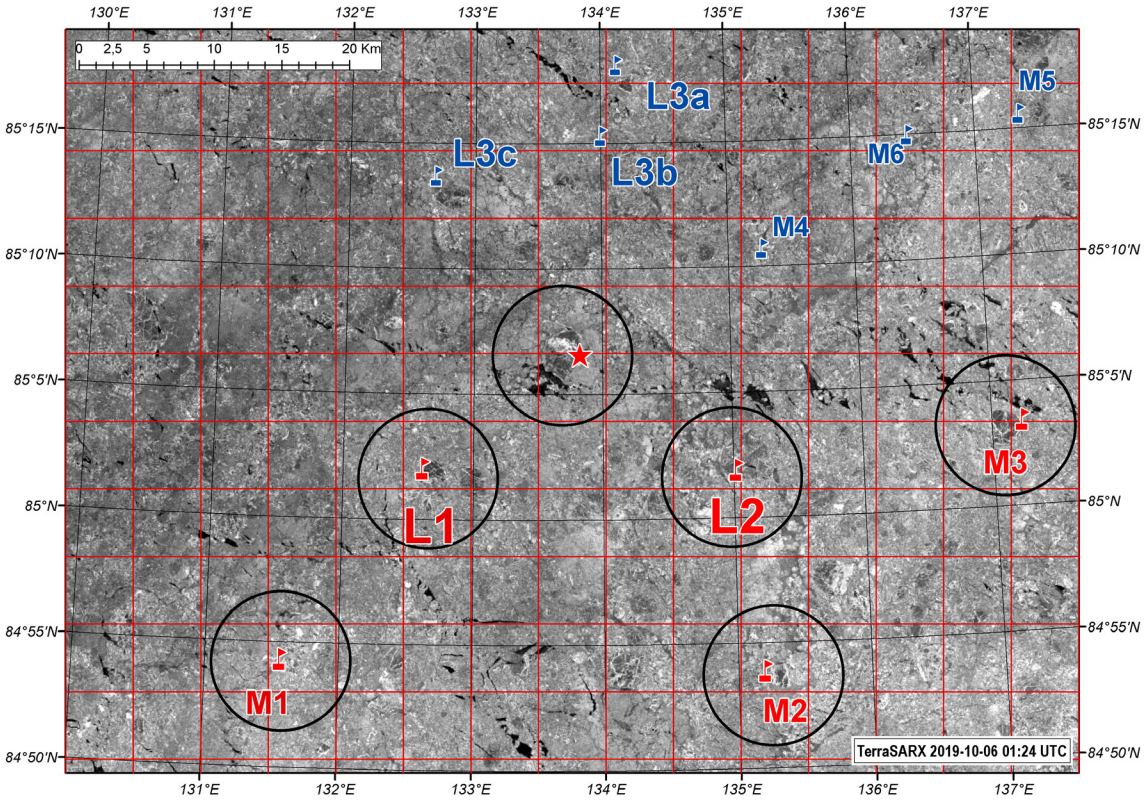

Fig. 5.1.7: Typical features of the ice floes on the X-band TerraSAR-X imagery used for identification of potential floes for L- and M-sites and ice routing between them. Background image – TerraSAR-X SAR for 2019-10-06 01:24UTC (credits: DLR, TSX/TDX AO: suman_OCE3562).

Sample imagery showing typical features of the ice floes on the X-band TerraSAR-X scene used for identification of the candidates for L- and M-sites deployment, is shown on Fig. 5.1.7. Typical necessary features included prominent darker color of the object from surrounding ice, well-formed roundish shape underlined by a whitish contour of the object edge, formed by the areas of ridged young ice round the object, and white lines of ridges serving as a skeleton for the level ice inside the floe. Objects identified by the specified criteria at the time of the shown

scene, included the L1, L2, M1, M2 and M3 floes marked by red color on Fig. 5.1.7. Objects marked by blue colour were chosen for further testing and deployments. It should be noted that not all of the selected objects met expectations. That included, for example, the first candidate for M2 (dark color floe 11 km westward), dark well-shaped floe marked as L3a, etc. Prior to flights, printed annotated imagery was distributed to helicopter pilots and ice specialists to facilitate the process of floe search.

Finally, the TerraSAR-X imagery together with the latest snapshot of the DN buoys was used to avoid collision of *Akademik Fedorov* with the buoys while escaping the area of DN. Route of the vessel moving westward from DN through the fracture zone on 18 October 2019 is shown on Fig. 5.1.8.

On October 18 3:20 MSK *Akademik Fedorov* started her return transit to the port of Tromsø from the point 84°46‘N 132°03’E. General ice conditions for the period 18 – 22 October are illustrated by the AARI ice analysis chart shown on Fig. 5.1.9. Due to continuous ice formation, sea ice conditions became more complicated for the ship routing. At several segments the vessel routed through the compact ice (10/10, no fractures) with average concentration of residual ice close to 5/10 (ice thicknesses 50-70 cm – 3-4/10, 70-100 cm – 1-2/10) in a form of giant floes. Up to 2/10 of freshly formed thin first-year ice first stage (30 cm-40 cm) were observed with remaining 2/10 of grey-white ice and 1/10 of nilas. Very small fractures were observed quite rarely across the ship route.

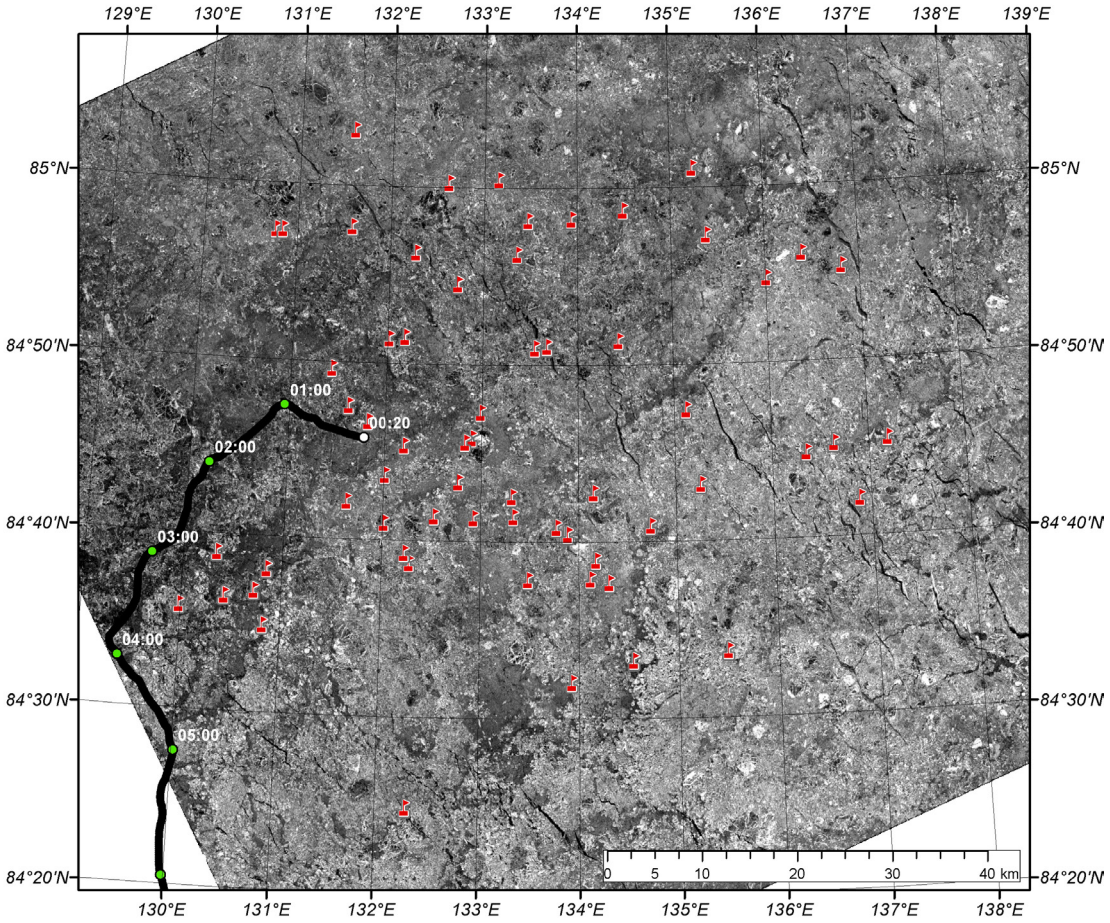

Fig. 5.1.8: Route of Akademik Fedorov while escaping the area of DN through the fracture zone on 18 October 2019 (hourly positions are shown). Background image – TerraSAR-X SAR for 2019-10-17 01:24UTC (credits: DLR, TSX/TDX AO: suman_OCE3562)

Bad visibility due to darkness, small and medium floes of residual ice consolidated into giant ones by the young and thin ice, presence of 10-20 high snow cover and considerable roughness of the ice cover on the ship ice radar embarrassed recognition of lighter conditions for ship routing. Several times the vessel was actually beset by complicated ice condition or inside floes of residual ice with averaged ice thickness distribution like 50-70 cm – 60 %; 70-120 cm- 30 %; 30-50 cm - 10 %. In such cases the vessel executed breaks through with a help of numerous attacks using power of all 4 engines.

Southward of 82°N predominant orientation of the fractures become NW-SE which allowed much easier ice routing. The sea ice remained compact but the predominant stage of development changed to grey-white ice with partial concentration 7-8/10. Closer to the ice edge partial concentration of residual ice was 5-6/10 again but its prevailing form was small and medium floes, with other tenths belonging to young and new ice.

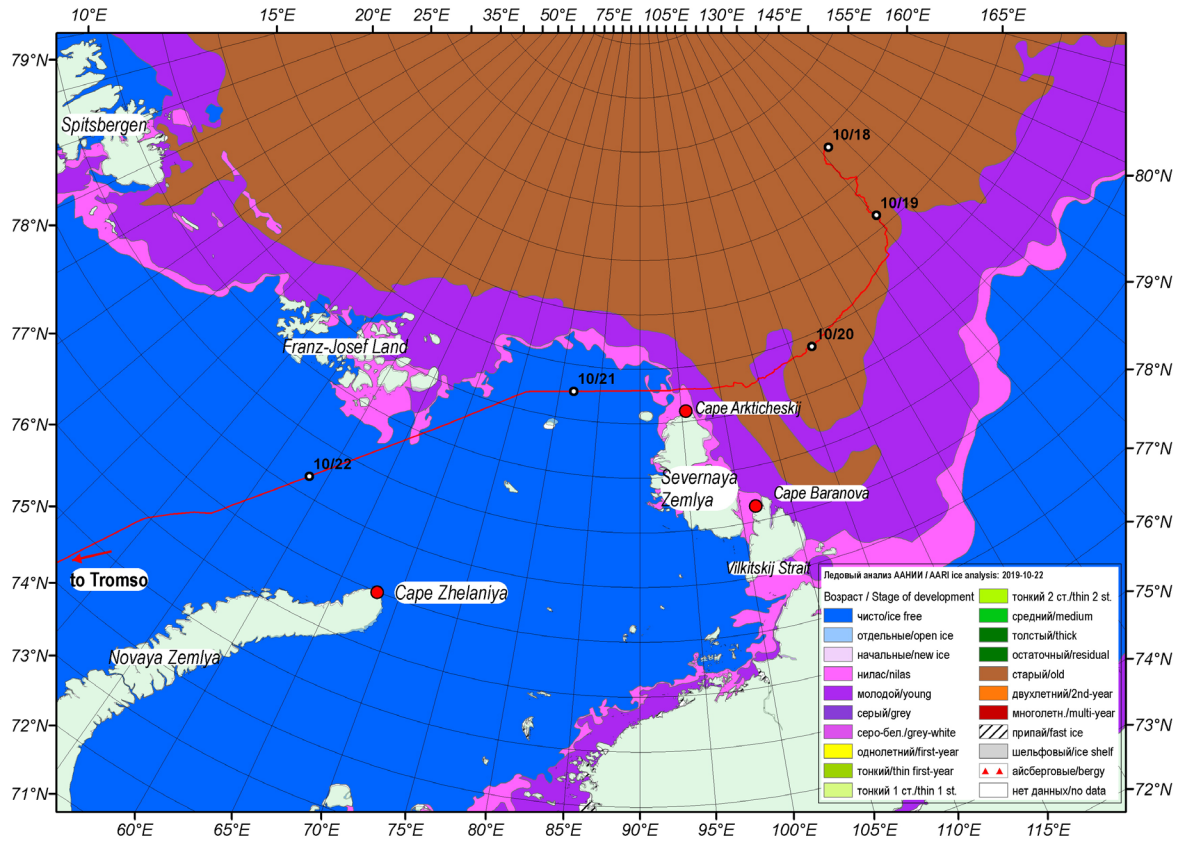

Fig. 5.1.9: Route of Akademik Fedorov from the area of MOSAiC experiment. Background image – AARI ice analysis chart for 22 October 2019, colouring based on predominant stage of ice development.

Ice observations were closed on October 20 at 19.37 MSK in coordinates 81°35'N 94°04'E after crossing diffuse ice edge in a form of a vast zone of pancake ice. Total length of ice navigation constituted approximately 2,600 km.

Preliminary results

Averaged ice thickness distribution: Results from bridge observations performed by AARI ice observer.

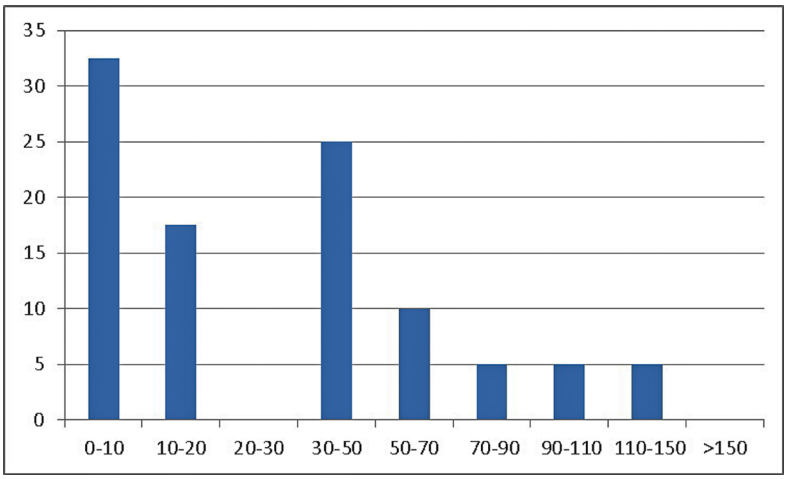

Fig. 5.1.10: Averaged ice thickness distribution on transit from Tromsø to the area of the MOSAiC main ice floe search

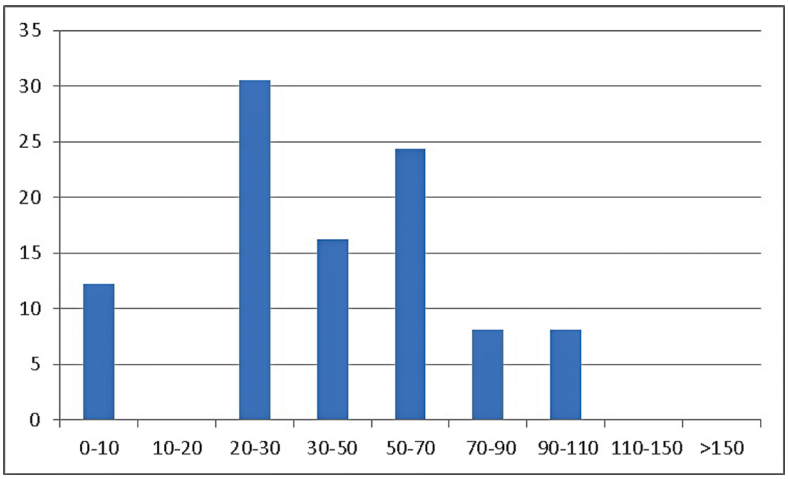

Fig. 5.1.11: Averaged ice thickness distribution at the area of search of the MOSAiC main ice floe and the distributed network (DN) deploying

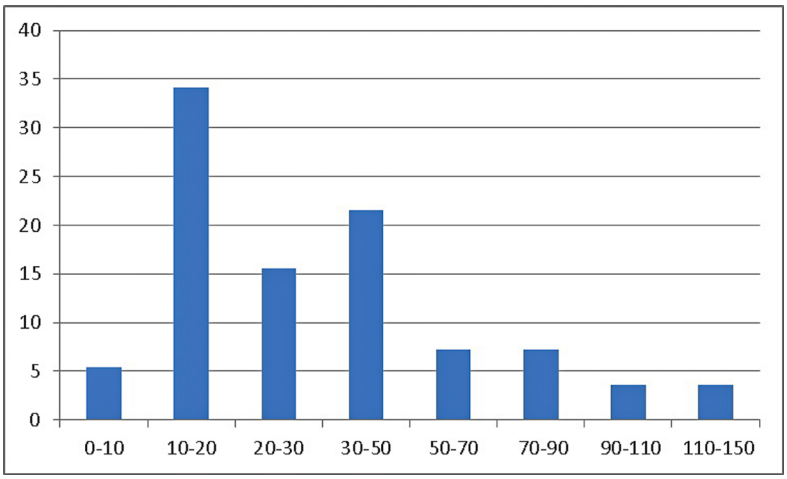

Fig. 5.1.12: Averaged ice thickness distribution on transit from the working area to the port of Tromsø

Data management

MOSAiC data in this project is published at the PANGAEA data repository (World Data Center PANGAEA Data Publisher for Earth & Environmental Science (www.pangaea.de)). All data are handled, documented, archived and published following the MOSAiC data policy.

- Smolyanitsky, Vasily (2019): Navigation track of Akademik Fedorov during pre-MOSAiC project phase with 10 minute interval for 21 September - 25 October 2019. PANGAEA, https://doi.org/10.1594/PANGAEA.909433.
- Sentinel-1 EW HH/HV scenes with 90 m resolution over the areas of search of the floes for MOSAiC experiment and Akademik Fedorov navigation for 18 September – 18 October 2019 – https://scihub.copernicus.eu/dhus/.
- Timofeeva, Anna; Smolyanitsky, Vasily; Bessonov, Vladimir; Petrovskiy, Tomash (2020): Special sea ice observations aboard Akademik Fedorov MOSAiC leg 1, 2019-09-25 - 2019-10-20. PANGAEA, https://doi.pangaea.de/10.1594/PANGAEA.912021.

References

AARI regional ice charts of the Arctic seas and ice covered seas of Russia for 1997-2019 in the WMO SIGRID-3 exchange format // World Data Center on Sea Ice – Global Digital Sea Ice Data Bank – http://wdc.aari.ru/datasets/d0004.

Buzuev AY, Dubovtsev VF, Zakharov VF and Smirnov VI (1988) Conditions of ship navigation in the seas of Northern Hemisphere (Uslovia plavaniya sudov vo l'dah Severnogo polushariya). In Russian. M.: Izd. GUNIO MOUSSR, 280 p.

Flanders Marine Institute (2018) IHO Sea Areas, version 3. Available online at http://www.marineregions.org/, https://doi.org/10.14284/323.

Manual on conduction of ice air reconnaissance (Rukovodstvo po proizvodstvu ledovoi aviarazvedki) (1981) In Russian. L. Gidrometeoizdat. 240 p.

SIGRID-3 (2014) A vector archive format for Sea Ice Georeferenced Information and Data - JCOMM Technical Report Series No. 23, WMO/TD-No.1214.

Ice Chart Colour Code Standard (2004) JCOMM Technical Report Series No. 24, WMO/TD-No.1215.

World Meteorological Organization (2017) Sea Ice Nomenclature, WMO-No.259.

5.2 Use of Satellite Data to Support the Search of the MOSAiC Ice Floe

Vladimir Bessonov[1] [1]AARI

Grant-No. AF-MOSAiC-1_00

Objectives

Prior the start of the MOSAiC campaign, Arctic and Antarctic Research Institute (AARI) monitored sea ice conditions in the area around 85°N, 130-140°E in order to identify suitable floes to establish the MOSAiC base camp. In this chapter, we briefly review the ice conditions prior the start and describe the floes that were identified as potential candidates for MOSAiC.

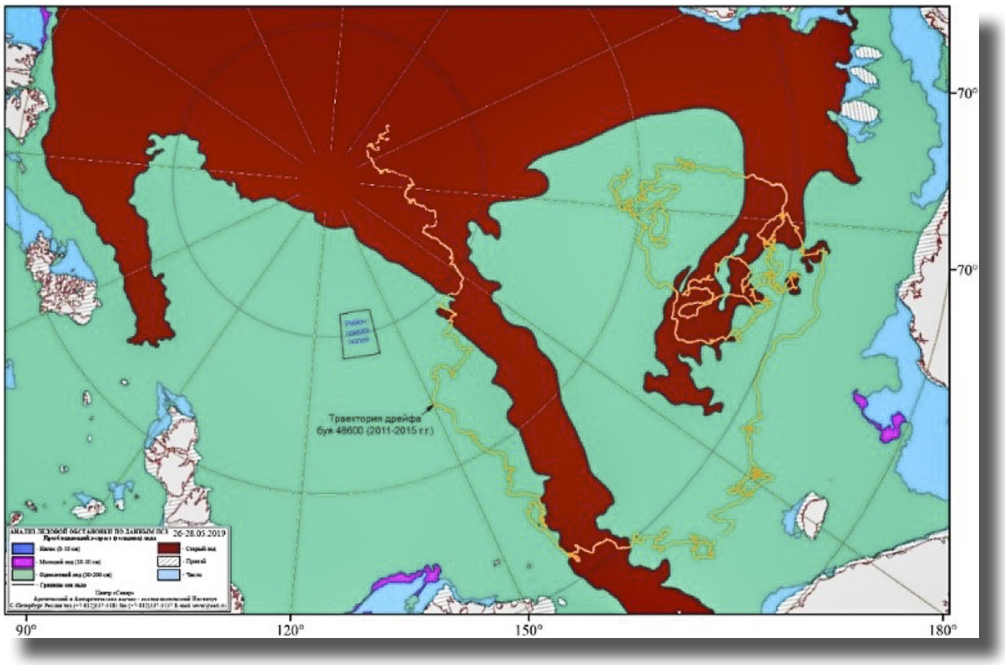

Fig. 5.2.1: The map of age distribution of the drifting ice in the Arctic basin for May 28, 2019 was prepared on the basis of radar imagery from the European satellites of the Sentinel-1 series

Work prior to the expedition

Continuous monitoring of ice conditions prior the start of the expedition has showed that the sea ice age distribution in the Arctic basin during the spring period of 2019 was characterized by a lack of the two-year and multiyear ice floes in the area of interest.

In recent years observations of trajectories of the movement of the drifting buoys and ice floes at the choice of one of them for the purpose of opening on it of the new drifting North Pole station showed that old ice never crossed in the western direction 150th meridian approximately before the latitude 86-87 degrees. It is confirmed by a drift track of a buoy 48600, which of all buoys drifted on the most western track. Collected information allowed to draw a conclusion about impossibility of a meeting of old ice in the planned area of search of ice floes.

With emergence at the end of August of pronounced ice floes there was the first possibility of separation from them some of the ice fields, which selected in comparison with surrounding ice floes around on many signs and to begin monitoring of them as potential ice floes from the point of view of creation on one of them of the base camp of the forthcoming expedition.

Potential ice floes were significantly distinguished from other ice fields thanks to the increased display brightness on satellite imagery and were well identified on data of visible range which arrived with the Terra and Aqua artificial satellite with the resolution of 250 m. Besides brightness of display, the ice field had the essential sizes, one of them reached the size of 10x10 km that considerably facilitated their identification on satellite images and when performing possible aviation ice investigations, especially in bad weather conditions that is the most frequent phenomenon in the Arctic. High brightness of display of this ice field, at times even through leaky cloudiness, was explained significantly by a smaller sea ice destruction of their top surface, and, therefore, and an indirect sign of the bigger ice thickness at this ice field in comparison with existing nearby that allowed to carry them to a number of potential ice fields. On this sign a number of ice floes was selected and continuous monitoring of them began with the second half of August.

At the same time potential ice floes were identified also on the radar images arriving with the Sentinel-1 artificial satellite that is extremely important monitoring element allowing to carry out it under any weather conditions which, as a rule, significantly complicate work of ice observers and analysts in the Arctic. Simultaneous monitoring of ice objects when using different types of satellite information (visible range, radar range) promotes obtaining the greatest possible continuous volume of information opening ample opportunities for the solution of a big circle of tasks in the Arctic.

Work at sea

With receiving on September 16, 2019 in the visible range with the Terra satellite on which the most part of the high latitude region of the Arctic was open from cloudiness similar ice objects worked well to add the satellite image to the existing number of potential ice floes some more. Further it was offered to break the extensive area, in which there were these ice fields, on 5 areas, started with the most east:

1 area (Site #1) was located around the 180th meridian. In this area a number of well remained ice floes among which on many signs the probability of presence here of old ice fields was rather high was observed. In case of the preliminary notice about interest in this area it would be possible to find in it not only old ice floes, but also multiyear ice floes. For obtaining such information it was required to carrying out a separate careful research.

In the 2nd area (Site #2) one well remained ice floe was located with a size of 6.6x7.2 km.

In the 3rd area (Site #3) one decent ice floe with a size of 3.7x4.6 km was identified (Fig. 5.2.4) Subsequently *Polarstern* found in the south of this area the ice floe, small by the sizes (2.6x3.9 km) which satisfied all not only on the structure, but the most important on the region of its location

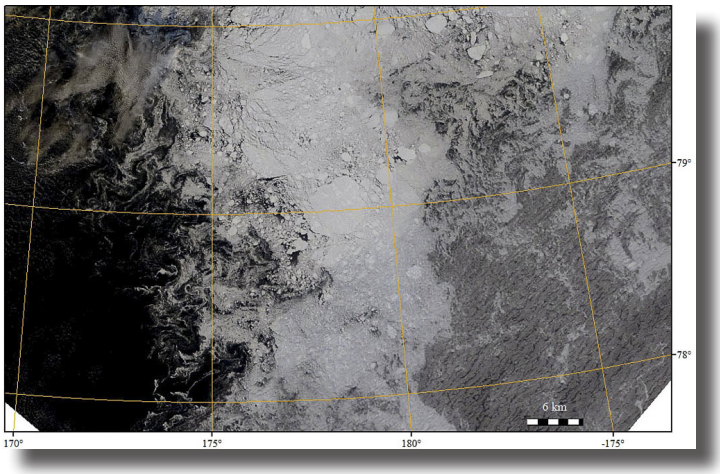

Fig. 5.2.2: Ice conditions in east region of the Arctic basin according to visible range from the Terra artificial satellite for September 18, 2019

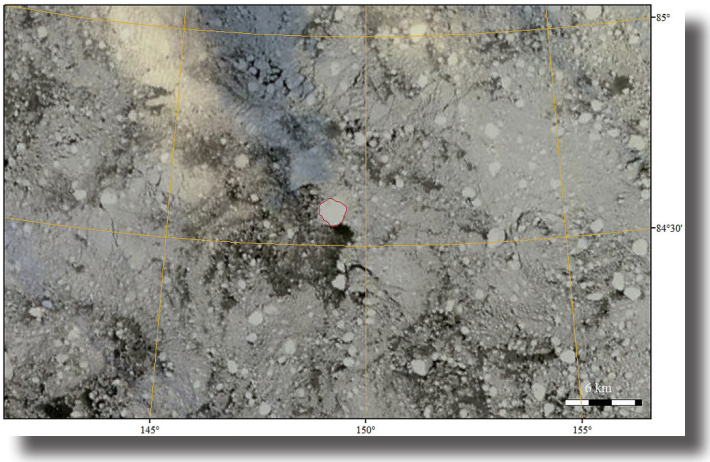

Fig. 5.2.3: Ice conditions in the high latitude region of the Arctic basin (the area 2) according to visible range from the Terra artificial satellite for September 16, 2019. The contour of the potential ice floe is highlighted with red color.

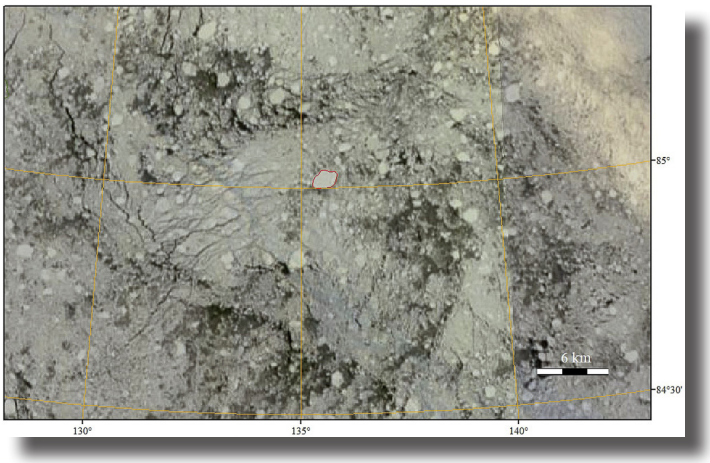

Fig. 5.2.4: Ice conditions in the high latitude region of the Arctic basin (the area 3) according to visible range from the Terra artificial satellite for September 16, 2019. The contour of the potential ice floe is highlighted in red colour.

4th area was broken into two subdistricts of "a" and "b" because of a large number of ice floes. Among this ice field in the area 4a (Site #4a) the most considerable ice floe by the sizes (10.5x10.5 km) was. Observations of it were the longest, since August 23. This ice field was selected with the maximum brightness of display on visible range satellite images and significantly distinguished from all drifting ice in radar pictures. The ice field was rounded shape that was a stability sign to splits possible in the future, and during the entire period of observations of it did not change the form, i.e. a splitting off of parts of this ice field was not observed. The only lack of this ice field was the unsatisfactory region of its location.

At the end of the day on September 28 *Akademik Fedorov* approached this ice field, then its research in an ice edge zone began. The first research of the similar potential ice floe showed that at its top surface there is a large number of puddle and ice thickness is non-uniform, fluctuating from 20 to 120 cm. The ship locator showed existence of a large number of ridges of hummocks which kept the ice field from destruction. It became obvious that all similar potential ice floes will have close characteristics.

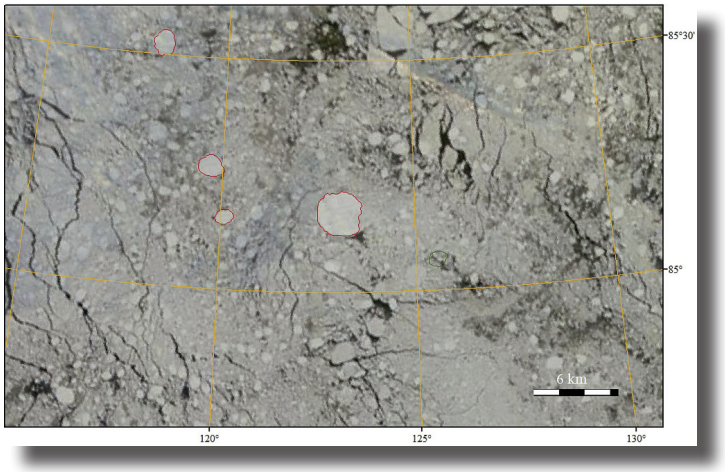

Fig. 5.2.5: Ice conditions in the high latitude region of the Arctic basin (the area 4a) according to visible range from the Terra artificial satellite for September 16, 2019. Contours of potential ice floes are highlighted in red colour.

The area 4b (Site #4b) on abundance of well remained potential ice floes and deployment of distributed network around the basic ice field was the most preferable. In a northern part of the area in the ice field of an ice breccia, big by the sizes, the extensive ice floe the sizes of 5.6x6.0 km which had according to radar shootings with the Sentinel-1 artificial satellite, the most level surface as against other potential ice fields was selected. In the future on this ice field it would be possible to equip a runway in any part of the ice field.

Summer drift of sea ice in this area promoted carrying out of this ice field from even more northern region of 87° N that more best condition of its surface and bigger ice thickness in comparison with other ice fields was an indirect sign. Its only short comings were besides its location and, according to the captain of the vessel *Akademik Fedorov*, a large number of the extensive ice floes which were sharply reducing freedom of maneuvering of the vessel during the work in the drifting ice during arrangement of the distributed network.

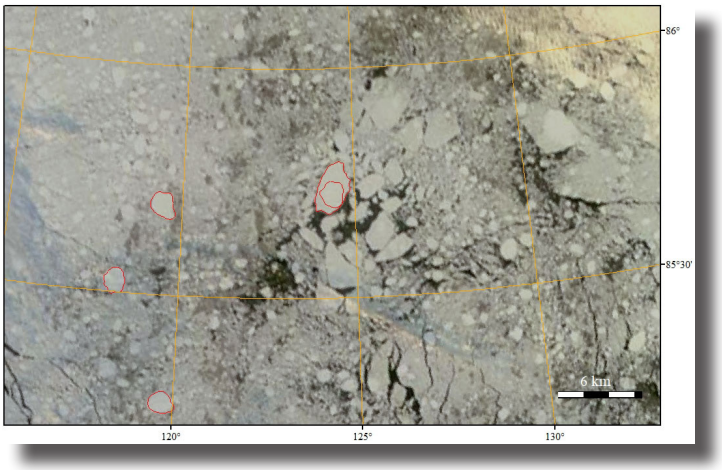

Fig. 5.2.6: Ice conditions in the high latitude region of the Arctic basin (the area 4b) according to visible range from the Terra artificial satellite for September 16, 2019. Contours of potential ice floes are highlighted in red colour

The area 5 (Site #5) was the most southern area at which there was the only potential ice floe extensive the size (7.6x10.9 km). As well as many potential ice floes, during the summer period this ice field moved as a result of drift from more northern area to southern, having appeared at the end of September near an edge of the drifting ice. The circumstance mentioned above promoted significantly bigger destruction of the ice field unlike other ice fields. Despite bigger destruction to which the ice field underwent it still kept the integrity.

Existence of a large number of hummocks ridges which kept the ice field from destruction served as the reason of it. It was confirmed with a ship locator of *Akademik Fedorov* which closely approached on September 28 it and made ice investigation by the vessel board, having cut through its northernmost tip according to satellite data representing the most destroyed part of the ice field.

During ice investigation information which showed that ice in this part of the ice field was strongly destroyed was obtained, a large number of sediment was observed, both in ice, and on its surface and its thickness in an ice edge zone fluctuated from 20-30 cm to 60-70 cm of sedimenta on ice and in it confirmed the place of origin of the ice field in shallow areas near the coast. *Polarstern* in more detail too investigated it after passing by it the Russian vessel and came to a conclusion about impossibility of its use.

Preliminary results

Wide use of satellite information in search of ice floes for the organization of the MOSAiC expedition base camp showed its high efficiency. Because of this information it was possible to carry out strategic search of ice floes and planning of the movement of vessels of an expedition at different stages. Satellite information was the main source of data on a surrounding ice conditions.

Data management

Not applicable.

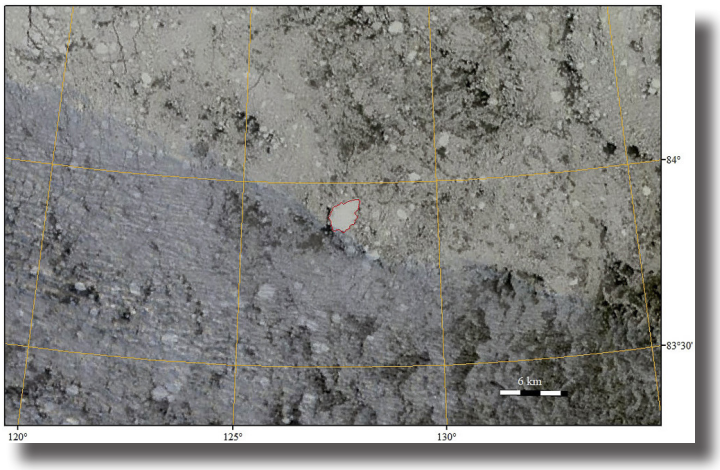

Fig. 5.2.7: Ice conditions in the high latitude region of the Arctic basin (the area 5) according to visible range from the Terra artificial satellite for September 16, 2019. The contour of the potential ice floe is highlighted in red color.

5.3 ASSIST ice watch observations

Daniel Watkins[1]
not on board: Jennifer Hutchings[1]

[1]Oregon State University

Grant-No. AF-MOSAiC-1_00

Objectives

Visual observations of sea ice provide information that is unavailable or unclear through satellite observations (Hutchings et al., 2018). Ice Watch observations using the Arctic Shipboard Sea Ice Standardization Tool (ASSIST) have been performed on ships throughout the Arctic starting in 2006 (Hutchings et al., 2016). The ASSIST protocol is based on the Antarctic Sea Ice Processes and Climate (ASPeCt) observation protocol, adapted to address differences between sea ice in the Arctic and the Antarctic. Ice analysis and ice watches to assist in navigation were provided by specialists from the Antarctic and Arctic Research Institute (AARI) of St. Petersburg. The purpose of conduct ASSIST-aided ice watches concurrently with AARI's observations is twofold. First, by coordinating Ice Watches on each of the six resupply cruises (including the Leg 1a cruise), we aim to compile a view of the seasonal progression of sea ice morphology over the MOSAiC year that will be compatible with Ice Watch observations from prior cruises. Second, through comparison with the continual, expert ice observations from AARI, we aim to quantify the biases introduced through hourly rather than continual sample, and the effect of using many inexperienced observers rather than a small number of experienced observers.

Work at sea

Volunteers were recruited via sign-up sheet following a brief presentation during the daily general meeting. Volunteers were then asked to attend a 45-minute presentation explaining the Ice Watch procedure and ASSIST software. When possible, volunteers were paired with experienced ice observers; however, for the vast majority of volunteers, this was the first opportunity for participating in an ice Watch.

While the ship was in transit, Ice Watches were carried out hourly, 24 hours per day. At the start of each hour, two volunteers climbed to the 8th deck and retrieved the camera and binoculars from an old radio room that the captain made available for Ice Watch. Walking out to the observation deck, observers spent five minutes on each side of the ship noting ice concentration, dominant ice types, floe size, topography, snow cover, weather conditions, and ,with the aid of a striped pole on attached to the port side by the crew, thickness of overturned sea ice. Ship data, either from the readouts in the dry lab or the mess hall, as also recorded. At least one photo was taken from each side of the vessel. After the 10 minute observation period, ASSIST software was used to record the observations. In addition to ice and weather observations, volunteers were asked to note if birds or marine mammals were noted. Very few fauna were observed.

Tab. 5.3.1: Typically Ice Watches are carried out by a small number of volunteers working in multiple shifts. Here, 46 members of the MOSAiC expedition participated in Ice Watches, including all 21 members of the MOSAiC school, bear guards, teachers, journalists, and scientists.

Volunteers	
Alex Mavrovic	Long Lin
Anika Happe	Marc Oggier
Anne Gold	Marlene Goering
Audrun Tholfsen	Marylou Athanase
Carrie Harris	Mauro Hermann
Chris Basque	Michel Tsamados
Chris Cox	Misha Krassowski
Christian Zoelly	Natalia Ribeiro Santos
Daisy Dunne	Nathan Kurtz
Daniel Watkins	Neil Aellen
Ewa Korejwo	Oguz Demir
Falk Ebert	Philipp Griess
Francesca Doglioni	Pierre Priou
Guangyu Zuo	Robbie Mallett
Hans Honold	Rosalie McKay
Ian Raphael	Ryleigh Moore
Igor Vasilevich	Sam Cornish
Jakob Belter	Sean Horvath
Jari Haapala	Thea Schneider
Josefine Lenz	Thomas Rackow
Julika Zinke	Trude Hohle
Katie Gavenus	Tatiana Matveeva
Lisa Craw	William Shaw

Preliminary results

Observations were primarily made during the transit to and from the Distributed Network area. Transit times between stations were short, so only a few observations were made within the network. Most ice observed was relatively thin first year ice, ranging from 30-50 cm except in a few areas of heavy ridging. Occasionally second-year ice was seen, with characteristic frozen-over meltponds and greater thickness. The ship preferentially traveled in leads. During the exit transit stage, much greater ice thickness was encountered. In one particularly thick section, the vessel required more than 40 attempts to break through a patch of thick second year ice. Ice concentration was noticeably higher on the return trip, with 10/10 compact ice up until shortly before the ice edge.

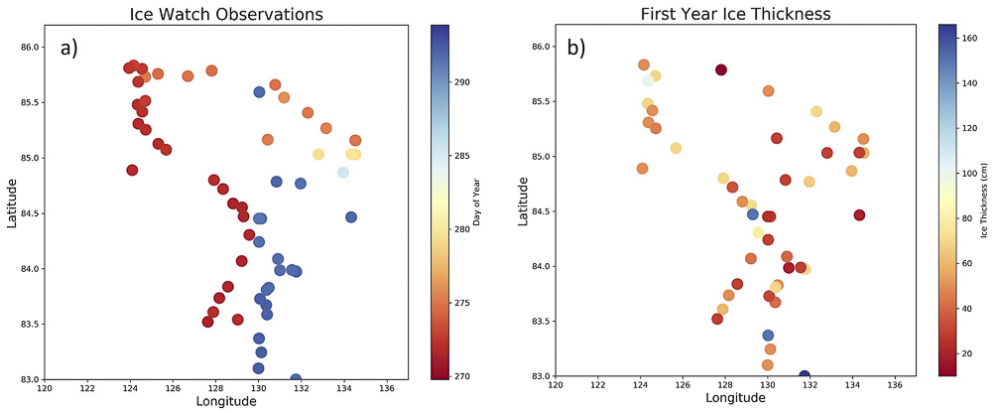

Fig. 5.3.1: (a) Ice watch observations by day of year (b) Thickness of first year ice along cruise track

Data management

Data access is provided through the Ice Watch website (icewatch.gina.alaska.edu). This data is open to the public, and visualization tools are provided.

Data will be stored at either at the PANGAEA data repository (World Data Center PANGAEA Data Publisher for Earth & Environmental Science www.pangaea.de or at the Arctic Data Center (arcticdata.io), which is supported by the National Science Foundation (NSF) and DOIs provided to PANGAEA according to the agreement between Arctic Data Centre and PANGAEA.

All data are handled, documented, archived and published following the MOSAiC data policy.

References

Hutchings JK, Hughes N, Orlich AR, MacFarlane S, Cowen A, Farmer L et al. (2016) Ice Watch: standardizing and expanding Arctic ship based sea ice observations. White paper presented at Arctic Observing Summit (Fairbanks, AK).

Hutchings JK and Faber MK (2018) Sea-Ice Morphology Change in the Canada Basin Summer: 2006 – 2015 Ship Observations Compared to Observations From the 1960s to the Early 1990s. Frontiers in Earth Science, 6(August), 2006–2015. https://doi.org/10.3389/feart.2018.00123

5.4 Weather and ice forecasts

Thomas Rackow[1], Jari Haapala[2], Thomas Krumpen[1], Andreas Raeke[3], Mauro Hermann[6], Tatiana Matveeva[6], Natalia Ribeiro Santos[6], Francesca Doglioni[6], Carrie Harris[6], Neil Aellen[6], Alex Mavrovich[6], Igor Vasilevich[6], Julika Zinke[6], Lisa Craw[6], Thea Schneider[6], Marylou Athanase[6], Anika Happe[6]
not on board: Helge F. Goessling[1], Jean-François Lemieux[4], Amy Solomon[5]

[1]AWI
[2]FMI
[3]DWD
[4]ECCC
[5]NOAA
[6]MOSAiC School

Grant No. AF-MOSAiC-1_00

Objectives

The purpose of the weather and ice forecasting efforts was to assist daily expedition planning, including informed decisions on feasibility of helicopter operations and likely ice conditions and their changes over time in the proximity of the various L and M site candidates. To this end, regular morning sessions were held where Jari Haapala and Thomas Rackow provided short overviews of the expected weather and ice conditions during the day to expedition lead (Fig. 5.4.1).

Data that has been used includes 10 m winds and 2 m temperature from ECMWF and DWD (see Table 5.4.1 below). All data was downloaded via FTP, using the Iridium satellite network. Due to the very limited bandwidth and frequent interruptions, global model data had often been split into smaller spatial subsets to speed up download times. For example, meteorological data from ECMWF and DWD was available for our local area of interest, centered around *Polarstern*. On request, Amy Solomon and Jean-François Lemieux quickly split the larger images into smaller subpanels, which greatly sped up individual download times and made use of the NOAA and ECCC sea ice forecasts possible during the setup phase of the *Distributed Network*. Their forecasts for sea ice divergence and information for likely gradients in sea ice thickness turned out to be very useful during the search for appropriate L and M sites as well as for the setup phase. In addition to the more localized weather information available to us, large-scale meteorological information on sea level pressure has also been provided by the Meteorological Office on board *Polarstern* via email, which facilitated interpretation of the more local weather information greatly.

Following his YOPP lecture on drift forecasts, Thomas Rackow prepared a hands-on session with the programming language Python where the participants of the MOSAiC School were able to implement a simple sea ice drift forecast for an arbitrary location in the Arctic Ocean. The approach is based on the “free-drift” assumption, using 10 m winds from ECMWF, with a sea ice drift speed of 2% of the wind speed and a turning angle (relative to the wind direction) of -22.5°. Applied to all GPS positions of the *Distributed Network* (provided by Daniel Watkins*),* these parameter choices later turned out to provide quite realistic forecasts for the development of the network positions 2-3 day ahead (Fig. 5.4.2) when compared to the observed trajectories of the network. The simple tool can be run easily on the ship using the available model data (in NetCDF format) from ECMWF. The forecast has also been compared to the operational SIDFEx forecast product (led by Helge F. Goessling), which provides a consensus drift forecast for the central observatory and surrounding positions that is available on board *Polarstern* during the course of the MOSAiC expedition.

Tab. 5.4.1: The most relevant data that has been used on *Akademik Fedorov* for the purpose of forecasting weather, ice, and visibility conditions.

Data	Content	Type / Typical file size
ECMWF	Ensemble forecasts (Meteograms)	Image (PDF) / 70 KB
ECMWF	10 m winds, rel. humidity, 2 m temperature, mean sea level pressure, ice cover	NetCDF / 200-500 KB
DWD	10 m winds, rel. humidity, 2 m temperature, mean sea level pressure	NetCDF / 200-500 KB
DWD	ICON model soundings (ICON_ timesects), vertical atmospheric profiles	*.csv file / 50 KB
DWD	Large-scale sea level pressure maps	Image (GIF) / 100 KB via daily email
DWD	MetMaster data	*.sgz file / 40-50 KB via daily email
ECCC	Different sea ice forecasts, e.g. for divergence or ice thickness	Image (PNG) / 300-500 KB per panel
NOAA	Different sea ice forecasts, e.g. for divergence or ice thickness	Image (PNG) / 100-300 KB per panel
TerraSAR	X-Band radar scene, DLR	Geo-referenced images (PNG + wld+xml) / 2 MB per image
Sentinel-1	C-band radar scene, ESA	Geo-referenced images (GeoTIFF) / 2 MB per image

Weather overviews during the General Meetings

Several MOSAiC School participants presented weather forecasts during the daily General Meetings to all expedition members, with support from Thomas Rackow and Andreas Raeke (during the return transit to Tromsø). The last weather forecasts also included forecasts for the expected wave height and swells along the projected cruise track, which were provided by Andreas Raeke using the MetMaster tool from DWD. The necessary input data to do this ('sgz' format) has been provided by the Meteorological Office on board *Polarstern* via email.

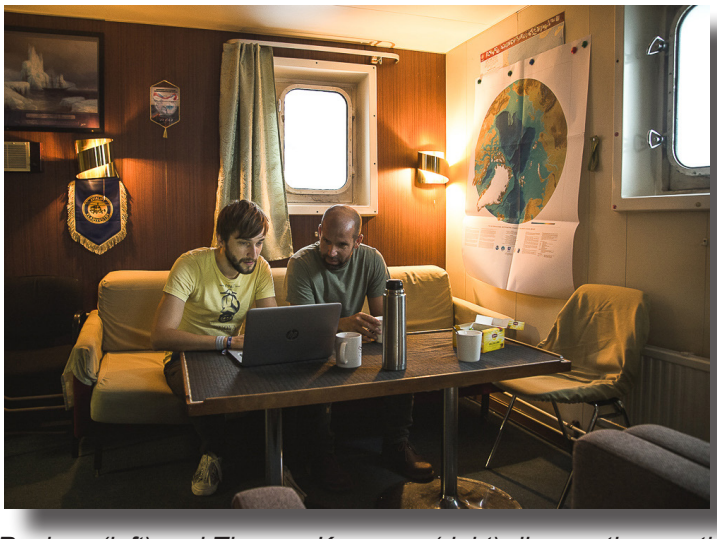

Fig. 5.4.1: Thomas Rackow (left) and Thomas Krumpen (right) discuss the weather, ice, and visibility forecasts for 26 September 2019 (photo by Thea Schneider).

Preliminary (expected) further results

During the cruise it became clear that ship navigation and floe selection, using satellite data with several hours or even up to a day of time lag between observations, can be very challenging since characteristic features and leads within the sea ice cover will be subject to drift during this time period. Because one cannot rely on the old positions alone, these features need to be somehow identified on the ship's radar to have a good idea about the exact ship position within the sea ice, especially because the large number of already deployed instruments of the *Distributed Network* must not be harmed. It is thus expected that the DN forecasting (Fig. 5.4.2) and the workflow for providing local weather information at limited available bandwidth will be of great use to upcoming supporting cruises during the other legs of the expedition.

Data and code management

All Python code and Jupyter notebooks will be made available at github.com. The code that was developed during the cruise will also be made available on a Ubuntu laptop (along with a documentation of the used workflow) and handed over to the next supporting vessels for the other legs of the MOSAiC expedition.

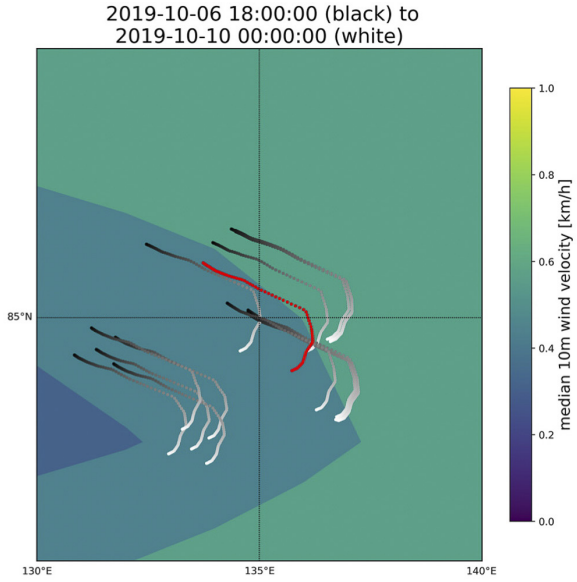

Fig. 5.4.2: A re-forecast for the positions of the Distributed Network, initialized on 6 October 2019 18:00:00 UTC. Red is Polarstern's 3-day forecast, the other trajectories are for all remaining GPS buoys that had already been deployed at that time (drift is from black to white). The forecast is based on ECMWF 10 m winds under the free-drift approximation. (The code will be available at github.com)

Links (FTP) to used data, requires registration

data.dwd.de (ICON and ECMWF model forecasts for relevant variables (ECMWF/ICON-MapView), profiles (ICON-soundings), meteograms, ensemble forecasts (ENS-ECMWF), …)

ftp1.esrl.noaa.gov (NOAA sea ice forecast data)

depot.cmc.ec.gc.ca (ECCC sea ice forecast data)

ftp.coas.oregonstate.edu (*Distributed Network* GPS positions)

5.5 Airborne ice thickness measurements

Thomas Krumpen[1], Jan Rohde[1], H. Jakob Belter[1], Anna Timofeeva[2]

[1]AWI
[2]AARI

Grant No. AF-MOSAiC-1_00

Objectives

To aid the search for the MOSAiC ice floe, MI-8 helicopters regularly took off from and landed on the accompanying Russian icebreaker *Akademik Fedorov*, taking aerial measurements with a sensor dubbed the electromagnetic (EM)-Bird. The device, which measures ice thickness in the direction of flight, makes it possible to initially survey potential ice floes, after which the ships can take a closer look at the most promising candidates. Once the MOSAiC floe was found additional more detailed survey flights were conducted above the floe and in its vicinity

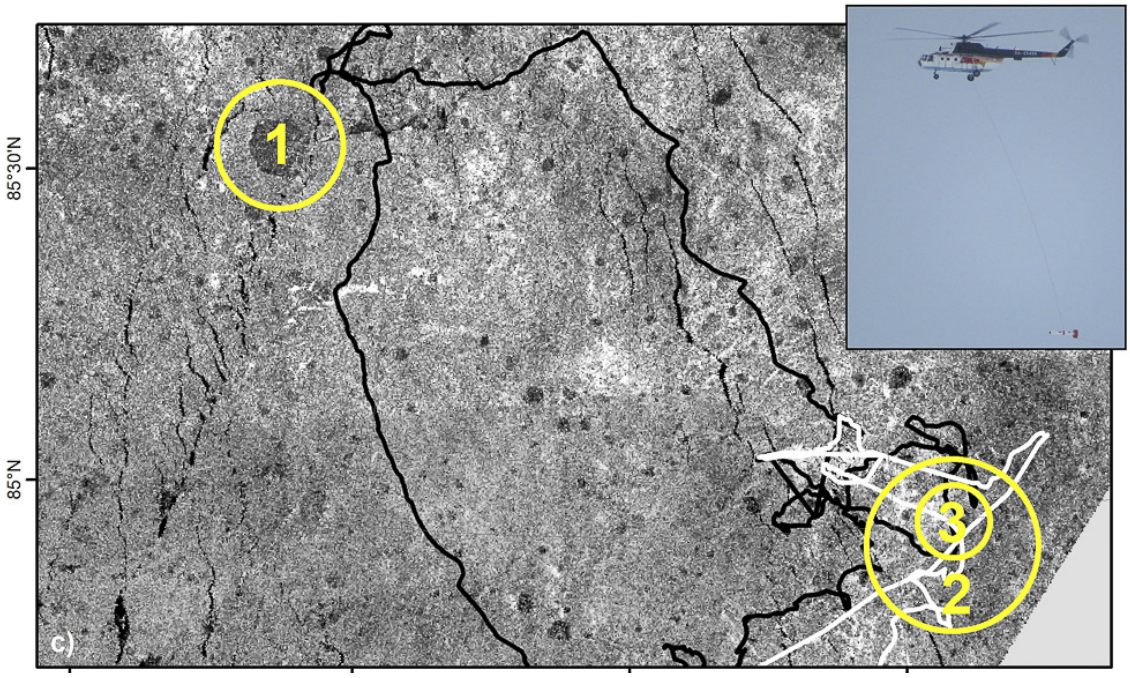

Fig. 5.5.1: EM-Bird surveys performed on 30 September, 2019 (yellow circle, #1), on 13 October, 2019 (yellow circle #2, vicinity of the MOSAiC floe) and on 14 October, 2019 (yellow circle #3, survey over MOSAiC floe).

Work at sea

An overview of all EM sea ice thickness measurements made during the cruise is given in Fig. 5.5.1. A table listing all flights performed between Sep. 30t, 2019 and October 15, 2019 is provided in the Appendix (Station List Helicopter Surveys). The EM method works as follows: EM ice thickness measurements utilize the contrast of electrical conductivity between sea water and sea ice to determine the distance of the instrument to the ice-water interface (Haas et al., 2009). Surveys were conducted with a MI-8 helicopter operated by Narjan-Marski from

the *Akademik Fedorov*. The accuracy of the EM measurements is in the order of ± 0.1 m over level sea ice (Pfaffling et al., 2007). The AEM thickness data enables us to determine the general thermodynamic and dynamic boundary conditions of ice formation (Thorndike et al., 1975). The most frequently occurring ice thickness, the mode of the distribution, represents level ice thickness and is the result of winter accretion and summer ablation. For details about data processing and handling we refer to (Haas et al., 2009; Krumpen et al., 2016).

Preliminary results

Not available yet.

Data management

All data will be made available shortly after the MOSAiC campaign on the MOSAiC Central Storage (MCS).

Data will be stored at the PANGAEA data repository (World Data Center PANGAEA Data Publisher for Earth & Environmental Science (www.pangaea.de)).

All data are handled, documented, archived and published following the MOSAiC data policy.

References

Haas C, Lobach J, Hendricks S, Rabenstein L, Pfaffling A (2009) Helicopter-borne measurements of sea ice thickness, using a small and lightweight, digital EM system. Journal of Applied Geophysics, 67(3):234-241.

Krumpen T, Gerdes R, Haas C, Hendricks S, Herber A, Selyuzhenok L, Smedsrud LH, Spreen G (2016) Recent summer sea ice thickness surveys in Fram Strait and associated ice volume fluxes. The Cryosphere, 10:523-534.

Pfaffling A, Haas C, Reid JE (2007) A direct helicopter EM sea ice thickness inversion, assessed with synthetic and field data. Geophysics, 72:F127-F137.

Thorndike AS, Rothrock DA, Maykut GA, Colony R (1975) The thickness distribution of sea ice. Journal of Geophysical Research, 80(33):4501-4513.

6. EDUCATION, OUTREACH, MEDIA

Josefine Lenz[1,2], Anne Gold[3],
Katharina Weiss-Tuider[1]

[1]AWI
[2]APECS
[3]U Colorado

Grant-No. AF-MOSAiC-1_00

General Objectives

The MOSAiC expedition and scientific activities provide a unique opportunity to inspire a wide audience and engage them in exploring MOSAiC science. By harnessing the public's fascination with the Arctic and the excitement of this year-long expedition, coordinated MOSAiC communication, outreach and education efforts promote a broader understanding of the changing Arctic and the societal implications of these changes, and inspire a future generation of potential scientists. The education, outreach and media activities aim to maximize the societal impact and broad reach of MOSAiC by working with across MOSAiC partner countries and organizations. The wealth of scientific knowledge and practical expertise onboard and during ice work further offers a unique opportunity to train the next generation of polar researchers. The education and outreach activities target to reach audiences from university graduate and undergraduate students, secondary students, teachers, science-interested public and visitors of informal science exhibits. The media activities and campaign additionally aim to inform the general public on science-related aspects of MOSAiC, e.g. the international collaboration and multidisciplinary approach of the expedition. Furthermore, the media activities include the production of sustainable and internationally recognized outreach products such as a high-end TV documentary.

6.1 MOSAiC School

Josefine Lenz[1,2], Thomas Rackow[1]
not on board: Gerlis Fugmann[1,2], Anja Sommerfeld[1], Andrea Schneider[2,3], Lisa Grosfeld[1,2]

[1]AWI
[2]APECS
[3]U Tromsø

Grant-No. H2020 ARICE Project Nr. 730965, further support was gratefully received from IASC, CliC and YOPP.

Objectives

A unique opportunity for a 6-week long training was offered to 20 early career researchers during leg 1a on *Akademik Fedorov* (Fig. 6.1.1). With the help of 30 reviewers, they have been selected from about 250 applications from 35 countries through a rigorous evaluation process. Coming from a wide background of environmental research backgrounds in physics, physical geography, glaciology, oceanography, geochemistry, geology, climate sciences, applied mathematics, biology, hydrology, remote sensing and modelling, and being early in their career, for most of them it was the first experience in the Arctic or on an icebreaking research vessel.

The aim of the MOSAiC School was to

- Train and educate the next generation of Arctic system science experts
- Provide support to the MOSAiC teams and
- Communicate the newly gained knowledge and experience by developing MOSAiC Ambassadors' projects

Fig. 6.1.1: Twenty early career researchers led by Josefine Lenz on the sea ice at site L3

In practical, the MOSAiC School was organized in 4 parts (Fig. 6.1.2), with 3 phases onboard *Akademik Fedorov*.

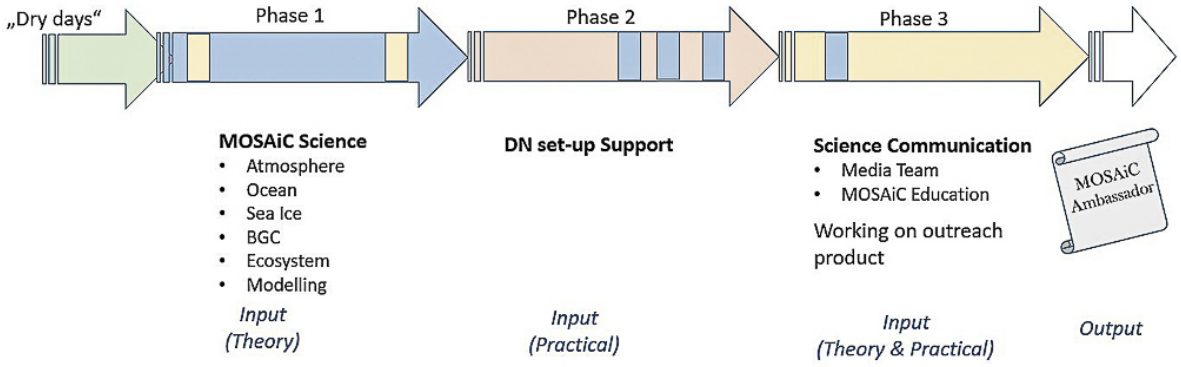

Fig. 6.1.2: The structure of the MOSAiC School in 3 phases (color coding according to table 6.1.1)

During the "dry days" in Tromsø/Norway (16-20 Sept 2019), the MOSAiC School focused on team building, logistical tasks and discussions on challenges on long ship-based expeditions. Also, first lectures were held on the MOSAiC project in general and its management by Markus Rex and Anja Sommerfeld, as well on social-economic impacts of Arctic Change by Stanislav Ksenofontov.

During the journey into the sea ice (phase 1, 21 Sep. - 4 Oct. 2019), lectures on the MOSAiC themes Atmosphere, Sea Ice, Ocean, Biogeochemistry, Ecosystem, as well as lectures and exercises on modelling were provided to the participants. Once the central MOSAiC ice floe was identified at around 85°N, all 20 participants were working on the ice to help setting up the distributed network of scientific stations around the central ice floe (phase 2, 5-18 Oct. 2019). Additionally, they were involved in logistic support, such as unloading/loading and snowmachine driving, as well as ice and bear watch. Lectures were reduced during phase 2. On the return journey to Tromsø (phase 3, 19-28 Oct 2019), lectures on science communication were given by journalists and educators, and all participants were working on their MOSAiC Ambassadors projects.

During the full year of the MOSAiC Expedition, the participants of the MOSAiC School will communicate their acquired knowledge and experience to their institutions, home countries and beyond.

All phases offered different educational focus but plans were adapted according to field plan changes in order to use time most efficiently, e.g. with intermediate science and communication lectures. Table 6.1.1 summarizes lectures and workshops held during the MOSAiC School.

Tab. 6.1.1: Lectures of the MOSAiC School (colors refer to figure 6.1: green=general preparation, blue=MOSAiC/Science themes, yellow=education, outreach & media themes)

Date	Presenter	Title	Affiliation	Category
17. Sep	Josefine Lenz & Gerlis Fugmann	Welcome, introduction to APECS and the MOSAiC School	APECS, AWI	General
17. Sep	Stanislav Ksenofonotov	Social-ecological systems in the context of global change	Ammosov North Eastern Federal University	General
18. Sep	Josefine Lenz	Communication & Conflict Management	APECS, AWI	General
18. Sep	Andrea Schneider	Panel discussion on Challenges on long ship-based expeditions with Alexey Pavlov, Elisabeth Jones & Matthias Forwick	APECS, UiT	General
19. Sep	Markus Rex	Introduction to MOSAiC	AWI	General
19. Sep	Anja Sommerfeld	Management of MOSAiC	AWI	General
22. Sep	Shannon Hall	Working with the media + Interview training + #AskMOSAiC Interview Exercise	Freelancer, Scientific American and others	Media
23. Sep	Chris Cox	Clouds in the Arctic System	University of Colorado/CIRES	Atmosphere
23. Sep	Jessie Creamean	Riding the wave: Microbes from the ocean and ice that form Arctic clouds	Colorado State U	Atmosphere/ Ecology
24. Sep	Michel Tsamados	Ocean physics and climate change	CPOM, UCL	Ocean
24. Sep	Tim Stanton	The Role of the Ocean in Arctic Change	NPS and MLMS	Ocean
25. Sep	Jari Haapala	Principles of sea-ice physics: thickness distibution – thermodynamics – dynamics + Group Exercise	Finnish Meteorological Institute	Sea Ice

Date	Presenter	Title	Affiliation	Category
25. Sep	Marc Oggier	Seasonal evolution of First-Year Ice Microstructure and physical properties	UAF, IARC	Sea Ice
25. Sep	Michel Tsamados	Sea ice dynamics	CPOM, UCL	Sea Ice/Ocean
25. Sep	Daniel Watkins	Introduction to Ice Watch	Oregon State U	Sea Ice
26. Sep	Tim Stanton	Introduction to L-Site plans	NPS and MLMS	General
26. Sep	Ying-Chih Fang	Introduction to M-Site plans	AWI	General
27. Sep	Stephen Archer	Trace gas exchange in the Arctic	University of Colorado/CIRES	Atmosphere
27. Sep	Allison Fong	Ecosystem Research in MOSAiC	AWI	Ecology
27. Sep	Matthew Shupe	Coupled System Science at MOSAiC + Group Exercise	University of Colorado/CIRES & NOAA	Atmosphere & General
28. Sep	Anne Gold	Broadening the Impact of your Science	University of Colorado/CIRES	Education & Outreach
29. Sep	Thomas Rackow	Drift forecasts – from sea ice over icebergs to Polarstern + Exercise	AWI	Modelling
02. Oct	Dorothea Bauch	How useful is tracer-oceanography in the Arctic in the middle of winter?	GEOMAR	BGC
08. Oct	Pauline Snoeijs Leijonmalm	Uncovering the largest blind spot on the map of the world's fish stocks	Stockholm University	Ecology
15. Oct	Michael Angelopoulos	Subaquatic permafrost and a brief introduction to planetary analogues	AWI	BGC
15. Oct	Sebastian Rokitta	Phytoplankton and how they interact with their environment -The basics of biogeochemistry	AWI	Ecology
16. Oct	Sebastian Rokitta	Cycling of biogenic elements	AWI	Ecology
18. Oct	Vera Schlindwein	Exploring seafloor spreading at Gakkel Ridge, Arctic Ocean	AWI	Geology
19. Oct	Friedericke Krüger	The Psychology of Learning	Integr. Gesamtschule Bothfeld	Education & Outreach
19. Oct	Falk Ebert	Understanding with your hands - Opportunities and limits of experiments in school + Group Exercise	Käthe-Kollwitz Gymnasium	Education & Outreach
20. Oct	Katie Gavenus	Understanding, Building From, and Honoring Students' Lived Experiences	PolarTREC/ Center for Alaskan Coastal Studies	Education & Outreach
22. Oct	Daisy Dunne	How to take on climate sceptics and win	Carbon Brief	Media
23. Oct	Chelsea Harvey	Writing About Science for Non-Scientists	E&E News	Media

Date	Presenter	Title	Affiliation	Category
23. Oct	Josefine Lenz	Panel discussion on field work preparation with Thomas Krumpen, Anne Morgenstern, Vera Schlindwein & Tim Stanton	AWI	General
24. Oct	Martha Henriques	Panel discussion on story telling with Martha Henriques, Marlene Göring and Philipp Griess	BBC	Media
24. Oct	Martha Henriques	Ethics in Climate Science	BBC	Media
25. Oct	Ravenna Koenig	Using Social Media to Communicate Your Science	National Public Radio	Media
26. Oct	Anne Gold	Evaluation of Projects	University of Colorado/CIRES	Education & Outreach

Besides a wide variety of lectures, exercises, panel discussions and workshops, all MOSAiC School participants were involved in Ice Watch, polar bear safety watch, creating weather forecast for the next day, helping with ice drift modelling, designing the poster profiling of all participants onboard, help answering the #AskMOSAiC questions and reporting of daily activities of the MOSAiC School.

As a result of the MOSAiC School, the participants will act as MOSAiC Ambassadors and pass their experience and therefor the legacy of MOSAiC to the public and young generation, e.g. by school visits, public talks, organizing teachers workshops, developing scout patches, photo exhibitions, creating video & audio material, blogs, cartoons and other outreach products. More information can be found on https://www.apecs.is/outreach/mosaic-school-outreach.html and on related distribution channels.

6.2 MOSAiC Education and Outreach

Anne Gold[1], Katie Gavenus[2], Friederike Krüger[3], Falk Ebert[4], Lisa-Marie Heusinger[5]
not on board: Lynne Harden[1], Jonathan Griffith[1], Katya Schloesser[1]

[1]U Colorado
[2]PolarTREC/CACS
[3]IGS Bothfeld
[4]Herder-Gymnasium
[5]AWI

Grant-No. NSF- OPP 1839104, NSF-OPP 1918637, NSF-OPP 1754290 (for US contribution)

Multimedia products

Captivating multimedia content and a number of products were created onboard *Akademik Fedorov* and further will be further developed and broadly disseminated during the full year of MOSAiC.

#Ask MOSAiC Questions

Students and the public submitted questions about the MOSAiC expedition and the time on the ship on different social media channels or through personal connections to education team members. These questions were answered by scientists, crew members and other expedition participants either in short video clips or in writing. The footage that we collected of scientists

answering these questions on the ship will be produced into short video clips under the #AskMOSAiC tab as well as posted on MOSAiC social media channels.

Fig. 6.2.1: The education team on board Akademik Fedorov

Videoclips to illustrate expedition and life on board

Short video clips illustrate science concepts and content, and transport emotions and especially impressions of the Arctic landscape in a way that is hard to illustrate in oral descriptions. The education team captured scenes from life on the ship, landscape scenes, short talks from scientists in the field and documented the equipment and the way science is conducted on the sea ice. Video clips will be edited and put in a framework to share with learners and interested public of all ages.

Planetarium show / 360° footage

One of the multimedia products from MOSAiC is a planetarium show that tells the story of MOSAiC in two dome productions - one short update film that will be release in the spring of 2020 and a full planetarium show that will be released after the completion of the expedition. 360° footage was collected during leg 1a on *Akademik Fedorov* to supplement the footage collected on *Polarstern*. Footage includes the instrument deployment on the ice for the distributed network and selected scenes of other data collection like the EM bird or flux chambers as well as people working on the ice.

Google Expeditions

Google Expeditions will serve as immersive explorations of the MOSAiC expedition. We collected 360° still images from field deployments on the L-sites that show the different instrumentation or onsite sampling. 360° still images will be embedded in Google Expeditions and allow students to explore the data collection field sites. Close ups of instruments, short videos and explanations will facilitate an in-depth learning about each instrument and the data that instruments collect.

Massive Open Online Course

An overview course that features all MOSAiC science is being developed as part of the outreach to the general public in the form of a Massive Open Online Course (MOOC). We filmed four lectures for the atmosphere and ocean modules during the cruise that will be embedded in the course. In addition, we developed the assessment for students for the sea ice course module: During the cruise, participants collected *ice watch* data hourly while the ship was moving through sea ice using the ASSIST network. Ice watch data will be compiled into a database

for all MOSAiC supply cruises; we plan to use the data as part of the MOOC sea ice module assessment. In addition, all lectures that were given as part of the MOSAiC School were filmed and the recordings will be supplied as background information for each of the MOOC modules.

Educational content

Development of educational materials is based on the Schloesser & Gold (2019) teacher needs assessment.

Materials for Lesson Plans

MOSAiC science will be featured in multiple lesson plans that focus on Arctic topics. The lesson plans are being developed based on teacher needs and on education standard requirements. The education team is developing a series of lesson plans (e.g. expedition planning, ocean acidification, polar processes), classroom activities (such as games, lesson that encourage work with data, hands on experiments) and educational texts for a variety of topics and subjects. Materials were partially developed during the expedition, or data and footage were gathered during the expedition to highlight MOSAiC science and embed as building blocks in materials later on. Numerous videos were developed that feature MOSAiC scientists, early-career scientists from the MOSAiC School and crew members to bring science concepts and expedition details to life. Some worksheets and educational activities were developed around the MOSAiC instruments, including graphics, photos, videos and simplified explanations. Profiles of scientists were collected and will be used to illustrate career paths and add a human face to the scientists.

Ship-to-Classroom calls

During the cruise, three ship-to-shore phone calls to classrooms were made via Iridium satellite phone, one to the Breia Middle School in Alaska, one to the Integrierte Gesamtschule Bothfeld in Germany and one to the Käthe-Kollwitz Gymnasium, Berlin. Students in Germany and the US prepared questions before the call and once on the phone asked questions about the expedition and life on board.

Journals

Katie Gavenus, the PolarTREC educator, wrote a total of 20 journal entries summarizing her experiences on board *Akademik Fedorov* (e.g. life in the ice, polar night, what are people reading), relevant science concepts that she experienced or learned about (e.g. wind, algae, sub-sea permafrost, foodweb, aurora borealis) as well as about topics that served documentation of the expedition (e.g. first sea ice, polar bear guarding, ice watch). Her journals were sent via email to PolarTREC and disseminated through PolarTREC channels to reach educators in Alaska, where Katie is from but also to educators across the U.S.

Experiments

Hands-on experiments are an effective way of engaging learners in the science. In collaboration with the MOSAiC School the education team developed, tested and refined a series of hands-on experiments that can be used to illustrate MOSAiC science concepts. The majority of the experiments already existed and were made relevant to MOSAiC. About five new experiments were developed. Worksheets are being created partially on board and partially after the expedition to support teaching about MOSAiC science concepts using hands-on experiences.

6.3 MOSAiC Media

Katharina Weiss-Tuider[1], Martha Henriques[2], Shannon Hall[3], Chelsea Harvey[4], Daisy Dunne[5], Ravenna Koenig[6], Marlene Göring[7], Nikolaus von Schlebrügge[8], Philipp Grieß[8]

[1]AWI
[2]BBC
[3]Scientific American
[4]E&E News
[5]Carbon Brief
[6]NPR
[7]Gruner & Jahr
[8]UFA

6.3.1. MOSAiC communications team and journalist's contributions

Contributions from international journalists and the MOSAiC communications team are aiming at informing and engaging the general public.

Media participation and coverage

Before the expedition, an international call for applications was issued to allow selected journalists/science communicators to take part in MOSAiC and to report from aboard the ships *Polarstern* and *Akademik Fedorov* during PS122/1, leg 1a. To facilitate the observation and coverage of MOSAiC science, international collaboration, and the challenging logistical aspects of the expedition, the journalists were given the opportunity to participate in logistical and scientific tasks, e.g. the deployment of the Distributed Network, the setup of the Ice Camp on the so-called "MOSAiC floe", the exchange of participants between the two research vessels. The journalists were mainly travelling onboard *Akademik Fedorov* and transferred to *Polarstern* for a certain period of time. In addition to their own observations of science activities, interviews with participating scientists as well as presentations and talks provided the relevant background information for the journalists' coverage in their respective media outlets. During the expedition, the participation of the journalists led to "live onboard" articles e.g. in the BBC (BBC Future), Scientific American, E&E News, as well as live interviews via Iridium telephone onboard for NPR (National Public Radio, USA). Due to the very limited access to internet for technical reasons, more extensive coverage, also including multimedia (such as picture and 3D video), will follow in the aftermath. Katharina Weiss-Tuider was responsible for the media coordination onboard *Akademik Fedorov*.

Live coverage via MOSAiC channels

In collaboration with the media coordination and photographer onboard *Polarstern*, blog posts and live pictures were published via the MOSAiC channels, such as the Progressive Web App, Twitter and Instagram. The articles published by the journalists aboard were collected and made available to the general public via MOSAiC channels such as the project website www.mosaic-expedition.org as well as Social Media channels.

Documentation of the expedition (interviews, pictures)

In accordance with the overall MOSAiC communications and outreach concept, a diverse spectrum of documentation material was produced and collected by the media coordination aboard *Akademik Fedorov* (pictures, video interviews, text interviews). This material will, to some part, be made available via the MOSAiC multimedia library, and to some part provide the basis for documentation formats such as website articles, interview videos etc., reporting on the mission of the *Akademik Fedorov* during MOSAiC leg 1a.

Sustainable outreach production processes

Sustainable outreach production processes onboard all legs of the MOSAiC expedition is established and supported.

TV Documentary

As the MOSAiC expedition will be accompanied by a TV documentary team (UFA Show & Factual) during all legs, the cruise of the *Akademik Fedorov* was also part of this documentary production. One member of the TV documentary team (Nikolaus von Schlebrügge) travelled on *Akademik Fedorov* and was provided access to, and participation in relevant and distinctive events (organizational, scientific, social) and tasks (scientific and logistic) during leg 1a. The footage taken during the cruise of *Akademik Fedorov* will be part of the various high-end documentary products produced by UFA Show & Factual and distributed internationally. Part of the footage will be made available in the MOSAiC multimedia library under CC-BY license.

6.3.2 Support of MOSAiC Education and Outreach

Participating journalists were providing support to the MOSAiC Education and Outreach efforts.

MOSAiC School

In accordance with their applications/proposals, participating journalists supported the MOSAiC School by giving lectures on media work and science communication. The MOSAiC School participants got insights e.g. into how to conduct and/or give interviews and how to explain complex scientific topics, how to use storytelling moments in their media work and how to react to climate change deniers in public media discussions. Group discussions were facilitated by panel discussions and exercises.

MOSAiC Outreach

In accordance with their applications/proposals, the journalists supported the MOSAiC Outreach campaign by providing pictures and blog posts.

Data management

All education, outreach and media products will be stored either on the MOSAiC website, the APECS website (for MOSAiC School content) or on closely related distribution channels (youtube channels, blogs).

References

Schloesser KA and Gold AU (2019) Bringing Polar Topics into the Classroom: Teacher Knowledge, Practices and Needs. Journal of Geoscience Education. (accepted)

APPENDIX

A.1 PARTICIPATING INSTITUTIONS

A.2 LIST OF PARTICIPANTS

A.3 STATION LIST

A.4 APPENDIX FOR ICE AND SNOW SURVEYS

A.1 TEILNEHMENDE INSTITUTE /PARTICIPATING INSTITUTIONS

Abbreviation	Institute
AARI	Arctic and Antarctic Research Institute, St Petersburg, Russia
APECS	Association of Polar Early Career Scientists, Germany
AWI	Alfred-Wegener-Institut Helmholtz-Zentrum für Polar- und Meeresforschung, Bremerhaven/Potsdam, Germany
BAS	British Antarctic Survey, Cambridge, United Kingdom
BBC	BBC, London, United Kingdom
BLOS	Bigelow Laboratory for Ocean Sciences, East Boothbay, USA
BNU	Beijing Normal University, Beijing, China
CACS	Centre for Alaskan Coastal Studies, Homer, USA
Carbon Brief	Carbon Brief, London, UK
CIRES	Cooperative Institute for Research in Environmental Sciences, University of Colorado, Boulder, USA
Colorado State University	Colorado State University, Fort Collins, USA
DOE	US Department of Energy, Atmospheric Radiation Measurement (ARM) user facility, Richland, USA
DWD	Deutscher Wetterdienst, Offenbach am Main, Germany
E&E News	E&E NEWS, Washington, USA
ETH	ETH Zurich, Zurich, Switzerland
FIELAX	FIELAX Gesellschaft für wissenschaftliche Datenverarbeitung mbH, Bremerhaven, Germany
FIO	First institute of Oceanography, Qingdao, China
FMI	Finnish Meteorological Institute, Helsinki, Finland
Gruner & Jahr	Gruner & Jahr GmbH, Hamburg, Germany
Herder-Gymnasium	Herder-Gymnasium, Berlin, Germany
HU Berlin	Humboldt University Berlin, Berlin, Germany
IARC	International Arctic Research Center, University of Alaska, Fairbanks, USA
IGS Bothfeld	Integrierte Gesamtschule Bothfeld, Germany
IOPAN	Institute of Oceanology Polish Academy of Sciences, Sopot, Poland

Abbreviation	Institute
LMSU	Lomonosov Moscow State University, Moscow, Russia
LOCEAN-IPSL	Laboratoire d'Océanographie et du Climat, Institut Pierre-Simon Laplace, Ile-De-France, France
MLML	Moss Landing Marine Laboratories, Moss Landing, USA
MSU	Montana State University, Bozeman, USA
MUN	Memorial University of Newfoundland, Fisheries and Marine Institute, Canada
NASA	National Aeronautics and Space Administration, Washington D.C., USA
NOAA	National Oceanic and Atmospheric Administration, Boulder, USA
NPR	National Public Radio, Washington, USA
NPS	Naval Postgraduate School, Monterey,USA
NSIDC	National Snow and Ice Data Center, Boulder, USA
NTNU	Norwegian University of Science and Technology, Trondheim, Norway
Ohio State University	The Ohio State University, Columbus, USA
Oregon State University	Oregon State University, Corvallis, USA
OUC	Ocean University of China, Qingdao, China
PolarTREC	PolarTREC, Arctic Research Consortium of the United States, University of Alaska, Fairbanks, USA
PRIC	Polar Research Institute of China, Shanghai, China
Scientific American	Scientific American, New York City, USA
SIO	Second Institute of Oceanography, Hangzhou, China
SLU	Swedish University of Agricultural Sciences, Uppsala, Sweden
Stockholm University	Stockholm University, Stockholm, Sweden
Thayer School	Thayer School of Engineering at Dartmouth, Dartmouth, USA
TUT	Taiyuan University of Technology, Taiyuan, China
UCL	University College London, London, United Kingdom
U Colorado	University of Colorado, Boulder, USA
UFA	UFA Show & Factual GmbH, Köln, Germany
U Oldenburg	Carl von Ossietzky University, Oldenburg, Germany
U Oxford	University of Oxford, Department of Earth Sciences, Oxford, UK

Abbreviation	Institute
U Potsdam	Mathematisch-Naturwissenschaftliche Fakultät, Potsdam-Golm, Germany
U Tasmania	University of Tasmania, Hobart, Australia
U Tromsø	University of Tromsø, Tromsø, Norway
U Utah	University of Utah, Salt Lake City, USA
UTR	Université du Québec à Trois-Rivières, Trois-Rivières, Canada
WHOI	Woods Hole Oceanographic Institution, Woods Hole, USA
ZJU	Zhejiang University, Zhejiang, China

A.2 FAHRTTEILNEHMER / CRUISE PARTICIPANTS

Name/ Last name	Vorname/ First name	Institut/ Institute	Beruf/Profession	Fachrichtung / Discipline
Aellen	Neil	ETH	Master Student	Atmosphere
Angelopolous	Michael	AWI	PhD Student	BGC
Archer	Steve	BLOS	Scientist	BGC
Athanase	Marylou	LOCEAN-IPSL	PhD Student	Ocean
Bai	Youcheng	SIO	Scientist	Ecosystem
Basque	Chris	WHOI	Scientist	Ocean
Belter	Jakob	AWI	PhD Student	Sea Ice
Bessonov	Vladimir	AARI	Scientist	Sea ice
Boyer	Matt	DOE	Scientist	Atmosphere
Buynov	Roman	AARI	Polarbear guard	Logistic
Christian	Boris	Laeisz	Administrator	IT
Chu	David	DOE	Scientist	Atmosphere
Chugunov	Andrey	AARI	Polarbear guard	Logistic
Cornish	Sam	U Oxford	PhD Student	Ocean
Costa	David	CIRES/NOAA	Engineer	Atmosphere
Cox	Christopher	NOAA	Scientist	Atmosphere
Craw	Lisa	U Tasmania	PhD Student	Sea Ice
Creamean	Jessie	Colorado State University	Scientist	Atmosphere
Dahlke	Sandro	AWI	PhD Student	Atmosphere
Davies	Andy	WHOI	Scientist	Atmosphere
Demir	Oguz	Ohio State University	PhD Student	Sea Ice
Doglioni	Francesca	AWI	PhD Student	Ocean
Dunne	Daisy	Carbon Brief	Reporter	Media
Ebert	Falk	Herder-Gymnasium	Teacher	Education & Outreach
Ellis	Jody	DOE	Scientist	Atmosphere
Fang	Ying-Chih	AWI	Scientist	Ocean
Fershter	Evgeny	AARI	Polarbear guard	Logistics
Garankin	Anton	AARI	Polarbear guard	Logistics
Gavenus	Katie	PolarTREC	Teacher	Education & Outreach
Gerchow	Peter	AWI	Scientist	Logistics
Gold	Anne	U Colorado	Scientist	Education & Outreach
Göring	Marlene	Gruner + Jahr	Reporter	Media

Name/ Last name	Vorname/ First name	Institut/ Institute	Beruf/Profession	Fachrichtung / Discipline
Grafov	Igor	AARI	Polarbear guard	Logistic
Graupner	Rainer	AWI	Scientist	Ocean
Greenamyer	Vernon	DOE	Scientist	Atmosphere
Grieß	Philipp	UFA	Reporter	Media
Grote	Sebastian	AWI	Manager	Education & Outreach
Haapala	Jari	FMI	Scientist	Sea Ice
Hall	Shannon	Freelancer	Reporter	Media
Happe	Anika	U Oldenburg	Master Student	Ecosystem
Harris	Carolynn	MSU	PhD Student	BGC
Harvey	Chelsea	E&E News	Reporter	Media
He	Hailun	SIO	Scientist	Ocean
Henriques	Martha	BBC	Reporter	Media
Hermann	Mauro	ETH	Master Student	Atmosphere
Hermansen	Gaute	Laeisz	Staff	Logistics
Heusinger	Lisa-Marie	AWI	Master Student	Education & Outreach
Hildebrandt	Nicole	AWI	Scientist	Ecosystem
Hohle	Trude	Laeisz	Staff	Logistics
Honold	Hans	Laeisz	Staff	Logistics
Hoppmann	Mario	AWI	Scientist	Ocean
Horvath	Sean	U Colorado	PhD Student	Sea Ice
Houchens	Todd	DOE	Scientist	Atmosphere
Hueber	Jacques	U Colorado	Scientist	Atmosphere
Kircher	Dietmar	Laeisz	Staff	Logistics
Kirchgaessner	Amelie	BAS	Scientist	Atmosphere
Kirk	Henning	AWI	Scientist	Ocean
Koenig	Ravenna	NPR	Reporter	Media
Kolabutin	Nikolai	AARI	Scientist	Sea Ice
Korejwo	Ewa	IOPAN	PhD Student	BGC
Krassowski	Misha	DOE	Scientist	Atmosphere
Krüger	Friederike	IGS Bothfeld	Teacher	Education & Outreach
Krumpen	Thomas	AWI	Scientist	Coordination
Kurtz	Nathan	NASA	Scientist	Atmosphere
Lan	Musheng	PRIC	Scientist	Ecosystem
Lei	Ruibo	PRIC	Scientist	Sea Ice
Lenz	Josefine	AWI	Scientist	Education & Outreach
Li	Tao	OUC	Scientist	Ocean

Name/ Last name	Vorname/ First name	Institut/ Institute	Beruf/Profession	Fachrichtung / Discipline
Lin	Long	SIO	Scientist	Ocean
Ma	Xiaobing	FIO	Scientist	Ocean
Mallett	Robbie	UCL	PhD Student	Sea Ice
Matero	Ilkka	AWI	Scientist	Sea Ice
Matveeva	Tatiana	LMSU	PhD Student	Atmosphere
Mavrovic	Alex	UTR	PhD Student	Sea Ice
McKay	Rosalie	NTNU	Master Student	BGC
Moore	Ryleigh	U Utah	PhD Student	Sea Ice
Morgenstern	Anne	AWI	Scientist	Coordination
Nehring	Franziska	Fielax	Staff	Data Managment
Oggier	Marc	IARC	Scientist	Sea Ice
Ortega	Paul	DOE	Scientist	Atmosphere
Paramzin	Andrey	AARI	Polarbear guard	Logistics
Persson	Ola	CIRES/NOAA	Scientist	Atmosphere
Petrovsky	Tomash	AARI	Scientist	Sea Ice
Priou	Pierre	MUN	PhD Student	Ecosystem
Rackow	Thomas	AWI	Scientist	Sea Ice
Raeke	Andreas	DWD	Staff	Logstics
Raphael	Ian	Thayer School	Master Student	Sea Ice
Ren	Jian	SIO	Scientist	Ecosystem
Ribeiro Santos	Natalia	U Tasmania	PhD Student	Ocean
Rohde	Jan	AWI	Engineer	Sea Ice
Rokitta	Sebastian	AWI	Scientist	Ecosystem
Schiller	Martin	AWI	Engineer	Sea Ice
Schlindwein	Vera	AWI	Scientist	Geophysics
Schneider	Thea	U Potsdam	Master Student	Sea Ice
Shaw	William	NPS	Scientist	Ocean
Shimanchuk	Egor	AARI	Scientist	Sea Ice
Smolyanitsky	Vasily	AARI	Scientist	Sea Ice
Snoeijs-Leijonmalm	Pauline	Stockholm University	Scientist	Ecosystem
Sokolov	Vladimir	AARI	Scientist	Coordination
Stanton	Tim	NPS	Scientist	Ocean
Sterbenz	Thomas	Laeisz	Staff	Logistics
Svenson	Anders	SLU	Scientist	Ecosystem
Tholfsen	Audun	Laeisz	Staff	Logistics
Timofeefa	Anna	AARI	Scientist	Sea Ice
Tsamados	Michel	UCL	Scientist	Sea Ice

Name/ Last name	**Vorname/ First name**	**Institut/ Institute**	**Beruf/Profession**	**Fachrichtung / Discipline**
Uin	Janek	DOE	Scientist	Atmosphere
Vasilevich	Igor	AARI	PhD Student	Ecosystem
von Schlebrügge	Nikolaus	UFA	Cinematographer	Media
Wang	Hangzhou	ZJU	Scientist	Ocean
Wang	Lei	BNU	Scientist	BGC
Watkins	Daniel	Oregon State University	Scientist	Sea Ice
Weiss-Tuider	Katharina	AWI	Media Manager	Education & Outreach
Zhu	Jialiang	OUC	Scientist	Ocean
Zinke	Julika	Stockholm University	PhD Student	Atmosphere
Zoelly	Christian	Laeisz	Staff	Logistics
Zuo	Guangyu	PRIC	Scientist	Sea Ice

A.3 STATIONSLISTE/STATION LIST

List 1

Station	Date	Time	Latitude	Longitude	Gear	Depth
AF-MOSAiC-1_44	2019-01-10	01:15:00	85.71339	123.24103	ICEGAUGE	n.a.
AF-MOSAiC-1_45	2019-03-10	01:24:00	85.19975	135.47300	ICEGAUGE	n.a.
AF-MOSAiC-1_154	2019-04-10	11:08:00	85.11570	133.13030	BUOY_ICE_TRACK	n.a.
AF-MOSAiC-1_39	2019-05-10	00:03:00	85.99834	132.94873	MAGNA	n.a.
AF-MOSAiC-1_77	2019-05-10	01:00:00	85.01130	132.77810	TBUOY	n.a.
AF-MOSAiC-1_46	2019-05-10	01:36:00	85.00556	132.90054	ICEGAUGE	n.a.
AF-MOSAiC-1_173	2019-05-10	02:27:00	84.95500	131.89580	ISVP	n.a.
AF-MOSAiC-1_148	2019-05-10	03:05:00	84.95900	131.18300	BUOY_ICE_TRACK	n.a.
AF-MOSAiC-1_147	2019-05-10	03:10:00	84.93870	131.74500	BUOY_ICE_TRACK	n.a.
AF-MOSAiC-1_145	2019-05-10	03:15:00	84.88600	131.69900	BUOY_ICE_TRACK	n.a.
AF-MOSAiC-1_143	2019-05-10	03:30:00	84.91070	130.75990	BUOY_ICE_TRACK	n.a.
AF-MOSAiC-1_170	2019-05-10	04:06:00	85.03000	134.88900	ISVP	n.a.
AF-MOSAiC-1_106	2019-05-10	04:40:00	84.91782	131.27920	AOFB	n.a.
AF-MOSAiC-1_70	2019-05-10	05:02:00	85.01340	132.72610	ITP	n.a.
AF-MOSAiC-1_73	2019-05-10	05:10:00	85.01283	132.73348	SIMB	n.a.
AF-MOSAiC-1_31	2019-05-10	05:16:00	85.01000	132.81800	BES	n.a.
AF-MOSAiC-1_37	2019-05-10	05:16:00	85.09249	133.84019	MAGNA	n.a.
AF-MOSAiC-1_105	2019-05-10	05:17:00	84.91894	131.26002	OCTDB	n.a.
AF-MOSAiC-1_103	2019-05-10	05:30:00	84.91888	131.26448	TBUOY	n.a.
AF-MOSAiC-1_81	2019-05-10	05:30:00	85.01222	132.75944	BUOY_FLO	n.a.
AF-MOSAiC-1_78	2019-05-10	05:43:00	85.01122	132.81339	BES	n.a.
AF-MOSAiC-1_22	2019-05-10	05:59:00	85.01131	132.81013	IC	n.a.
AF-MOSAiC-1_6	2019-05-10	05:59:00	85.01131	132.81012	hCTD	n.a.
AF-MOSAiC-1_79	2019-05-10	06:01:00	85.01283	132.77030	BES	n.a.
AF-MOSAiC-1_76	2019-05-10	06:01:00	85.01282	132.73650	MRS	n.a.
AF-MOSAiC-1_75	2019-05-10	08:27:00	85.09442	133.78993	ASFS	n.a.
AF-MOSAiC-1_80	2019-05-10	08:29:00	85.01440	132.79348	BES	n.a.
AF-MOSAiC-1_74	2019-05-10	09:34:00	85.01334	132.72975	AOFB	n.a.
AF-MOSAiC-1_135	2019-05-10	10:22:00	84.87110	131.17320	ISVP	n.a.
AF-MOSAiC-1_125	2019-05-11	12:00:00	85.93894	118.43960	TBUOY	n.a.
AF-MOSAiC-1_153	2019-06-10	03:30:00	85.03670	134.13240	BUOY_ICE_TRACK	n.a.
AF-MOSAiC-1_149	2019-06-10	04:00:00	85.02440	134.57410	BUOY_ICE_TRACK	n.a.
AF-MOSAiC-1_47	2019-06-10	06:18:00	85.01414	134.67150	ICEGAUGE	n.a.

Station	Date	Time	Latitude	Longitude	Gear	Depth
AF-MOSAiC-1_91	2019-06-10	06:58:00	85.01270	134.66550	BES	n.a.
AF-MOSAiC-1_38	2019-06-10	07:00:00	84.01273	132.66551	MAGNA	n.a.
AF-MOSAiC-1_23	2019-06-10	07:33:00	85.01253	134.67199	IC	n.a.
AF-MOSAiC-1_8	2019-06-10	07:33:00	85.01253	134.67199	hCTD	n.a.
AF-MOSAiC-1_24	2019-06-10	08:24:00	85.01217	134.67903	IC	n.a.
AF-MOSAiC-1_25	2019-06-10	08:42:00	85.01190	134.68006	IC	n.a.
AF-MOSAiC-1_90	2019-07-10	01:00:00	84.99744	134.99664	TBUOY	n.a.
AF-MOSAiC-1_132	2019-07-10	01:15:00	84.86900	136.85300	ISVP	n.a.
AF-MOSAiC-1_42	2019-07-10	01:33:00	84.99649	135.01960	hCTD	n.a.
AF-MOSAiC-1_168	2019-07-10	01:48:00	85.00920	136.88000	ISVP	n.a.
AF-MOSAiC-1_108	2019-07-10	02:00:00	84.87130	135.75825	BUOY_SNOW	n.a.
AF-MOSAiC-1_26	2019-07-10	02:00:00	84.99616	135.03325	IC	n.a.
AF-MOSAiC-1_175	2019-07-10	02:05:00	85.25100	136.58400	ISVP	n.a.
AF-MOSAiC-1_174	2019-07-10	02:09:00	85.22300	133.63950	ISVP	n.a.
AF-MOSAiC-1_171	2019-07-10	02:19:00	85.26700	134.69700	ISVP	n.a.
AF-MOSAiC-1_55	2019-07-10	02:30:00	85.08973	134.20123	SSG	n.a.
AF-MOSAiC-1_110	2019-07-10	02:30:00	84.87100	135.75150	AOFB	n.a.
AF-MOSAiC-1_144	2019-07-10	02:34:00	85.03300	133.38000	BUOY_ICE_TRACK	n.a.
AF-MOSAiC-1_56	2019-07-10	02:35:00	85.08962	134.20410	SSG	n.a.
AF-MOSAiC-1_142	2019-07-10	02:39:00	84.96900	135.37500	BUOY_ICE_TRACK	n.a.
AF-MOSAiC-1_146	2019-07-10	02:42:00	84.95460	134.64700	BUOY_ICE_TRACK	n.a.
AF-MOSAiC-1_107	2019-07-10	03:00:00	84.87130	135.75825	TBUOY	n.a.
AF-MOSAiC-1_89	2019-07-10	03:00:00	84.99640	135.03130	TBUOY	n.a.
AF-MOSAiC-1_109	2019-07-10	03:22:00	84.87110	135.78467	OCTDB	n.a.
AF-MOSAiC-1_104	2019-07-10	04:00:00	84.91890	131.26450	BUOY_SNOW	n.a.
AF-MOSAiC-1_41	2019-07-10	04:40:00	84.99260	135.13137	hCTD	n.a.
AF-MOSAiC-1_88	2019-07-10	04:40:00	84.99326	135.00144	BRS	n.a.
AF-MOSAiC-1_53	2019-07-10	05:05:00	85.08592	134.30186	SSG	n.a.
AF-MOSAiC-1_72	2019-07-10	05:09:00	85.01383	132.72716	BUOY_SNOW	n.a.
AF-MOSAiC-1_54	2019-07-10	05:10:00	85.08575	134.30532	SSG	n.a.
AF-MOSAiC-1_83	2019-07-10	05:15:00	84.99308	135.00132	MRS	n.a.
AF-MOSAiC-1_84	2019-07-10	05:16:00	84.99323	135.00133	AOFB	n.a.
AF-MOSAiC-1_27	2019-07-10	05:18:00	84.99136	135.15634	IC	n.a.
AF-MOSAiC-1_9	2019-07-10	05:18:00	84.99136	135.15634	hCTD	n.a.
AF-MOSAiC-1_86	2019-07-10	05:20:00	84.99326	135.00140	ITP	n.a.

Station	Date	Time	Latitude	Longitude	Gear	Depth
AF-MOSAiC-1_87	2019-07-10	05:21:00	84.99330	135.00140	BUOY_SNOW	n.a.
AF-MOSAiC-1_71	2019-07-10	05:24:00	84.99330	132.00140	BRS	n.a.
AF-MOSAiC-1_92	2019-07-10	05:30:00	84.98917	135.19417	BUOY_ITP	n.a.
AF-MOSAiC-1_85	2019-07-10	05:43:00	84.99920	134.57682	SIMB	n.a.
AF-MOSAiC-1_134	2019-07-10	06:14:00	85.06100	137.61000	ISVP	n.a.
AF-MOSAiC-1_112	2019-07-10	06:30:00	85.05358	137.80755	BUOY_SNOW	n.a.
AF-MOSAiC-1_133	2019-07-10	06:32:00	85.31400	138.64600	ISVP	n.a.
AF-MOSAiC-1_172	2019-07-10	06:40:00	85.27300	135.69900	ISVP	n.a.
AF-MOSAiC-1_32	2019-07-10	06:58:00	85.01000	134.66500	BES	n.a.
AF-MOSAiC-1_151	2019-07-10	06:58:00	85.20000	134.68000	BUOY_ICE_TRACK	n.a.
AF-MOSAiC-1_157	2019-07-10	07:02:00	85.34100	134.58200	BUOY_ICE_TRACK	n.a.
AF-MOSAiC-1_152	2019-07-10	07:05:00	85.34200	134.00100	BUOY_ICE_TRACK	n.a.
AF-MOSAiC-1_114	2019-07-10	07:10:00	85.05297	137.81910	AOFB	n.a.
AF-MOSAiC-1_160	2019-07-10	07:13:00	85.24100	134.09700	BUOY_ICE_TRACK	n.a.
AF-MOSAiC-1_150	2019-07-10	07:24:00	85.27500	133.62000	BUOY_ICE_TRACK	n.a.
AF-MOSAiC-1_111	2019-07-10	07:30:00	85.05358	137.80755	TBUOY	n.a.
AF-MOSAiC-1_113	2019-07-10	08:05:00	85.05133	137.85214	OCTDB	n.a.
AF-MOSAiC-1_82	2019-07-10	09:33:00	85.07534	134.47262	ASFS	n.a.
AF-MOSAiC-1_33	2019-08-10	00:14:00	85.11500	136.10700	BES	n.a.
AF-MOSAiC-1_115	2019-08-10	01:00:00	85.11112	136.19598	TBUOY	n.a.
AF-MOSAiC-1_116	2019-08-10	01:00:00	85.11083	136.20480	BUOY_SNOW	n.a.
AF-MOSAiC-1_48	2019-08-10	01:21:00	85.02137	135.59813	ICEGAUGE	n.a.
AF-MOSAiC-1_117	2019-08-10	01:30:00	85.10932	136.24055	AOFB	n.a.
AF-MOSAiC-1_57	2019-08-10	02:21:00	85.01696	135.70129	SSG	n.a.
AF-MOSAiC-1_167	2019-08-11	12:30:00	85.89674	116.02703	ISVP	n.a.
AF-MOSAiC-1_99	2019-09-10	01:00:00	85.12820	135.67800	TBUOY	n.a.
AF-MOSAiC-1_118	2019-09-10	01:00:00	85.05380	139.02060	TBUOY	n.a.
AF-MOSAiC-1_119	2019-09-10	01:00:00	85.05380	139.02060	BUOY_SNOW	n.a.
AF-MOSAiC-1_141	2019-09-10	01:29:00	84.87600	131.97300	ISVP	n.a.
AF-MOSAiC-1_49	2019-09-10	01:30:00	84.91119	136.05788	ICEGAUGE	n.a.
AF-MOSAiC-1_58	2019-09-10	02:50:00	85.05261	139.04993	SSG	n.a.
AF-MOSAiC-1_159	2019-09-10	02:50:00	84.88000	134.93200	BUOY_ICE_TRACK	n.a.
AF-MOSAiC-1_163	2019-09-10	02:55:00	84.85400	134.53600	BUOY_ICE_TRACK	n.a.
AF-MOSAiC-1_138	2019-09-10	02:58:00	85.28500	135.82000	ISVP	n.a.
AF-MOSAiC-1_179	2019-09-10	03:01:00	84.79900	134.53600	ISVP	n.a.

Station	Date	Time	Latitude	Longitude	Gear	Depth
AF-MOSAiC-1_156	2019-09-10	03:08:00	84.79500	135.19800	BUOY_ICE_TRACK	n.a.
AF-MOSAiC-1_50	2019-09-10	03:12:00	84.91014	136.01556	ICEGAUGE	n.a.
AF-MOSAiC-1_162	2019-09-10	03:15:00	84.83500	135.40000	BUOY_ICE_TRACK	n.a.
AF-MOSAiC-1_166	2019-09-10	03:30:00	84.54500	135.25400	BUOY_UNIV_ TRACK	n.a.
AF-MOSAiC-1_169	2019-09-10	03:39:00	84.67000	135.55700	ISVP	n.a.
AF-MOSAiC-1_34	2019-09-10	03:43:00	85.12200	136.16500	BES	n.a.
AF-MOSAiC-1_120	2019-09-10	04:00:00	85.05383	139.02108	OCTDB	n.a.
AF-MOSAiC-1_40	2019-09-10	04:34:00	85.12271	136.16564	MAGNA	n.a.
AF-MOSAiC-1_28	2019-09-10	04:48:00	85.12344	136.14807	IC	n.a.
AF-MOSAiC-1_10	2019-09-10	04:48:00	85.12344	136.14807	hCTD	n.a.
AF-MOSAiC-1_59	2019-09-10	05:23:00	85.72999	136.13649	SSG	n.a.
AF-MOSAiC-1_29	2019-09-10	07:32:00	85.12141	136.13585	IC	n.a.
AF-MOSAiC-1_11	2019-09-10	07:32:00	85.12141	136.13585	hCTD	n.a.
AF-MOSAiC-1_101	2019-09-10	14:00:00	85.05380	139.02060	DCSFS	n.a.
AF-MOSAiC-1_139	2019-09-29	00:36:00	85.53700	139.03100	ISVP	n.a.
AF-MOSAiC-1_3	2019-09-30	00:01:00	85.12439	137.98501	HELI	n.a.
AF-MOSAiC-1_1	2019-09-30	03:15:00	85.12085	137.85481	BES	n.a.
AF-MOSAiC-1_43	2019-09-30	03:21:00	85.78149	123.69648	ICEGAUGE	n.a.
AF-MOSAiC-1_36	2019-09-30	06:54:00	85.10939	137.70180	BES	n.a.
AF-MOSAiC-1_164	2019-09-30	12:00:00	85.83000	118.19000	BUOY_UNIV_ TRACK	n.a.
AF-MOSAiC-1_165	2019-09-30	12:00:00	86.18000	125.37000	BUOY_UNIV_ TRACK	n.a.
AF-MOSAiC-1_140	2019-10-10	00:27:00	85.15100	139.25000	ISVP	n.a.
AF-MOSAiC-1_155	2019-10-10	02:01:00	84.86680	135.73800	BUOY_ICE_TRACK	n.a.
AF-MOSAiC-1_123	2019-10-10	02:30:00	85.12870	133.17010	BUOY_SNOW	n.a.
AF-MOSAiC-1_178	2019-10-10	02:32:00	85.00600	133.34000	ISVP	n.a.
AF-MOSAiC-1_177	2019-10-10	02:42:00	84.98400	135.19500	ISVP	n.a.
AF-MOSAiC-1_161	2019-10-10	02:46:00	84.94900	135.41900	BUOY_ICE_TRACK	n.a.
AF-MOSAiC-1_137	2019-10-10	02:51:00	84.95000	135.89400	ISVP	n.a.
AF-MOSAiC-1_60	2019-10-10	02:57:00	85.12722	133.23459	SSG	n.a.
AF-MOSAiC-1_158	2019-10-10	03:06:00	84.87600	135.21000	BUOY_ICE_TRACK	n.a.
AF-MOSAiC-1_124	2019-10-10	03:10:00	85.12722	133.23459	AOFB	n.a.
AF-MOSAiC-1_122	2019-10-10	03:30:00	85.12870	133.17010	TBUOY	n.a.
AF-MOSAiC-1_136	2019-10-10	03:56:00	84.91000	136.17300	ISVP	n.a.

Station	Date	Time	Latitude	Longitude	Gear	Depth
AF-MOSAiC-1_94	2019-10-10	04:41:00	85.13255	135.52630	ITP	n.a.
AF-MOSAiC-1_100	2019-10-10	04:46:00	85.12832	135.52887	BUOY_SI	n.a.
AF-MOSAiC-1_96	2019-10-10	04:50:00	85.13314	135.51829	AOFB	n.a.
AF-MOSAiC-1_98	2019-10-10	04:54:00	85.13323	135.51678	SIMB	n.a.
AF-MOSAiC-1_95	2019-10-10	06:00:00	85.13291	135.51478	BUOY_SNOW	n.a.
AF-MOSAiC-1_93	2019-10-10	06:00:00	85.12320	136.13400	BUOY_SI	n.a.
AF-MOSAiC-1_97	2019-10-10	08:21:00	84.92152	135.34570	ASFS	n.a.
AF-MOSAiC-1_102	2019-10-10	10:30:00	85.13400	135.48000	DCSFS	n.a.
AF-MOSAiC-1_180	2019-10-10	23:00:00	85.01920	134.21960	ISVP	n.a.
AF-MOSAiC-1_181	2019-10-10	23:00:00	85.01410	134.26240	ISVP	n.a.
AF-MOSAiC-1_52	2019-10-13	02:09:00	84.98663	134.47101	ICEGAUGE	n.a.
AF-MOSAiC-1_182	2019-10-13	04:35:00	84.89332	133.22596	TBUOY	n.a.
AF-MOSAiC-1_12	2019-10-13	04:47:00	84.89452	133.21277	hCTD	n.a.
AF-MOSAiC-1_30	2019-10-13	04:47:00	84.89452	133.21277	IC	n.a.
AF-MOSAiC-1_2	2019-10-13	04:47:00	84.89452	133.21277	IC	n.a.
AF-MOSAiC-1_4	2019-10-13	05:34:00	84.85776	135.01034	HELI	n.a.
AF-MOSAiC-1_5	2019-10-14	02:17:00	84.79185	134.62028	HELI	n.a.
AF-MOSAiC-1_183	2019-10-14	06:08:00	84.78111	134.49621	AOFB	n.a.
AF-MOSAiC-1_121	2019-10-19	01:20:00	85.05383	139.02062	AOFB	n.a.
AF-MOSAiC-1_127	2019-10-25	20:20:00	85.45047	127.70028	AOFB	n.a.
AF-MOSAiC-1_131	2019-10-26	04:00:00	85.45226	127.53864	AOFB	n.a.
AF-MOSAiC-1_176	2019-10-28	12:30:00	85.59137	126.12912	ISVP	n.a.
AF-MOSAiC-1_51	2019-11-10	00:10:00	84.98992	134.46822	ICEGAUGE	n.a.
AF-MOSAiC-1_35	2019-11-10	00:12:00	84.88942	135.45221	BES	n.a.
AF-MOSAiC-1_129	2019-11-10	01:00:00	84.98725	134.48903	BUOY_SNOW	n.a.
AF-MOSAiC-1_128	2019-11-10	02:00:00	84.98725	134.48903	TBUOY	n.a.
AF-MOSAiC-1_126	2019-11-10	02:00:00	84.73815	135.84716	BUOY_SNOW	n.a.
AF-MOSAiC-1_130	2019-11-10	02:30:00	84.98651	134.49061	OCTDB	n.a.
AF-MOSAiC-1_61	2019-11-10	02:55:00	84.87712	135.50429	SSG	n.a.

Gear abbreviations	Gear
AOFB	Autonomous Ocean Flux Buoy
ASFS	Atmospheric Surface Flux Station
BES	Broadband electromagnetic sensor
BRS	Buoy, radiation station
BUOY_FLO	Fixed-Layer Ocean Buoy
BUOY_ICE_TRACK	Buoy, ice tracker
BUOY_ITP	Ice-Tethered Profiler Buoy
BUOY_SI	Sea ice buoy
BUOY_SNOW	Snow buoy
BUOY_UNIV_TRACK	Buoy, universal tracker
DCSFS	Dynamic chamber surface flux system
hCTD	CTD, handheld
HELI	Helicopter Polarstern
IC	Ice corer
ICEGAUGE	Ice Thickness Gauge
ISVP	Surface velocity profiler
ITP	Ice Tethered Profiler
MAGNA	Magnaprobe
MRS	Mobile radiation suite
OCTDB	Ocean CTD buoy
SIMB	Seasonal Ice Mass Balance buoy
SSG	Snow Sampler Glove
TBUOY	Thermistor buoy

List 2

Station	Sensor Id	Comment Old Labels
AF-MOSAiC-1_44	https://sensor.awi.de/?site=search&q=pack_ice:ice_ps:ice_gauge	PS122/1_3-44
AF-MOSAiC-1_45	https://sensor.awi.de/?site=search&q=pack_ice:ice_ps:ice_gauge	PS122/1_3-45
AF-MOSAiC-1_154	https://sensor.awi.de/?site=search&q=buoy:2019p197	OSU-IT-0013,PS122/1_1-191
AF-MOSAiC-1_39	https://sensor.awi.de/?site=search&q=pack_ice:ice_ps:magnaprobe-anja	L2_MAGNA_2_AWI_20191007,PS122/1_3-39
AF-MOSAiC-1_77	https://sensor.awi.de/?site=search&q=buoy:2019t67	L1_SIMBA_1_PRIC_20191005,PS122/1_1-314
AF-MOSAiC-1_46	https://sensor.awi.de/?site=search&q=pack_ice:ice_ps:ice_gauge	L1_DRILLING_AARI_20191005,PS122/1_3-46
AF-MOSAiC-1_173	https://sensor.awi.de/?site=search&q=buoy:2019p142	TUT-GPS-8,PS122/1_1-213
AF-MOSAiC-1_148	https://sensor.awi.de/?site=search&q=buoy:2019p194	OSU-IT-0007,PS122/1_1-188
AF-MOSAiC-1_147	https://sensor.awi.de/?site=search&q=buoy:2019p189	OSU-IT-0006,PS122/1_1-183
AF-MOSAiC-1_145	https://sensor.awi.de/?site=search&q=buoy:2019p192	OSU-IT-0004,PS122/1_1-186
AF-MOSAiC-1_143	https://sensor.awi.de/?site=search&q=buoy:2019p191	OSU-IT-0002,PS122/1_1-185
AF-MOSAiC-1_170	https://sensor.awi.de/?site=search&q=buoy:2019p138	TUT-GPS-4,PS122/1_1-210
AF-MOSAiC-1_106	https://sensor.awi.de/?site=search&q=buoy:2019o1	M1_SIT_1_AWI_20191005,PS122/1_1-148
AF-MOSAiC-1_70	https://sensor.awi.de/?site=search&q=buoy:2019w4	L1_ITP_WHOI_20191005,PS122/1_1-170
AF-MOSAiC-1_73	https://sensor.awi.de/?site=search&q=buoy:2019i1	L1_SIMB3_1_Dartmouth_20191005, PS122/1_1-204
AF-MOSAiC-1_31	https://sensor.awi.de/?site=search&q=pack_ice:ice_ps:gem2-556	L1_GEM_1_AWI_20191005,PS122/1_3-31
AF-MOSAiC-1_37	https://sensor.awi.de/?site=search&q=pack_ice:ice_ps:magnaprobe-anja	L1_MAGNA_1_AWI_20191005,PS122/1_3-37
AF-MOSAiC-1_105	https://sensor.awi.de/?site=search&q=buoy:2019v1	M1_DTOP_1_OUC_20191005,PS122/1_1-275
AF-MOSAiC-1_103	https://sensor.awi.de/?site=search&q=buoy:2019t68	M1_SIMBA5_PRIC_20191005,PS122/1_1-171
AF-MOSAiC-1_81	https://sensor.awi.de/?site=search&q=buoy:fio_fio	
AF-MOSAiC-1_78	https://sensor.awi.de/?site=search&q=pack_ice:ice_ps:gem2-556	
AF-MOSAiC-1_22	https://sensor.awi.de/?site=search&q=pack_ice:ice_ps:si_corer_9cm	L1_CORE_01_AWI_20191005, L1_CORE_02_AWI_20191005, L1_CORE_03_AWI_20191005, L1_CORE_04_AWI_20191005,PS122/1_3-22
AF-MOSAiC-1_6	https://sensor.awi.de/?site=search&q=pack_ice:ice_ps:orange-crush-ctd	L1_CDT_AWI_20191005,PS122/1_3-6
AF-MOSAiC-1_79	https://sensor.awi.de/?site=search&q=pack_ice:ice_ps:gem2-556	
AF-MOSAiC-1_76	https://sensor.awi.de/?site=search&q=pack_ice:ice_ps:mrs_1_ucb	
AF-MOSAiC-1_75	https://sensor.awi.de/?site=search&q=pack_ice:ice_ps:asfs_40_ucb	L1_ASFS_CIRES_20191005,PS122/1_1-241
AF-MOSAiC-1_80	https://sensor.awi.de/?site=search&q=pack_ice:ice_ps:gem2-556	
AF-MOSAiC-1_74	https://sensor.awi.de/?site=search&q=buoy:2019f1	L1_AOFB_NPS_20191005,PS122/1_1-227

Station	Sensor Id	Comment Old Labels
AF-MOSAiC-1_135	https://sensor.awi.de/?site=search&q=buoy:2019p92	AWI-UTAP-0009,PS122/1_1-163
AF-MOSAiC-1_125	https://sensor.awi.de/?site=search&q=buoy:2019t71	M7_SIMBA11_ PRIC,FMI_20191011,PS122/1_1-174
AF-MOSAiC-1_153	https://sensor.awi.de/?site=search&q=buoy:2019p199	OSU-IT-0012,PS122/1_1-193
AF-MOSAiC-1_149	https://sensor.awi.de/?site=search&q=buoy:2019p195	OSU-IT-0008,PS122/1_1-189
AF-MOSAiC-1_47	https://sensor.awi.de/?site=search&q=pack_ice:ice_ps:ice_ gauge	L2_DRILLING_ AARI_20191006,PS122/1_3-47
AF-MOSAiC-1_91	https://sensor.awi.de/?site=search&q=pack_ice:ice_ ps:gem2-556	
AF-MOSAiC-1_38	https://sensor.awi.de/?site=search&q=pack_ice:ice_ ps:magnaprobe-anja	L1_MAGNA_1_ AWI_20191007,PS122/1_3-38
AF-MOSAiC-1_23	https://sensor.awi.de/?site=search&q=pack_ice:ice_ps:si_ corer_9cm	L2_CORE_1_ AWI_20191006,PS122/1_3-23
AF-MOSAiC-1_8	https://sensor.awi.de/?site=search&q=pack_ice:ice_ps:orange- crush-ctd	L2_CTD_1_AWI_20191006,PS122/1_3-8
AF-MOSAiC-1_24	https://sensor.awi.de/?site=search&q=pack_ice:ice_ps:si_ corer_9cm	L2_CORE_2_ AWI_20191006,PS122/1_3-24
AF-MOSAiC-1_25	https://sensor.awi.de/?site=search&q=pack_ice:ice_ps:si_ corer_9cm	L2_CORE_3_ AWI_20191006,PS122/1_3-25
AF-MOSAiC-1_90	https://sensor.awi.de/?site=search&q=buoy:2019t63	L2_SIMBA3_ PRIC_20191007,PS122/1_1-224
AF-MOSAiC-1_132	https://sensor.awi.de/?site=search&q=buoy:2019p88	AWI-UTAP-0005,PS122/1_1-160
AF-MOSAiC-1_42	https://sensor.awi.de/?site=search&q=pack_ice:ice_ps:orange- crush-ctd	PS122/1_3-42
AF-MOSAiC-1_168	https://sensor.awi.de/?site=search&q=buoy:2019p136	TUT-GPS-2,PS122/1_1-208
AF-MOSAiC-1_108	https://sensor.awi.de/?site=search&q=buoy:2019s79	M2_SB05_ AWI_20191007,PS122/1_1-146
AF-MOSAiC-1_26	https://sensor.awi.de/?site=search&q=pack_ice:ice_ps:si_ corer_9cm	L2_CORE_4_ AWI_20191007,PS122/1_3-26
AF-MOSAiC-1_175	https://sensor.awi.de/?site=search&q=buoy:2019p144	TUT-GPS-10,PS122/1_1-215
AF-MOSAiC-1_174	https://sensor.awi.de/?site=search&q=buoy:2019p143	TUT-GPS-9,PS122/1_1-214
AF-MOSAiC-1_171	https://sensor.awi.de/?site=search&q=buoy:2019p139	TUT-GPS-5,PS122/1_1-211
AF-MOSAiC-1_55	https://sensor.awi.de/?site=search&q=pack_ice:ice_ps:snow_ sampler_glove	PS122/1_3-55
AF-MOSAiC-1_110	https://sensor.awi.de/?site=search&q=buoy:2019o2	M2_SIT_2_ AWI_20191007,PS122/1_1-149
AF-MOSAiC-1_144	https://sensor.awi.de/?site=search&q=buoy:2019p193	OSU-IT-0003,PS122/1_1-187
AF-MOSAiC-1_56	https://sensor.awi.de/?site=search&q=pack_ice:ice_ps:snow_ sampler_glove	PS122/1_3-56
AF-MOSAiC-1_142	https://sensor.awi.de/?site=search&q=buoy:2019p188	OSU-IT-0001,PS122/1_1-182
AF-MOSAiC-1_146	https://sensor.awi.de/?site=search&q=buoy:2019p190	OSU-IT-0005,PS122/1_1-184
AF-MOSAiC-1_107	https://sensor.awi.de/?site=search&q=buoy:2019t57	M2_SIMBA6_ PRIC_20191007,PS122/1_1-176
AF-MOSAiC-1_89	https://sensor.awi.de/?site=search&q=buoy:2019t65	L2_SIMBA2_ PRIC_20191007,PS122/1_1-226
AF-MOSAiC-1_109	https://sensor.awi.de/?site=search&q=buoy:2019v1	M2_DTOP_2_ OUC_20191007,PS122/1_1-276
AF-MOSAiC-1_104	https://sensor.awi.de/?site=search&q=buoy:2019s84	M1_SB04_ AWI_20191005,PS122/1_1-147

Station	Sensor Id	Comment Old Labels
AF-MOSAiC-1_41	https://sensor.awi.de/?site=search&q=pack_ice:ice_ps:orange-crush-ctd	PS122/1_3-41
AF-MOSAiC-1_88	https://sensor.awi.de/?site=search&q=buoy:2019r8	L2_IT_BOB_ AWI_20191005,PS122/1_1-167
AF-MOSAiC-1_53	https://sensor.awi.de/?site=search&q=pack_ice:ice_ps:snow_ sampler_glove	L2_SNOW_1_BNU_1007,PS122/1_3-53
AF-MOSAiC-1_72	https://sensor.awi.de/?site=search&q=buoy:2019s92	L1_SNOW_BUOY_ AWI_20191005,PS122/1_1-137
AF-MOSAiC-1_54	https://sensor.awi.de/?site=search&q=pack_ice:ice_ps:snow_ sampler_glove	L2_SNOW_2_BNU_1007,PS122/1_3-54
AF-MOSAiC-1_83	https://sensor.awi.de/?site=search&q=pack_ice:ice_ps:mrs_1_ ucb	
AF-MOSAiC-1_84	https://sensor.awi.de/?site=search&q=buoy:2019f2	L2_AOFB_1_ NPS_20191007,PS122/1_1-261
AF-MOSAiC-1_27	https://sensor.awi.de/?site=search&q=pack_ice:ice_ps:si_ corer_9cm	L2_CORE_5_AWI_20191007,L2_ CORE_6_AWI_20191007,PS122/1_3-27
AF-MOSAiC-1_9	https://sensor.awi.de/?site=search&q=pack_ice:ice_ps:orange-crush-ctd	L2_CTD_2_AWI_20191007,PS122/1_3-9
AF-MOSAiC-1_86	https://sensor.awi.de/?site=search&q=buoy:2019w2	L2_ITP_1_ WHOI_20191007,PS122/1_1-168
AF-MOSAiC-1_87	https://sensor.awi.de/?site=search&q=buoy:2019s93	L2_SNOW_BUOY_2_ AWI_20191007,PS122/1_1-138
AF-MOSAiC-1_71	https://sensor.awi.de/?site=search&q=buoy:2019r9	PS122/1_1-313,L2_IT_BOB_ AWI_20191007
AF-MOSAiC-1_92	https://sensor.awi.de/?site=search&q=buoy:fio_itp	
AF-MOSAiC-1_85	https://sensor.awi.de/?site=search&q=buoy:2019i2	L2_SIMB3_1_Dartmouth_20191007, PS122/1_1-205
AF-MOSAiC-1_134	https://sensor.awi.de/?site=search&q=buoy:2019p91	AWI-UTAP-0008,PS122/1_1-162
AF-MOSAiC-1_112	https://sensor.awi.de/?site=search&q=buoy:2019s81	M3_SB06_ AWI_20191007,PS122/1_1-145
AF-MOSAiC-1_133	https://sensor.awi.de/?site=search&q=buoy:2019p90	AWI-UTAP-0007,PS122/1_1-161
AF-MOSAiC-1_172	https://sensor.awi.de/?site=search&q=buoy:2019p140	TUT-GPS-6,PS122/1_1-212
AF-MOSAiC-1_32	https://sensor.awi.de/?site=search&q=pack_ice:ice_ ps:gem2-556	L1_GEM_2_ AWI_20191007,PS122/1_3-32
AF-MOSAiC-1_151	https://sensor.awi.de/?site=search&q=buoy:2019p200	OSU-IT-0010,PS122/1_1-194
AF-MOSAiC-1_157	https://sensor.awi.de/?site=search&q=buoy:2019p203	OSU-IT-0016,PS122/1_1-197
AF-MOSAiC-1_152	https://sensor.awi.de/?site=search&q=buoy:2019p198	OSU-IT-0011,PS122/1_1-192
AF-MOSAiC-1_114	https://sensor.awi.de/?site=search&q=buoy:2019o3	M3_SIT_3_ AWI_20191007,PS122/1_1-150
AF-MOSAiC-1_160	https://sensor.awi.de/?site=search&q=buoy:2019p206	OSU-IT-0019,PS122/1_1-200
AF-MOSAiC-1_150	https://sensor.awi.de/?site=search&q=buoy:2019p196	OSU-IT-0009,PS122/1_1-190
AF-MOSAiC-1_111	https://sensor.awi.de/?site=search&q=buoy:2019t59	M3_SIMBA7_ PRIC_20191007,PS122/1_1-178
AF-MOSAiC-1_113	https://sensor.awi.de/?site=search&q=buoy:2019v1	M3_DTOP_3_ OUC_20191007,PS122/1_1-277
AF-MOSAiC-1_82	https://sensor.awi.de/?site=search&q=pack_ice:ice_ps:asfs_40_ ucb	L2_ASFS_ CIRES_20191007,PS122/1_1-240; Device Failed Measurement: Comment: PS122/1_1-240
AF-MOSAiC-1_33	https://sensor.awi.de/?site=search&q=pack_ice:ice_ ps:gem2-556	PS122/1_3-33

Station	Sensor Id	Comment Old Labels
AF-MOSAiC-1_115	https://sensor.awi.de/?site=search&q=buoy:2019t58	M4_SIMBA8_ PRIC_20191008,PS122/1_1-177
AF-MOSAiC-1_116	https://sensor.awi.de/?site=search&q=buoy:2019s80	M4_SB07_ AWI_20191008,PS122/1_1-144
AF-MOSAiC-1_48	https://sensor.awi.de/?site=search&q=pack_ice:ice_ps:ice_gauge	M4_DRILLING_ AARI_20191008,PS122/1_3-48
AF-MOSAiC-1_117	https://sensor.awi.de/?site=search&q=buoy:2019o4	M4_SIT_3_ AWI_20191008,PS122/1_1-151
AF-MOSAiC-1_57	https://sensor.awi.de/?site=search&q=pack_ice:ice_ps:snow_sampler_glove	PS122/1_3-57
AF-MOSAiC-1_167	https://sensor.awi.de/?site=search&q=buoy:2019p135	TUT-GPS-1,PS122/1_1-207
AF-MOSAiC-1_99	https://sensor.awi.de/?site=search&q=buoy:2019t70	L3_SIMBA4_ PRIC_20191010,PS122/1_1-173
AF-MOSAiC-1_118	https://sensor.awi.de/?site=search&q=buoy:2019t72	M5_SIMBA9_ PRIC,FMI_20191009,PS122/1_1-175
AF-MOSAiC-1_119	https://sensor.awi.de/?site=search&q=buoy:2019s87	M5_SB08_ AWI_20191009,PS122/1_1-143
AF-MOSAiC-1_141	https://sensor.awi.de/?site=search&q=buoy:2019p126	MO_SVP-I-BXGS-AP,PS122/1_1-159
AF-MOSAiC-1_49	https://sensor.awi.de/?site=search&q=pack_ice:ice_ps:ice_gauge	PS122/1_3-49
AF-MOSAiC-1_58	https://sensor.awi.de/?site=search&q=pack_ice:ice_ps:snow_sampler_glove	PS122/1_3-58
AF-MOSAiC-1_159	https://sensor.awi.de/?site=search&q=buoy:2019p205	OSU-IT-0018,PS122/1_1-199
AF-MOSAiC-1_163	https://sensor.awi.de/?site=search&q=buoy:2019p209	OSU-IT-0022,PS122/1_1-203
AF-MOSAiC-1_138	https://sensor.awi.de/?site=search&q=buoy:2019p122	MO_SVP-I-BXGS-AP,PS122/1_1-156
AF-MOSAiC-1_179	https://sensor.awi.de/?site=search&q=buoy:2019p149	TUT-GPS-19,PS122/1_1-219
AF-MOSAiC-1_156	https://sensor.awi.de/?site=search&q=buoy:2019p202	OSU-IT-0015,PS122/1_1-196
AF-MOSAiC-1_50	https://sensor.awi.de/?site=search&q=pack_ice:ice_ps:ice_gauge	L3_DRILLING_ AARI_20191009,PS122/1_3-50
AF-MOSAiC-1_162	https://sensor.awi.de/?site=search&q=buoy:2019p208	OSU-IT-0021,PS122/1_1-202
AF-MOSAiC-1_166	https://sensor.awi.de/?site=search&q=buoy:2019p187	OSU-UT-0006,PS122/1_1-181
AF-MOSAiC-1_169	https://sensor.awi.de/?site=search&q=buoy:2019p137	TUT-GPS-3,PS122/1_1-209
AF-MOSAiC-1_34	https://sensor.awi.de/?site=search&q=pack_ice:ice_ps:gem2-556	L3_GEM_1_ AWI_20191009,PS122/1_3-34
AF-MOSAiC-1_120	https://sensor.awi.de/?site=search&q=buoy:2019v1	M5_DTOP_5_ OUC_20191009,PS122/1_1-278
AF-MOSAiC-1_40	https://sensor.awi.de/?site=search&q=pack_ice:ice_ps:magnaprobe-anja	L3_MAGNA_1_ AWI_20191007,PS122/1_3-40
AF-MOSAiC-1_28	https://sensor.awi.de/?site=search&q=pack_ice:ice_ps:si_corer_9cm	L3_CORE_1_AWI_20191009, L3_CORE_2_AWI_20191009, L3_CORE_3_AWI_20191009,PS122/1_3-28
AF-MOSAiC-1_10	https://sensor.awi.de/?site=search&q=pack_ice:ice_ps:orange-crush-ctd	L3_CTD_1_ AWI_20191009,PS122/1_3-10
AF-MOSAiC-1_59	https://sensor.awi.de/?site=search&q=pack_ice:ice_ps:snow_sampler_glove	L3_SNOW_7_BNU_1010,PS122/1_3-59
AF-MOSAiC-1_29	https://sensor.awi.de/?site=search&q=pack_ice:ice_ps:si_corer_9cm	L3_CORE_4_AWI_20191009, L3_CORE_5_AWI_20191009, L3_CORE_6_AWI_20191009,PS122/1_3-29
AF-MOSAiC-1_11	https://sensor.awi.de/?site=search&q=pack_ice:ice_ps:orange-crush-ctd	L3_CTD_2_ AWI_20191009,PS122/1_3-11

Station	Sensor Id	Comment Old Labels
AF-MOSAiC-1_101	https://sensor.awi.de/?site=search&q=pack_ice:ice_ps:co2_ch4_chamber_portable	
AF-MOSAiC-1_139	https://sensor.awi.de/?site=search&q=buoy:2019p124	MO_SVP-I-BXGS-AP,PS122/1_1-157
AF-MOSAiC-1_3	https://sensor.awi.de/?site=search&q=aircraft:heli-ps	HELI_AEM_AWI_20190930,PS122/1_3-3
AF-MOSAiC-1_1	https://sensor.awi.de/?site=search&q=pack_ice:ice_ps:gem2-556	PS122/1_3-1
AF-MOSAiC-1_43	https://sensor.awi.de/?site=search&q=pack_ice:ice_ps:ice_gauge	PS122/1_3-43
AF-MOSAiC-1_36	https://sensor.awi.de/?site=search&q=pack_ice:ice_ps:gem2-556	PS122/1_3-36
AF-MOSAiC-1_164	https://sensor.awi.de/?site=search&q=buoy:2019p182	OSU-UT-0001,PS122/1_1-179
AF-MOSAiC-1_165	https://sensor.awi.de/?site=search&q=buoy:2019p184	OSU-UT-0003,PS122/1_1-180
AF-MOSAiC-1_140	https://sensor.awi.de/?site=search&q=buoy:2019p125	MO_SVP-I-BXGS-AP,PS122/1_1-158
AF-MOSAiC-1_155	https://sensor.awi.de/?site=search&q=buoy:2019p201	OSU-IT-0014,PS122/1_1-195
AF-MOSAiC-1_123	https://sensor.awi.de/?site=search&q=buoy:2019s86	M6_SB09_AWI_20191010,PS122/1_1-142
AF-MOSAiC-1_178	https://sensor.awi.de/?site=search&q=buoy:2019p148	TUT-GPS-14,PS122/1_1-218
AF-MOSAiC-1_177	https://sensor.awi.de/?site=search&q=buoy:2019p146	TUT-GPS-12,PS122/1_1-217
AF-MOSAiC-1_161	https://sensor.awi.de/?site=search&q=buoy:2019p207	OSU-IT-0020,PS122/1_1-201
AF-MOSAiC-1_137	https://sensor.awi.de/?site=search&q=buoy:2019p103	AWI-UTA-0010,PS122/1_1-165
AF-MOSAiC-1_60	https://sensor.awi.de/?site=search&q=pack_ice:ice_ps:snow_sampler_glove	PS122/1_3-60
AF-MOSAiC-1_158	https://sensor.awi.de/?site=search&q=buoy:2019p204	OSU-IT-0017,PS122/1_1-198
AF-MOSAiC-1_124	https://sensor.awi.de/?site=search&q=buoy:2019o6	M6_SIT_6_AWI_20191010,PS122/1_1-153
AF-MOSAiC-1_122	https://sensor.awi.de/?site=search&q=buoy:2019t64	M6_SIMBA10_PRIC,FMI_20191010,PS122/1_1-225
AF-MOSAiC-1_136	https://sensor.awi.de/?site=search&q=buoy:2019p101	AWI-UTA-0008,PS122/1_1-164
AF-MOSAiC-1_94	https://sensor.awi.de/?site=search&q=buoy:2019w3	L3_ITP102_WHOI_20191010,PS122/1_1-169
AF-MOSAiC-1_100	https://sensor.awi.de/?site=search&q=buoy:unis_pric	L3_UNMANED_ICE_PRIC_20191010,PS122/1_1-263
AF-MOSAiC-1_96	https://sensor.awi.de/?site=search&q=buoy:2019f3	L3_AOFB_1_NPS_20191010,PS122/1_1-262
AF-MOSAiC-1_98	https://sensor.awi.de/?site=search&q=buoy:2019i3	L3_SIMB3_1_Dartmouth_20191010, PS122/1_1-206
AF-MOSAiC-1_95	https://sensor.awi.de/?site=search&q=buoy:2019s94	L3_SNOW_BUOY_3_AWI_20191010,PS122/1_1-139
AF-MOSAiC-1_93	https://sensor.awi.de/?site=search&q=buoy:2019m30	L3_IT_BOB_AWI_20191009,PS122/1_1-166
AF-MOSAiC-1_97	https://sensor.awi.de/?site=search&q=pack_ice:ice_ps:asfs_40_ucb	L3_ASFS_CIRES_20191010,PS122/1_1-242
AF-MOSAiC-1_102	https://sensor.awi.de/?site=search&q=pack_ice:ice_ps:dms_chamber_portable	
AF-MOSAiC-1_180	https://sensor.awi.de/?site=search&q=buoy:2019p22	MO_SVP-B,PS122/1_1-350
AF-MOSAiC-1_181	https://sensor.awi.de/?site=search&q=buoy:2019p123	MO_SVP-I-BXGS-AP-16,PS122/1_1-346
AF-MOSAiC-1_52	https://sensor.awi.de/?site=search&q=pack_ice:ice_ps:ice_gauge	PS122/1_3-52
AF-MOSAiC-1_182	https://sensor.awi.de/?site=search&q=buoy:2019t47	PS122/1_1-285

Station	Sensor Id	Comment Old Labels
AF-MOSAiC-1_12	https://sensor.awi.de/?site=search&q=pack_ice:ice_ps:orange-crush-ctd	PS122/1_3-12
AF-MOSAiC-1_30	https://sensor.awi.de/?site=search&q=pack_ice:ice_ps:si_corer_9cm	PS122/1_3-30
AF-MOSAiC-1_2	https://sensor.awi.de/?site=search&q=pack_ice:ice_ps:si_corer_9cm	PS122/1_3-2
AF-MOSAiC-1_4	https://sensor.awi.de/?site=search&q=aircraft:heli-ps	HELI_AEM_AWI_20191013,PS122/1_3-4
AF-MOSAiC-1_5	https://sensor.awi.de/?site=search&q=aircraft:heli-ps	HELI_AEM_AWI_20191014,PS122/1_3-5
AF-MOSAiC-1_183	https://sensor.awi.de/?site=search&q=buoy:2019f4	PS122/1_1-304
AF-MOSAiC-1_121	https://sensor.awi.de/?site=search&q=buoy:2019o5	M5_SIT_5_ AWI_20191009,PS122/1_1-152
AF-MOSAiC-1_127	https://sensor.awi.de/?site=search&q=buoy:2019o7	M7_SIT_7_ AWI_20191011,PS122/1_1-154
AF-MOSAiC-1_131	https://sensor.awi.de/?site=search&q=buoy:2019o8	M8_SIT_8_ AWI_20191011,PS122/1_1-155
AF-MOSAiC-1_176	https://sensor.awi.de/?site=search&q=buoy:2019p145	TUT-GPS-11,PS122/1_1-216
AF-MOSAiC-1_51	https://sensor.awi.de/?site=search&q=pack_ice:ice_ps:ice_gauge	M7_DRILLING_ AARI_20191011,PS122/1_3-51
AF-MOSAiC-1_35	https://sensor.awi.de/?site=search&q=pack_ice:ice_ps:gem2-556	PS122/1_3-35
AF-MOSAiC-1_129	https://sensor.awi.de/?site=search&q=buoy:2019s90	M8_SB11_ AWI_20191011,PS122/1_1-141
AF-MOSAiC-1_128	https://sensor.awi.de/?site=search&q=buoy:2019t69	M8_SIMBA12_ PRIC,FMI_20191011,PS122/1_1-172
AF-MOSAiC-1_126	https://sensor.awi.de/?site=search&q=buoy:2019s95	M7_SB10_ AWI_20191011,PS122/1_1-140
AF-MOSAiC-1_130	https://sensor.awi.de/?site=search&q=buoy:2019v1	M8_DTOP_4_ OUC_20191011,PS122/1_1-279
AF-MOSAiC-1_61	https://sensor.awi.de/?site=search&q=pack_ice:ice_ps:snow_sampler_glove	PS122/1_3-61

A.4 APPENDIX FOR ICE AND SNOW SURVEYS

Photos of instruments deployed on L1

The instruments deployed at L1 are shown in the photos below with acronyms consistent with the station book (Appendix station book).

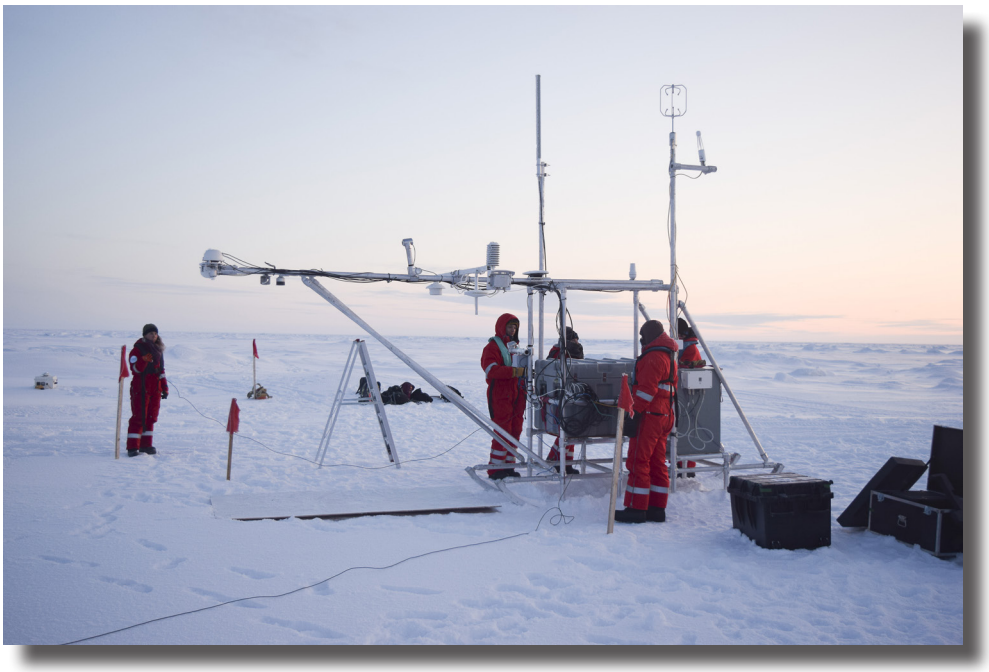

Fig. A4.1: ASF

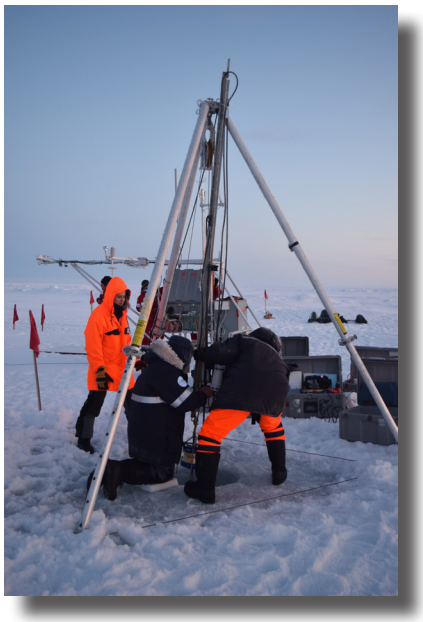

Fig. A4.2: AOFB

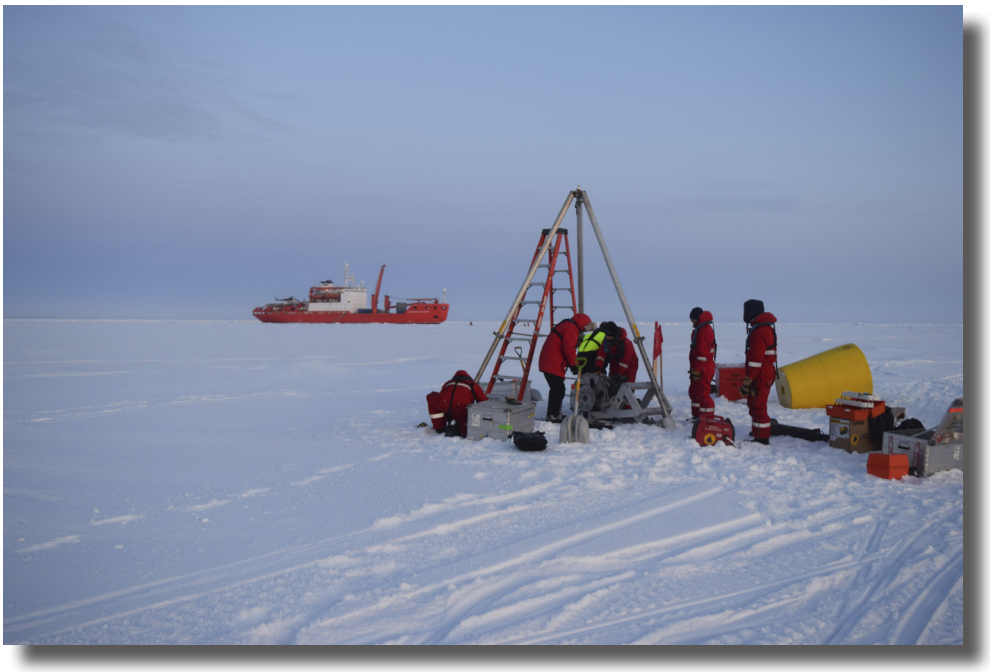

Fig. A4.3: ITP

Fig. A4.4: BIOB

Fig. A4.5: SIMB3

Fig. A4.6: GEM calibration site

Photos of instruments deployed on L2.

The instruments deployed at L2 are shown in the photos below with acronyms consistent with the station book (Appendix station book).

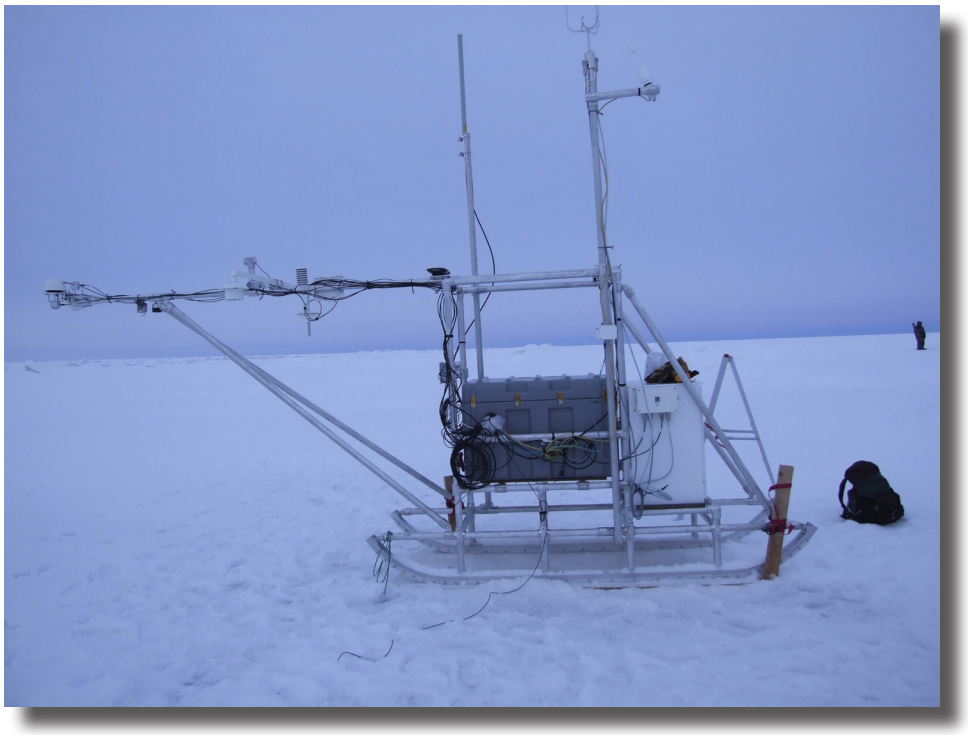

Fig. A4.7: ASFS

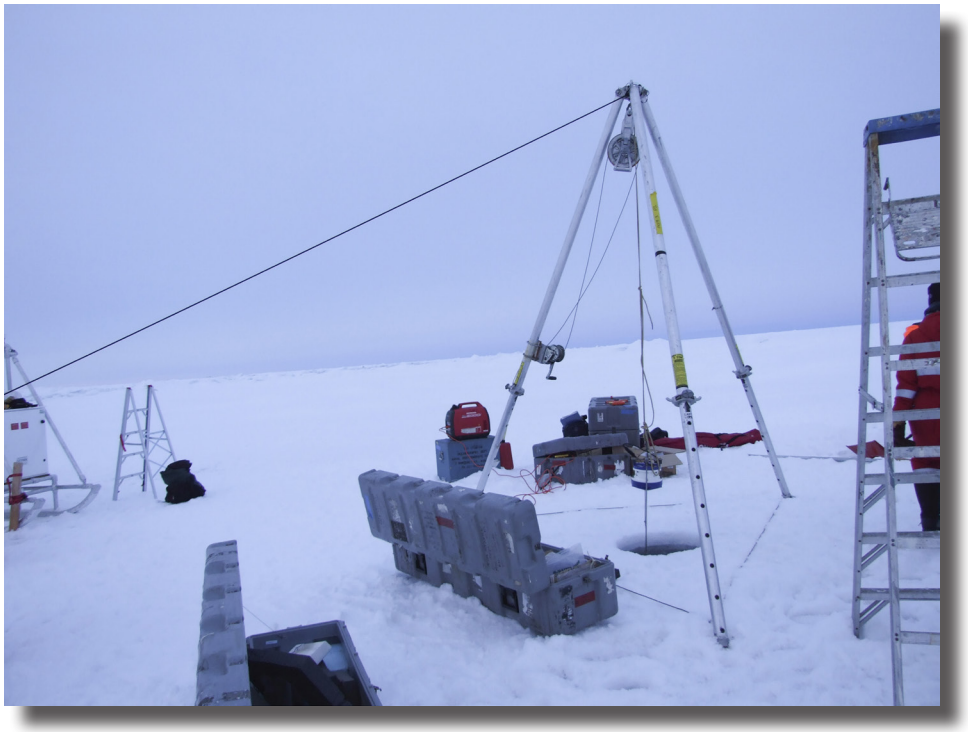

Fig. A4.8: AOFB

Fig. A4.9: ITP

Fig. A4.10: SIMB3

Fig. A4.11: Snow buoy

Fig. A4.12: AWI FLUX Station

Photos of instruments deployed on L3.

The instruments deployed at L3 are shown in the photos below with acronyms consistent with the station book (Appendix station book).

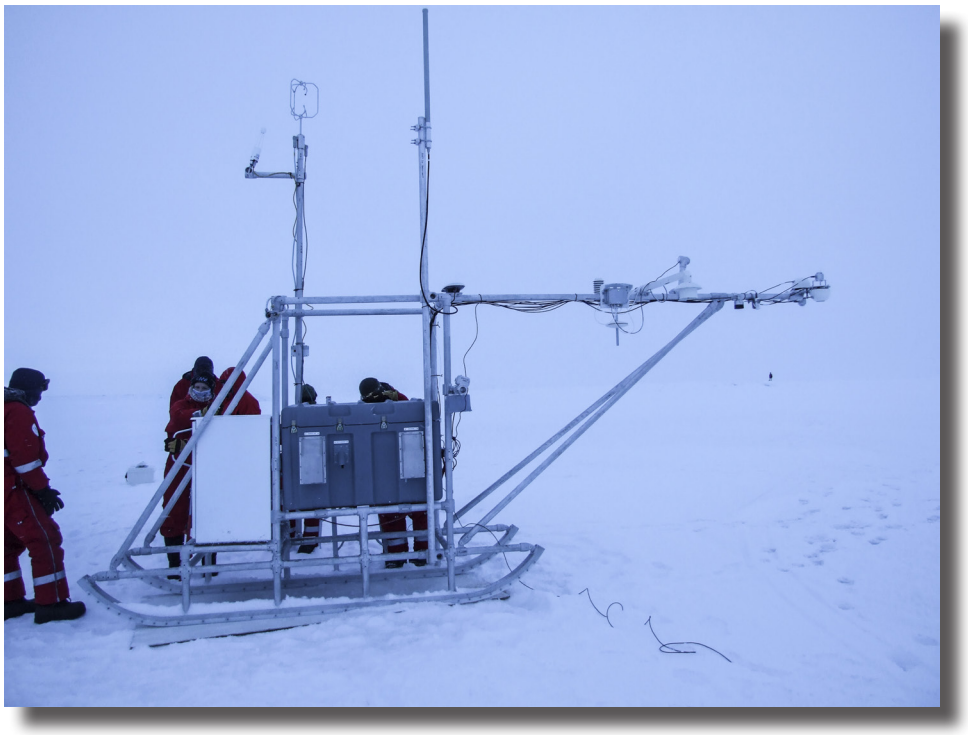

Fig. A4.13: ASFS

Fig. A4.14: AOFB

Fig. A4.15: SIMB3

Fig. A4.16: SIMBA

Die **Berichte zur Polar- und Meeresforschung** (ISSN 1866-3192) werden beginnend mit dem Band 569 (2008) als Open-Access-Publikation herausgegeben. Ein Verzeichnis aller Bände einschließlich der Druckausgaben (ISSN 1618-3193, Band 377-568, von 2000 bis 2008) sowie der früheren **Berichte zur Polarforschung** (ISSN 0176-5027, Band 1-376, von 1981 bis 2000) befindet sich im electronic Publication Information Center **(ePIC)** des Alfred-Wegener-Instituts, Helmholtz-Zentrum für Polar- und Meeresforschung (AWI); see https://epic.awi.de. Durch Auswahl “Reports on Polar- and Marine Research“ (via “browse”/”type”) wird eine Liste der Publikationen, sortiert nach Bandnummer, innerhalb der absteigenden chronologischen Reihenfolge der Jahrgänge mit Verweis auf das jeweilige pdf-Symbol zum Herunterladen angezeigt.

The **Reports on Polar and Marine Research** (ISSN 1866-3192) are available as open access publications since 2008. A table of all volumes including the printed issues (ISSN 1618-3193, Vol. 377-568, from 2000 until 2008), as well as the earlier **Reports on Polar Research** (ISSN 0176-5027, Vol. 1-376, from 1981 until 2000) is provided by the electronic Publication Information Center **(ePIC)** of the Alfred Wegener Institute, Helmholtz Centre for Polar and Marine Research (AWI); see URL https://epic.awi.de. To generate a list of all Reports, use the URL http://epic.awi.de and select “browse”/ ”type” to browse ”Reports on Polar and Marine Research”. A chronological list in declining order will be presented, and pdf-icons displayed for downloading.

Zuletzt erschienene Ausgaben:

Recently published issues:

743 (2020) The Expedition AF122/1 Setting up the MOSAiC Distributed Network in October 2019 with Research Vessel AKADEMIK FEDOROV, edited by Thomas Krumpen and Vladimir Sokolov

743 (2020) The Expedition to the Peel River in 2019: Fluvial Transport Across a Permafrost Landscape, edited by Frederieke Miesner, P. Paul Overduin, Kirsi Keskitalo, Niek J. Speetjens, Jorien Vonk, Sebastian Westermann

742 (2020) Das Alfred-Wegener-Institut in der Geschichte der Polarforschung - Einführung und Chronik, von Christian R. Salewski, Reinhard A. Krause, Elias Angele

741 (2020) The MOSES Sternfahrt Expeditions of the Research Vessels LITTORINA, LUDWIG PRANDTL, MYA II, and UTHÖRN to the inner German Bight in 2019, edited by Ingeborg Bussmann, Holger Brix, Mario Esposito, Madlen Friedrich, Philipp Fischer

740 (2020) The Expedition PS120 of the Research Vessel POLARSTERN to the Atlantic Ocean in 2019, edited by Karen H. Wiltshire and Eva-Maria Brodte

739 (2020) Focus Siberian Permafrost – Terrestrial Cryosphere and Climate Change, International Symposium, Hamburg, 23 – 27 March 2020, Institute of Soil Science - Universität Hamburg, Germany, edited by E.M. Pfeiffer, T. Eckhardt, L. Kutzbach, I. Fedorova, L. Tsibizov, C. Beer

738 (2020) The Expedition PS121 of the Research Vessel POLARSTERN to the Fram Strait in 2019, edited by Katja Metfies

737 (2019) The Expedition PS105 of the Research Vessel POLARSTERN to the Atlantic Ocean in 2017, edited by Rainer Knust

736 (2019) The Expedition PS119 of the Research Vessel POLARSTERN to the Eastern Scotia Sea in 2019, edited by Gerhard Bohrmann

735 (2019) The Expedition PS118 of the Research Vessel POLARSTERN to the Weddell Sea in 2019, edited by Boris Dorschel

ALFRED-WEGENER-INSTITUT
HELMHOLTZ-ZENTRUM FÜR POLAR-
UND MEERESFORSCHUNG

BREMERHAVEN

Am Handelshafen 12
27570 Bremerhaven
Telefon 0471 4831-0
Telefax 0471 4831-1149
www.awi.de

HELMHOLTZ